LATERAL STRENGTH AND DUCTILE BEHAVIOR OF A MORTISE-TENON CONNECTED TIMBER FRAME

A Thesis

presented to

the Faculty of California Polytechnic State University,

San Luis Obispo

In Partial Fulfillment

of the Requirements for the Degree

Master of Architecture with an emphasis in Architectural Engineering

by

Alexandros Kouromenos

March 2017

COMMITTEE MEMBERSHIP

TITLE: Lateral Strength and Ductile Behavior of a Mortise-Tenon Connected Timber Frame

AUTHOR: Alexandros Kouromenos

DATE SUBMITTED: March 2017

COMMITTEE CHAIR: James Mwangi, Ph.D., S.E.
Professor of Structural engineering

COMMITTEE MEMBER: Jill Nelson, S.E., P.M.P.,
Professor of Structural engineering

COMMITTEE MEMBER: Cole McDaniel, Ph.D., P.E.
Professor of Structural engineering

ABSTRACT

Lateral Strength and Ductile Behavior of a Mortise-Tenon Connected Timber Frame

Alexandros Kouromenos

The primary goals of this project were to examine the amount of lateral force resisted by a single-bay mortise-tenon connected timber moment frame, and to introduce ductile behavior into the mortise-tenon connections by adding a steel sleeve around a traditional wood peg. This research aimed to provide proof that traditional timber frames are capable of ductile racking while reliably complying with ASCE 7-10 building code drift specifications, implying an increase in the ASCE 7-10 ductility factor (R) for wood frames when used as lateral force resisting elements.

A secondary goal was to promote traditional heavy timber framing as a main structural system. Modern structural framing is dominated by light-wood, steel, and concrete framing. The exploration in this project aspires to demonstrate that heavy timber frames can achieve comparable lateral performance and frame behavior to other current lateral systems, reassuring the reliability of traditional timber frames.

ACKNOWLEDGMENTS

Bill Hurley is the owner of Dos Osos Timber Works Incorporated in Los Osos, CA. With over twenty years of experience as a timber frame designer and fabricator, Mr. Hurley's vast knowledge of wood-working techniques were passed down to this project. Access to the Dos Osos Timber Works Incorporated wood shop resources also made fabricating the full scale test frame possible.

Ray Ward, the architectural engineering technician at Cal Poly in San Luis Obispo, CA, assisted in coordinating the full scale testing set up. This included placing the frame in its test position, calibrating deflection and force measuring devices, and writing a script in LabView that recorded force and displacement.

Garret McElveny is a Project Engineer at Taylor & Syfan in San Luis Obispo, CA, and a former employee at Dos Osos Timber Works Incorporated. Mr. McElveny is passionate about timber framing, and believes that timber frames can be more commonly used as reliable framing systems in seismic zones. Mr. McElveny introduced the initial subject, and contributed his experience with timber structure to guide the growth of concepts in this research.

Hayward Lumber is a timber distribution company in San Luis Obispo, CA. Although they did not offer discounts for educational research projects, their services allowed completion of this project within a reasonable budget.

TABLE OF CONTENTS

LIST OF TABLES

LIST OF FIGURES

1 LITERATURE REVIEW

Figure 1. Hugh Lofting Timber Framing, Carriage Shed.

This project researched the lateral strength and ductility of a timber post-beam frame with angled kick braces triangulating the top two corners, using traditional heavy timber connections. All joints were connected by inserting a tenon into a mortise pocket and sliding a dowel through pre-drilled holes. The dowel was in double shear as it held the tenon inside the mortise pocket.

Heavy timber frames of this configuration have potential to be used as a reliable lateral force-resisting element because as the beam translates laterally, the changes in geometry can be accommodated by isolating damage into the dowels that connect all of the members, especially the dowels connecting the kick braces to the beam and columns. Essentially, the changes in the geometry impose forces into the members, primarily the kick braces. The forces that generates in the kick braces then flow to the dowels then into the main member that houses the connection, either the beam or the column. If the dowel holding the connections together is engineered yield without rupturing the frame can accept changes in the geometry (permanent deformations), the dowel can be used as a non-linear plastic hinge element, and in general the frame will dampen structure movement. Control of the frame's racking

behaviour was achieved by designing the dowels to form plastic hinge zones, similar to a reduced beam section in steel moment frames, before any of the main timber members fail in these modes: compression parallel and perpendicular to grain, bolt tear out, or tension parallel and perpendicular to grain. As long as the dowel hinging is engaged before the previously listed failure modes, the main structural elements that hold up the building against an earthquake or gust of wind will not fail and collapse. Traditionally wholly wood pegs are used to connect all of the members, but in this research wood pegs were inserted into a metal tube sleeve creating a composite cross section with wood on the inside and a thin-walled metal pipe layer on the outside. The wood peg inserts were used to guide the deformed shape of the metal tubes. The metal material is used for slow, inelastic deformation, which translates into energy dissipation, as it controls the global frame action with ductile and stable behaviour; maintaining the overall structural integrity of the frame supporting the building, preventing collapse. The dowel and the main structural members were sized such that the heavy timber withstood the forces imposed by the dowels at each connection to the kick braces, forcing the ductile dowel to be the only element that yields.

1.1 Historic Relevance

A post and beam timber frame with kick braces used to triangulate the corners is an ancient timber construction method. In fact these frames have been used for thousands of years getting their earliest start in Japan and Europe. "The oldest temple in Japan…The Horyu-ji Temple, which was built around the start of the eighth century…[has] withstood devastating earthquake[s]…outperforming other building types" (Globalstructures, 2010). Many wood churches in Europe are still common tourist attractions "dating back to the 12th and 13th centuries" (Globalstructures, 2010). These historic timber structures have endured many years and remain both

beautiful and sturdy. In a book about timber framing the author speaks of visiting Switzerland and being asked to guess the age of the post-beam timber structure that provides comforting shelter to this day. It turns out the home was 500 years old (Roy, 2004). The members that make up the frame are most commonly connected together by slotting a key (tenon) into a carved out joint (mortise) then pegging them together with a dowel. "A recent rebirth of this technique is seeing hundreds of new joinery-connected buildings being constructed each year" (Brungraber, 1985). However, there have been few attempts to apply either a modern analysis to evaluate the strength of these frames or modern concepts to improve the behavior of this frame.

1.2 Structural Relevance

Wood frames with mortise tenon connections held together with dowels are perhaps the most common connection type found in traditional timber framed structures. "They are relatively easy to fabricate, enable efficient frame assembly, and are effective in transferring shear forces" (Schmidt, 2007). We luckily still get to enjoy ancient wood structures today, considering many have lasted decades without being destroyed by one of the many threats to wood: fungal and pest attacks, decay, dry rot, shrinkage, earthquakes, and fires. Wood has been a trusted structural building material for centuries but modern design methods have helped demonstrate its superior performance "in thousands of buildings during the last one hundred and fifty years, many of which are still in satisfactory use." (AWC, 2013). The main structural elements in a wood structure are typically sized to be heavy timber. Wood members are considered to be heavy timber when their net cross sections measure five inches by five inches or larger nominally. All members in this project exceeded these dimensions (AWC, 2013). This is important because timber members meeting this size requirement perform well in fires, especially compared to steel frames (ASTM E199,

2016). Steel weakens dramatically once its temperature exceeds 450°F, retaining only 10 percent of its strength at 1,380°F. After 30 minutes in a 1,380°F fire, an exposed large wooden beam will have lost roughly 25 percent of its strength, and retain structural integrity. A steel beam will have lost 90 percent strength and will have failed (ASTM E119, 2016). Heavy timber members, composite or sawn cut, will char in a fire as opposed to burn. What this means for an owner is that during a fire the main structure will hold up for enough time allowing occupants or firefighters to evacuate the building.

Parallel Strand Lumber (PSL) is a harder and stiffer material than sawn cut timber, obtaining higher design level stress values. PSLs are made by drying small 1 inch strips of lumber and gluing, then compressing them together (Busta & Honesty, 2013) a more uniform and homogeneous cross section is created, discarding errors in the natural growth of wood such as knots and other undesirable features from a strength standpoint. This manufacturing process also creates less waste. "Up to 65% of a whole log can be converted into high-grade structural lumber" (Strand, 2007). In general, "Production and use of structural composite lumber (SCL) products are increasing" (McKeever 1997, Schuler and others, 2001) because of their reliable and controlled physical properties.

For situations that weaken PSLs over time such as pest attacks and dry rot there is a separate PSL manual featuring Parallel Strand Lumber with Wolmanized Preservative Protection (Weyerhauser, 2016). Although design stresses are reduced, this treated composite lumber "effectively resists fungal decay and termite attack." And is "ideal for ground, fresh, and saltwater splash applications" (Weyerhauser, 2016). When it comes to shrinkage, both treated and untreated PSLs "resist bowing, twisting, and shrinking—both before and after installation" (Weyerhauser, 2016).

Wood is a less weighty building material compared to steel or concrete. Not

only does a lighter material result in cheaper shipping costs, but it also results in a lighter structure, in pounds. During a seismic event, materials that are heavier have more inertia and will require a larger opposing force to prevent lateral deflections compared to a building constructed of a lighter material. A building with less weight can be laterally supported during an earthquake with less material.

Images in timber framing books, such as A Timber Framer's Workshop, a common frame size is between 8-16 feet wide and 8-12 feet tall (Chappell, 1998). Knowing common bay dimensions allows for the approximation of the structural requirements of each member and the architectural space they create. Although an aspect ratio closer to 2:1 is more common in timber framing, the eight foot by eight foot frame tested in this research can be compared to a wood shear wall with two sheets of sheathing side by side. An aspect ratio of 1:1 also can be seen as a conservative configuration because larger overturning axial forces will develope in the columns than if the width of the frame was larger than the height. This imposes large compressive and tensile axial forces in the columns, combined with a bending force in the column from the axial kick braces tests the combined stress capacity of the columns. A wider frame racks more than it overturns. Racking is more desirable for the frame being tested because racking deformation ensures engagement of the plastic hinging dowels. Using 8 foot long members also made managing the members by hand more feasible.

From the perspective of a structural engineer the major questions that remains is: Can a dowel in a mortise tenon connection be used to reliably transfer significant axial loads, upwards of 3,000 pounds, from the kick braces into the columns and beam that develope when a lateral load is imposed along the frame's beam? Based on research done at Stanford (Brungraber, 1985), the answer is yes. Brungraber (Brungraber, 1985) conducted an in depth analysis using modern technologies to

predict the capacity of these connections within a frame. The Stanford research (Brungraber, 1985) went deep into the finite element modeling of these connections, then compared analysis to physical testing of full scale mortise-tenon connections. Data and results will not be referenced in this paper because the specific values do not apply to this research, but the general conclusion of Brungraber's paper is that the dowels do in fact provide reliable resistance to the tenon pulling out of or pushing into the mortise pocket (Brungraber, 1985). This translates into the global frame being capable of resisting lateral forces. How much? That depends on many variables, but that is not the point of Brungraber's research. The only conclusion needed to be withdrawn from The Modern Analysis of Traditional Timber Joinery is that traditional mortise-tenon connected timber frames do resist lateral load by transferring horizontal load from the beam, into the kick braces, then into the dowels. The timber joinery in this project took this concept one step further by creating a dowel that forms two nonlinear plastic hinges similar to the way plastic hinging is used in a reduced beam section steel moment frame. The dowel's steel sleeve encasement will be the material used to achieve plastic hinging in this ductile, energy dissipating, connection. If no steel is used the structure would be relying on brittle wood dowels that do not fatigue before failing, after being overstressed once wood dowels are unable to support stabile frame racking after one cycle.

1.3 Sustainability

Timber structural elements are renewable and sustainable, assuming proper deforesting. Trees "absorb carbon dioxide" (Globalstructures, 2010) out of the atmosphere, storing it in the form of a building material. New trees can be planted to continue this process and help decontaminate the atmosphere. Glue lam beams and other engineered wood products (such as the PSLs to be used in this project) can be

made from recycled wood and used to replace new sawn lumber. But in general "The manufacture of wood products consumes little energy" (Globalstructures, 2010), and according to the same article (Globalstructures, 2010) these energy efficient timber products make up roughly 70% of the homes built in the western world. However, within the last 100 years designers have relied heavily on new materials such as steel and concrete, without realizing how costly they are to the environment. "In the present time, [humans] are increasingly called upon to consider the ecological consequences of [their] actions" (Stung, 2001). With these considerations, and with recent innovations in the wood industry, such as engineered lumber, sustainable wood construction is making a comeback. In an article about the sustainability of wood in Europe many respected professors were quoted on the need to bring back the use of wood for its sustainability benefits. Prof. Dr. Callum Hill (Kuzman, M. K., & Kutnar, 2014) professed that "Human society faces one of its greatest challenges due to climate change driven by anthropogenic emissions of greenhouse gases." (Kuzman, M. K., & Kutnar, 2014). Although increasing levels of carbon dioxide have been made public, the push for clean energy has been slow. "One very effective strategy of dealing with this serious problem is the use of timber in construction" (Kuzman, M. K., & Kutnar, 2014). Another professor (Kuzman, M. K., & Kutnar, 2014) whose focus is in architecture, Mag. Peter Gabrijelčič from the University of Ljubljana in Slovenia, condones wood construction for its aesthetic charm and structural strength as well as environmental characteristics by saying, "The growing use of this renewable resource is sustainable because the growth of European forest resources exceeds consumption." (Kuzman, M. K., & Kutnar, 2014). Continuing sustainable forestry creates opportunities for innovation in timber construction and architecture. To evaluate the sustainability benefits when using wood a comparison must be made to different building materials examining the net energy used to produce a material product over its full life cycle.

"From harvest of raw materials through manufacturing, transportation, installation, use, maintenance and disposal or recycling—wood performs better than concrete and steel in terms of embodied energy, air and water pollution, and carbon footprint" (Ritter, Skog, Bergman, 2011). The sustainability benefits for using timber as a building material are overpowering. In this day and age it now important for us to start questioning the purpose of our projects and condone sustainable building by not glorifying "what can we build" and start prioritizing "what should we build."

1.4 Architectural Relevance

The biggest benefit of this type of frame is the creation of open space. Walls are good, and important, but some situations call for capitalizing on open space or astounding views. It is possible to cut holes in walls but their structural requirements increase along with costs via design time, construction processes, and materials needed to compensate the loss in strength. This frame could also be covered up for situations that require separation from the environment or partitioning. Or, the open space could be used for windows, doors, or even a garage structure (Figure 1). The amount of open space, also known as bay size, that timber frames are able to create varies from 8-16 feet wide, and 8-12 feet tall (Roy, 2004). Coinciding with an open and light structure, wood frames are aesthetically and physically more comforting than most other materials. Wood has a warmer look and has a softer touch to the hand compared to a cold and rough steel or concrete surface. There is just something about the way wood looks; almost everybody wants a nice wood cabin.

1.5 Potentials

The frame members could be shop manufactured using Computer Numerical Control (CNC) technology for the mortise-tenon connections to make fabrication

faster and easier. The frame tested will be observed for reusability since all significant damage occurs only in the dowels. After the steel sleeved dowels have been damaged and deformed they can be replaced by some means of drilling or cutting them out and hammering in new ones. The frame members were designed and sized so that the beams, posts, and kick braces do not crush or shear and can be used at least two times. Using traditional timber frames in high seismic regions, categories D through F per the American Society of Civil Engineers (ASCE 7-10), and in multi-story or high-rise or buildings with a lot of mass would require more testing. The main potential demonstrated by this project was within residential design and small commercial buildings in seismic design categories A through C.

1.6 Limitations

This project promotes using Parallel Strand Lumber everywhere in a traditionally timber framed structure, however using PSLs may not be desired because the engineered wood is toxic when burned, due to the glue that adheres the strips of wood. Burning any pressure treated wood or composite lumber can have serious health implications when the smoke is inhaled in (Croft, W., Henry, P., Woolson, E., Darcey, B., Olson, M., 1984). So despite Engineered PSLs having an equivalent fire rating to sawn cut dimensional lumber (White, 2006) there are still toxic fumes that will be released from the glue burning. However, engineered wood products, such as plywood sheathing are already widely used justifying the use of PSLs for a heavy timber frame where fire hazards are a design parameter.

Fabrication limitations of heavy timber framing are also an issue. Traditionally, these frames have been very labor intensive with a lot of carpentry. However, these limitations are minor when compared to concrete or steel construction. With steel framing welders need to be paid, and weld inspectors, along with larger cranes to

place all of the heavy components. In concrete design the costs of formwork and paying the workers to construct them make up anywhere from 40 to 60% of the cost of concrete structures (R.H. Lab, 2007). Wood is generally locally sourced saving shipping expenses compared to alternative building materials. Assembly of wood structures, custom or prefabricated, is quick and efficient (Ritter, Skog, Bergman, 2011). There are certainly costs associated with wood framing, however when compared to the other options wood is generally still a cheaper solution.

Long-term exposure to weather and other natural elements or insects can diminish the strength of wood but no building material lasts forever and the life of a wood building can be just as long as steel or concrete if protection is detailed carefully.

2 DOWEL TESTING

Figure 2. Stainless steel tube dowel post compression test.

2.1 Theory

The timber frame configuration researched in this project is a post-beam wood frame with two kick braces triangulating the top two frame corners. True pinned base connections and kick brace connections, and a pinned beam to column connection hold the members in their desired configuration. What makes the frame to be tested in this project unique compared to traditional timber frames is the use of a steel tube sleeve that encases a wood peg. This engineered dowel, and detailing around that dowel inside of the mortise-tenon connection, allow the composite peg to isolate permanent frame damage and changes in frame geometry as it racks into two plastic hinges, see Figures 3, 4, and 5. The metal pipe is necessary because metal can endure many cycles of fatigue and strain, unlike a traditional and brittle wood peg. The challenge was engineering the optimum ratio of dowel strength to the strength of the surrounding wood housing (mortise tenon connection), such that wood failure in the main wood members is avoided. As a starting point, a very thin walled metal pipe shall be used to encase a wood peg. Using thin walled pipes weakens the stiffer metal material by encouraging local wall buckling. The dowel is not expected to fail in shear

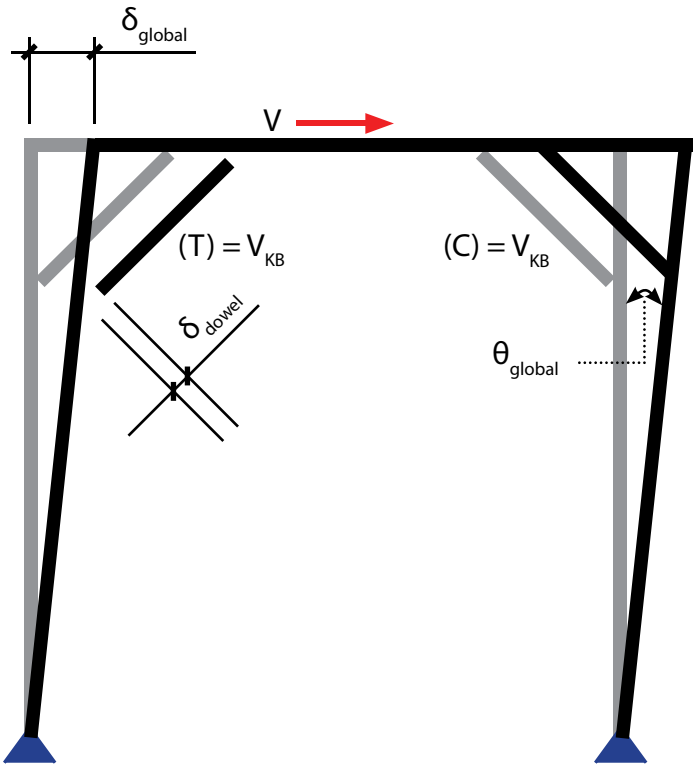

Figure 3. Changes in geometry caused by frame racking.

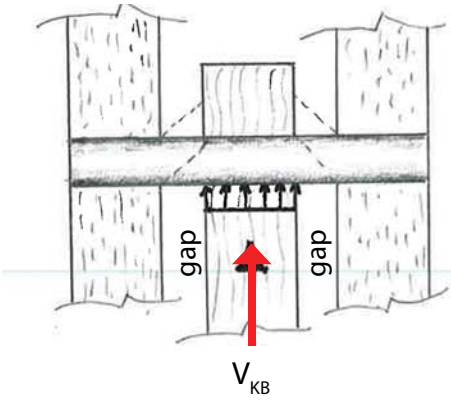

Figure 4. Dowel section for an undeflected frame.

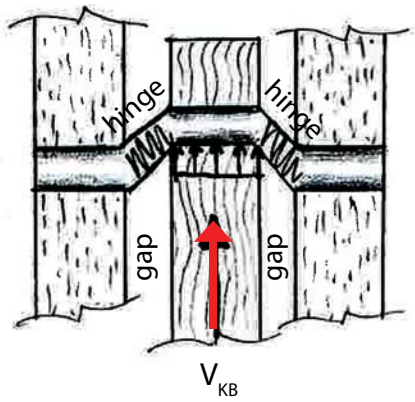

Figure 5. Dowel section for a deflected frame.

because local buckling is expected to govern. A gap between the mortise and tenon outer surfaces was detailed to ensure the thin metal pipe walls deform and buckle locally in the desired plastic hinge regions. Including a gap voids the National Design Specifications (AWC, 2014) for Wood Construction provision to analyze different yield modes with dowel connections because the gap forces only one major yield mode, Mode IV (AWC, 2014).

The other factor controlling the flexibility of the metal tubes is the yield stress of the material. Steel is the favorable metal in structural engineering because it has desirable behavior in the nonlinear range; metal can endure large deformations before rupturing. From testing done in Great Britain (Forrest, 1970), steel is the metal that

can endure the most fatigue cycles, a desirable characteristic when the material is being used to resist cyclic lateral loads. Two other metals, however, shall be explored. Aluminum and Copper are common building materials and both aesthetically look good when paired with wood.

A PSL housing was constructed to test various metal dowels, see Figures 6 and 7. The main housing member was conservatively oriented so that it would be compressed perpendicular to grain, testing the weakest failure mode of the housing. During full scale testing, for the proposed frame configuration, the dowel would be pulling or pushing on the grain of a beam or column mortise pocket at a forty-five degree angle to the parallel strands of lumber, generating a smaller perpendicular to grain force than the force imposed on the main housing member during dowel testing. The test housing was limited in width because of the test machine allowances. PSL was used for the housing to observe the behavior of the wood because PSL was planned to be used as the full frame material. The housing was made to simulate a mortise pocket. Two rectangular boards were cut, one and a half inches thick, with two 2.25 inch spacers in between. The spacers would also be used as legs to support the jig. The two boards were to be bolted into the spacers, two bolts on each side.

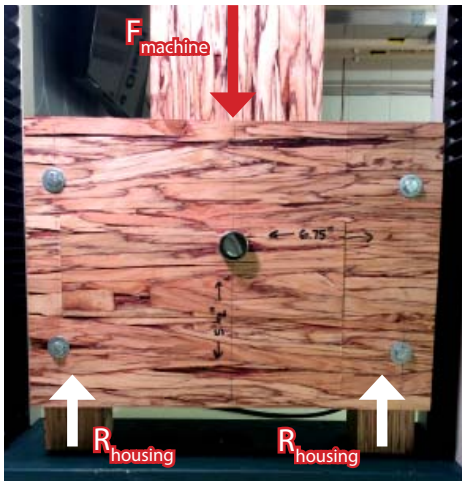

Figure 6. Hollow metal pipe compression test arrangement in the Tinius Olsen Testing machine.

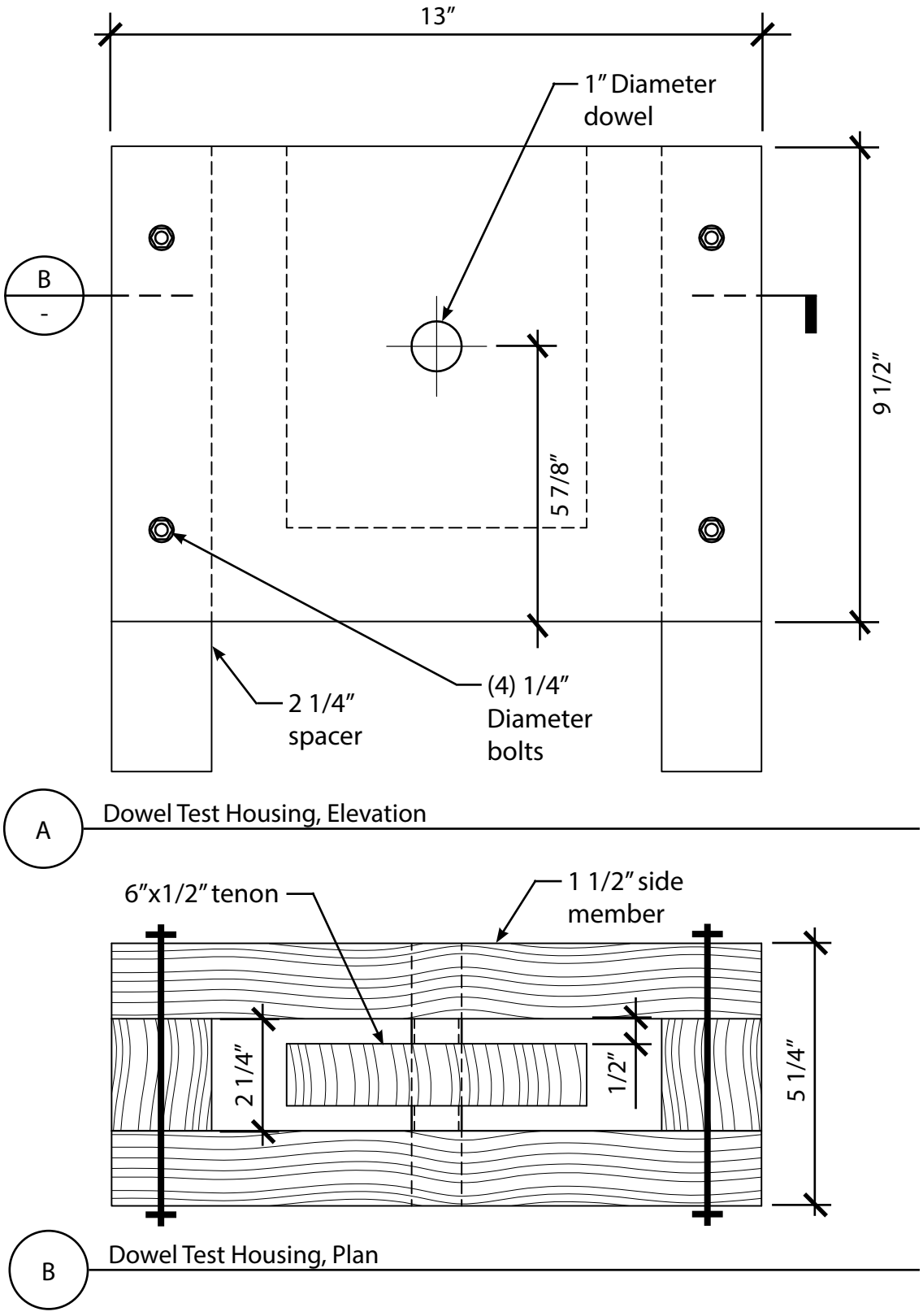

Figure 7. Dowel Test Housing Details.

To achieve ductile behavior in the frame, metal must be introduced for its ductile qualities. Metal, however, is stronger than wood. The stiffness of the dowel needed to be a particular ratio such that the dowel fails before crushing or rupturing the surrounding wood housing. The stiffness of the metal dowel and the stiffness of the wood housing material were made proportional by selecting a thin-walled round pipe. Using a thin-walled hollow pipe reduced the moment of inertia of dowel and allowed for localized buckling to occur before crushing or rupturing any wood. To achieve the perfect dowel stiffness, two controlling parameters were tested: the yield stress of the metal and the wall thickness. Three different metals of varying yield stresses and wall thicknesses were tested, see Table 1 and Table 2. The logic behind the selections was this: a low yield stress would be compensated by thicker walls. The one exception was the aluminum dowel, however, between the three tests enough information was deduced to conclude on the proper dowel needed for the full scale frame testing.

2.2 Metal Tube Compression Test

The Metal Tube Compression Test was used to examine the strength and deformation properties of three one inch diameter metal tube dowels.

A one inch diameter pipe dowel was inserted into the PSL housing connecting the vertical tenon member. The head of the compression machine was gently lowered so that the compression head was barely touching the top of the tenon, only keeping it from rotating, this was the zero deflection starting point. The system was compressed at a rate of half an inch per second; until it was clear the dowel had failed.

The results of the test can be seen in Figures 8, 9, 10, and 11. Wall thickness was the controlling factor and not yield stress when it came to getting the desired deformed shape of the dowel. The copper dowel, which has a yield stress of only

Table 1. Metal pipe material specifications for the copper (C122 CO) (ASTMB88-16, 2016), aluminum (6061-T6 AL) (ASTM B241M-16, 2016), and stainless steel (304 SS) (ASTM A312 / A312M-00c) dowels.

Dowel	Ultimate Tensile Strength (psi)	Yield Strength (psi)	Copper %	Carbon % max	Manganese % max
C122 CO	32,000	10,000	99.9	N/A	N/A
6061-T6 AL	45,000	40,000	0.15-0.40	0.08	0.15
304 SS	73,200	31,200	N/A	N/A	2.0

Table 2. Metal tube length, diameter, and wall thickness.

Dowel	Length (inches)	Outer Diameter (inches)	Wall Thickness (inches)
CO	6	1	0.065
AL	6	1	0.035
SS	6	1	0.020

Figure 8. Deformed steel pipe dowels post compression testing. Aluminum (a), Steel (b), and Copper (c).

Table 3. Compressive test results for the metal pipe dowels.

Dowel	Yield Load (pounds)	Yield Deflection (inches)	Ultimate Load (pounds)	Ultimate Deflection (inches)
CO	3,450	0.190	4,933	0.425
AL	2,200	0.165	2,525	0.450
SS	1,400	0.140	1,900	0.765

10 ksi (Table 1), and was hardly strained because the walls were so thick. Scarce signs of permanent deformations demonstrates that the yield and ultimate load of a tube perpendicular to its length is highly dependent on wall thickness and is less dependent on the yield stress of the material. This is not surprising because the metal tube walls were very slender. The next thickest tube was the aluminum and it was

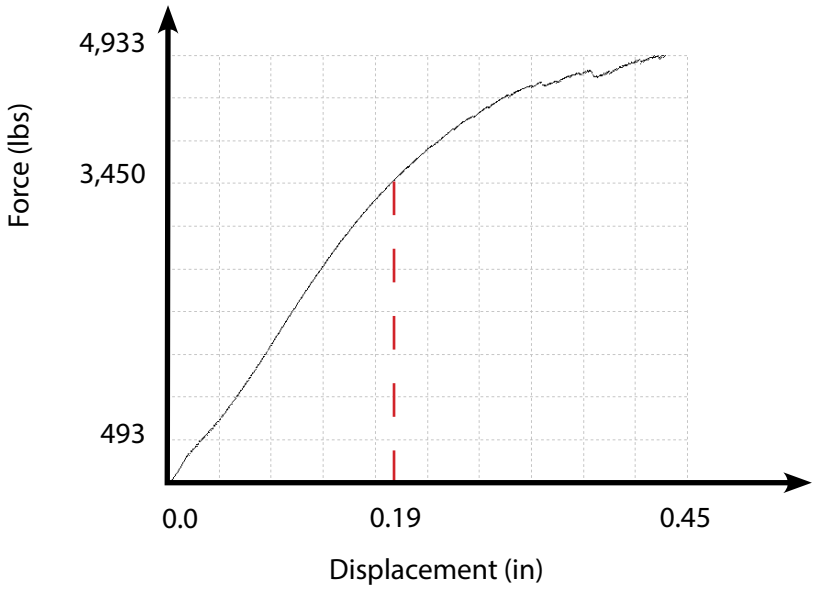

Figure 9. Copper pipe compression test results.

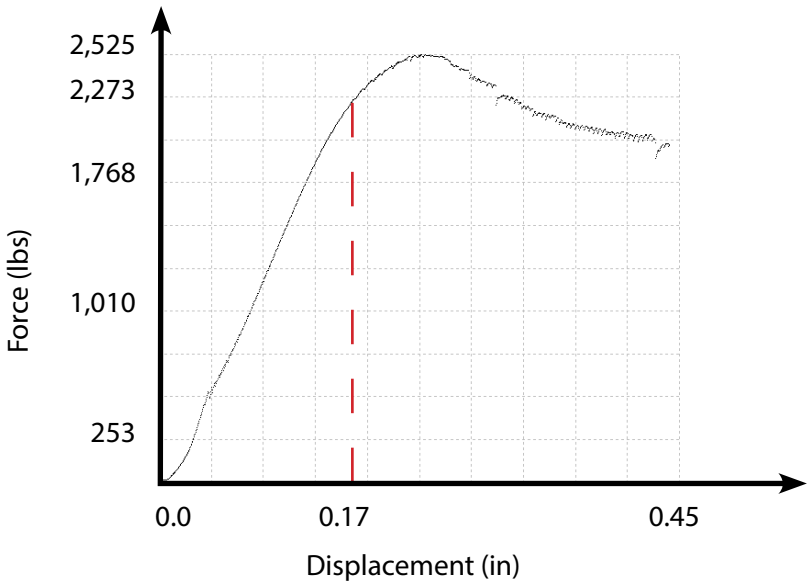

Figure 10. Aluminum pipe compression test results.

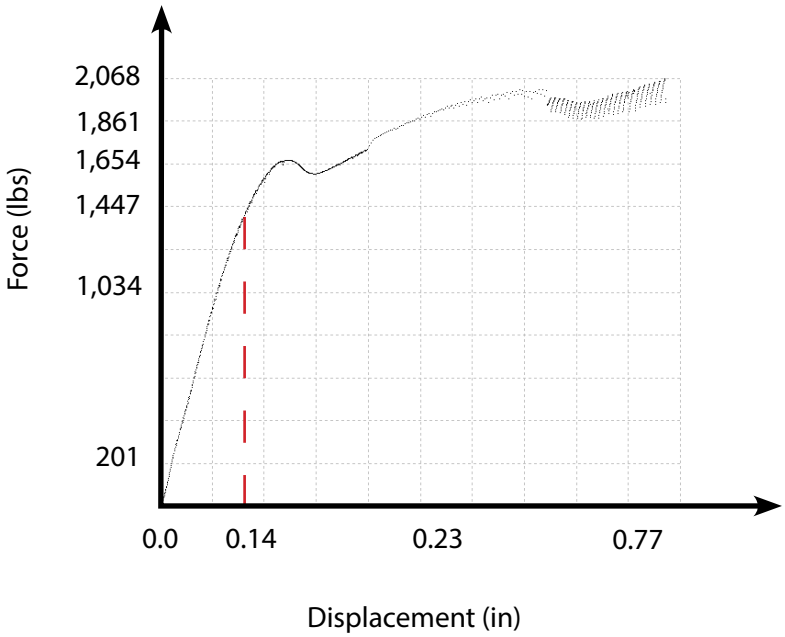

Figure 11. Stainless steel pipe compression test results.

the second strongest and deformed the second least. Then the steel had the thinnest walls and the smallest yield and ultimate load, although it deformed the most. More tests could be done with varying materials and wall thicknesses but it was determined to move forward with the stainless steel and aluminum tubes. For this project it was desired to exaggerate the frame behavior and dowel deformation in order to make obvious the capability of this frame to deform without collapsing, so the thinnest walled and least stiff stainless steel dowel was used. The copper dowel performed very well from a strength standpoint, but to ensure prevention of failures in the timber frame members to be tested in this project a metal tube of this strength will not be used. The aluminum tube held the second most load, and it had the second thickest walls. It has a negative sloping nonlinear region. The shape of the curve for the stainless steel pipe is identical to the curve given from a tensile steel force-versus-displacement test. The stainless steel tube resulted in the lowest yield and ultimate load, see Table 3, but deformed the largest distance without rupturing or shearing. The thin walls forced local buckling to be the governing failure mode, which is the

desired failure mode as opposed to shearing because the local buckling deforms slowly, giving warning of failure without rupturing. One of the steel tube specimens deformed so much it was impossible to extract from the tenon member.

Figure 12. Stainless steel pipe compressed around the edges of the tenon hole.

Removing the deformed dowels from the housing and the tenon was very difficult. Each time the bolted housing had to be disassembled. To prevent this from being an issue in the future, the amount of local buckling of each pipe will need to be reduced. In this first dowel test the tenon split perpendicular to grain when testing the 0.035 inch wall thickness aluminum dowel. As the top and bottom of the tube crushed, the side walls moved outwards pushing against the wood, eventually splitting it apart perpendicular to grain. The 0.02 inch wall thickness stainless steel dowel deformed similarly, however it did not split the tenon. The stainless steel dowel deformed around the hole barely crushing even the cornered edges of the hole, as seen in Figure 12. The bolts holding the housing together were examined. Upon removal the bolts were slightly bent. This means they accounted for a small amount of the measured deflection, however, the force-versus-displacement graphs will be approximated to the most conservative force and displacement values. The next step is to add stiffeners to the dowel to prevent it from buckling in the portions that are embedded within the main timber members.

Figures 12 and 13 demonstrate how much crushing and local buckling can occur without causing significant harm to the wood. PSL wood appears to be so hard, most likely because of all the glue, that the thin steel tube has even bent around the corner edges of the hole.

Figure 13. Stainless steel pipe compressed around the edges of the tenon hole.

2.3 Tube Sleeve with a Wood Peg Dowel Compression Test

This test was used to observe the behavior of a steel and aluminum tube with a one inch outer diameter filled in with a wood peg insert, see Figure 14. The same stainless steel (SS) and aluminum (AL) tubes as the first dowel test were to be used, copper was excluded from further testing. The wood peg insert was used as a guide, it controlled the geometry of the deforming metal tube. The wood insert was predicted to prevent major local buckling and flattening of the metal casing throughout the entire connection. The notched areas in the wood inserts are there to ensure the dowel forms a plastic hinge in a half inch open area inside of the mortise pocket. This is essentially the same idea as a reduced beam section in a steel moment frame. This portion of the dowel is desired to be the location of large deformations and strains in order to make the entire piece a sacrificial element. The notched regions

will break and the wood will become a deformation guide as shown in Figure 15. The wood insert will add stiffness to the dowel because it will not allow the metal tube encasement to locally buckle and crush as dramatically as the hollow tube dowels in the first dowel test.

Figure 14. Stainless steel pipe below the notched wood insert.

A wood peg was fabricated with 1/8"-3/16" deep, and half inch wide, notches in the specified locations, per Figure 16. A taper was not used in this test because the mortise and tenon holes were easily aligned by hand. The wood insert was sanded down until it fit snuggly inside the metal pipe. The composite dowel was pushed into place, no adhesives were used. Using the same Tinius Olsen Testing Machine, shown in Figure 17, the system was loaded in compression at one half of an inch per second, until the system became unstable or until the desired data was collected. If the PSL test housing survives and the dowel is compressed as expected, once the test was over, the level of difficulty to remove the dowel was recorded.

As the machine compressed some minor cracking could be heard, this was the sound of the test housing settling. Eventually some louder cracks were heard however nothing seemed to be happening to the test housing, so it was clear that this noise

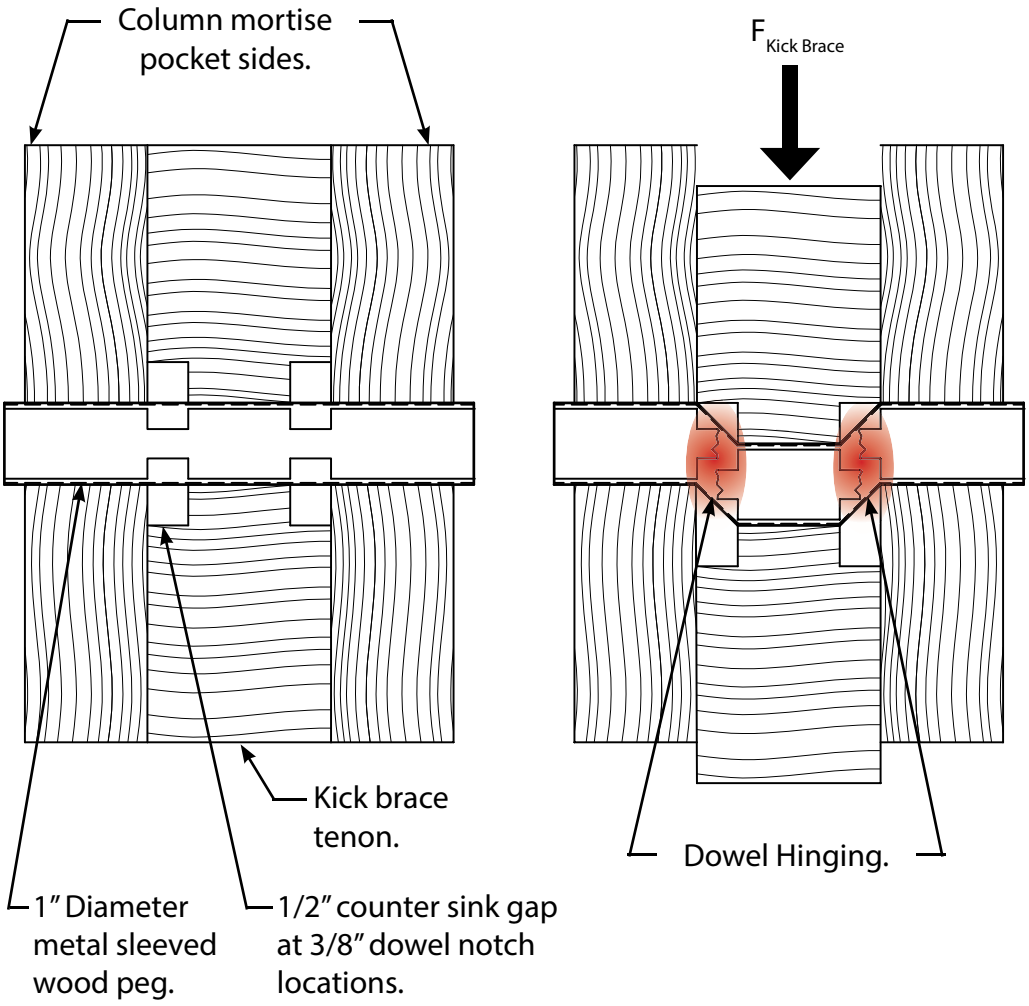

Figure 15. Wood dowel with metal pipe sleeve deformation behavior.

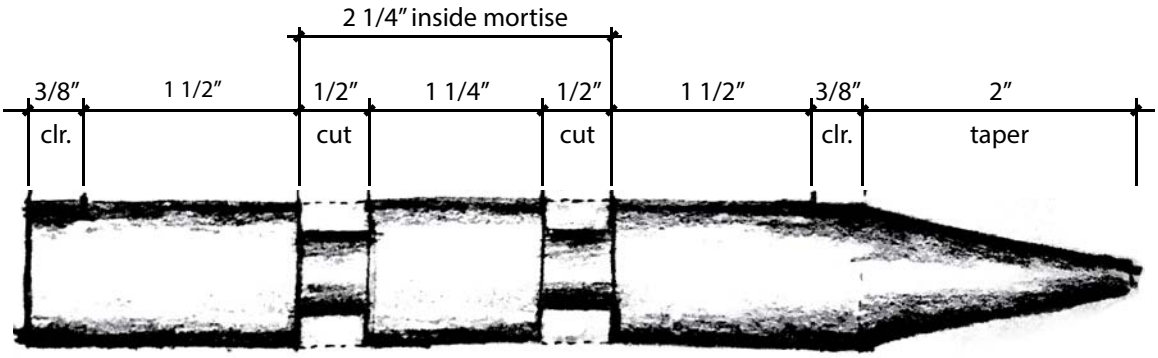

Figure 16. Wood peg insert for metal sleeve.

came from the wood peg insert breaking at the notches. Even though the wood peg inserts broke, the dowel continued to resist increasing loads until around one half inch of deflection, for both steel and aluminum. The ultimate load of the dowel was 3,500 pounds for the stainless steel and just over 4,100 pounds for the aluminum, see Table 4. The thicker aluminum dowel held more load and had less local bucking, but the aluminum dowel had more of a curved deformed shape as opposed to a more abrupt offset in the middle of the dowel for the thinner walled stainless steel dowel. In both tests there was a large amount of deformation in the one half inch gap, as can been seen in Figures 18 and 19. Because of the thicker walls, the aluminum dowel did not show as much localized buckling, it deformed in a more subtle manner. The steel tube had more creasing and wall buckling. The test jig had to be taken apart every time to retrieve the dowel because the dowels were being compressed so much that their deformed shape made it impossible for them to easily slide out.

Figure 17. Wood filled pipe compression test arrangement in the Tinius Olsen Testing Machine.

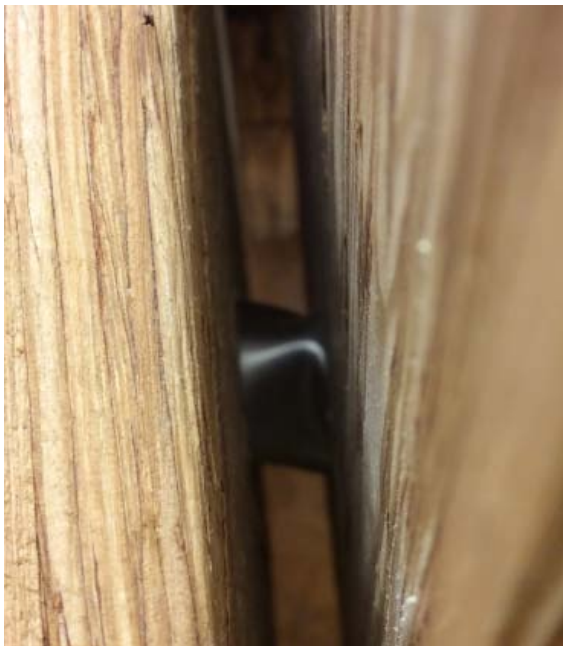

Figure 18. Visible dowel strains within the 1/2" gap region.

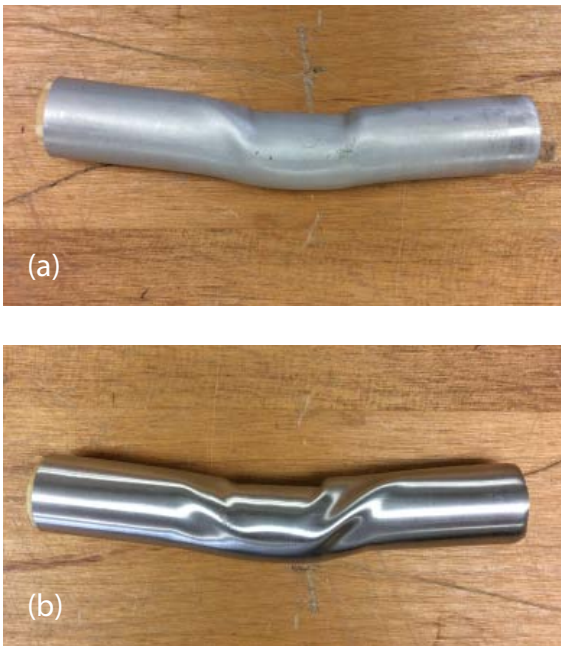

Figure 19. Test results from the aluminum (a) and steel (b) dowels with wood inserts.

Table 4. Compressive test results for the aluminum (a) and stainless steel (b) sleeved dowels with wood peg inserts.

Dowel	Yield Load (lbs)	Yield Deflection (in)	Ultimate Load (lbs)	Ultimate Deflection (in)
AL	2,800	0.201	4,100	0.591
SS	2,500	0.267	3,500	0.591

The aluminum tube and wood insert resulted in a steep jump in stiffness and a yield load that occurred at a smaller displacement, roughly 0.201 inches, than the stainless steel dowel. The stainless steel tube and wood insert produced a consistent stiffness until the yield plateau occurring at 0.53 inches. The jumps in the data are caused by the wood insert fracturing and the metal pipe taking some time to regain stiffness. Once the dowel regained stiffness, the slope of the curve is almost the same as the slope of the data curve before the wood inserts fractured. The steel dowel has

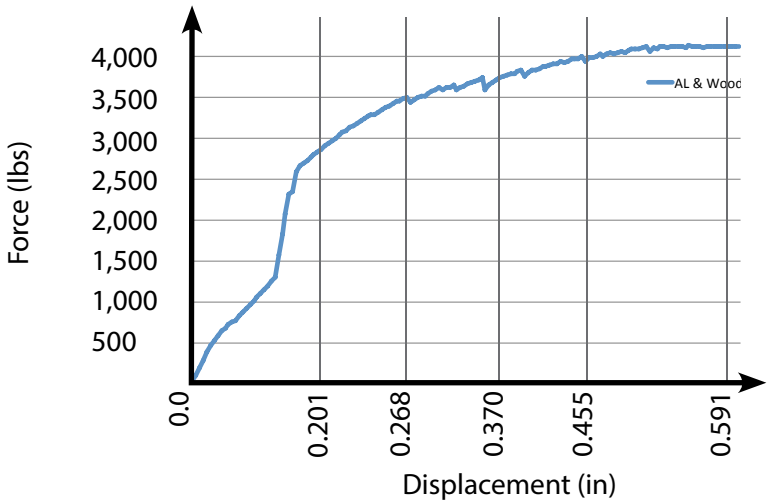

Figure 20. Compression test results for the aluminum tube with a wood insert.

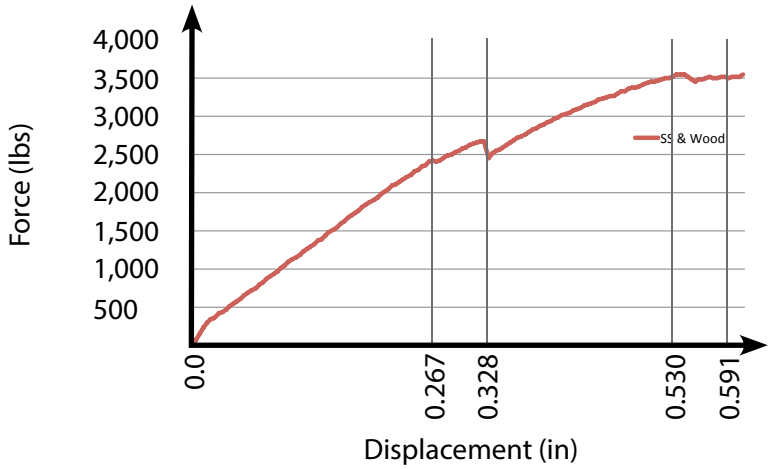

Figure 21. Compression test results for the stainless steel tube with a wood insert.

a longer and steadier elastic region. The aluminum dowel took more load, but that is expected because 6061-T6 aluminum has a higher yield stress than 304 stainless steel by 10 ksi and the aluminum tube had thicker walls than the steel tube, by double. These dowels provided enough elastic stiffness and inelastic energy absorption to be considered used as reliable dowels that hold together critical connections in a traditional timber frame. In both graphs there are dips in the data. At 0.37 inches of deflection for the aluminum and 0.328 inches for the steel, the wood peg inserts broke at the notched locations, as expected, creating plastic hinges in the two desired locations, similar to a the reduced beam section locations in a special steel moment frame. Both aluminum and steel sleeved dowels could be used for the full frame testing, but the less stiff steel sleeved dowel shall be used. Choosing the weakest one is conservative as it ensures the wood members will not be significantly damaged, and ductile behavior will be magnified. Steel has also been discovered to retain material strength under many cycles of loading far better than any other metal (Forrest, 1970), aluminum and copper in this research, making it a preferred building material when it is known the structure will endure fatiguing cyclic loading, also known as wind or earthquake forces. The reason for steel being tough and able to endure cyclic loading is that it is a ferrous metal, meaning it is composed of iron. Metals containing iron have a high fatigue limit, unlike aluminum or copper alloys. This is explained in a paper written solely about fatigue in metals from the Ministry of Technology in England (Forrest, 1970).

3 FRAME ANALYSIS

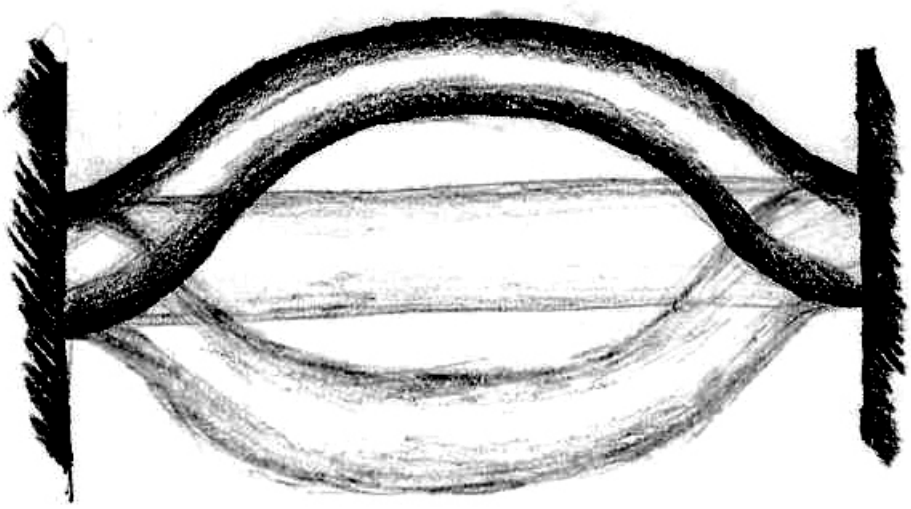

Figure 22. Dowel plastic hinging sketch.

3.1 Analysis

RISA-2D 2013, ETABS 2015, and MATLAB 2013 were used to analyze the eight foot by eight foot timber moment frame structure made up of PSL members that were 9 ½" deep by 5 ¼" wide for the beams and columns and 8" deep by 2 ¼" wide for the kick braces creating a frame with an aspect ratio of 1:1. All three programs

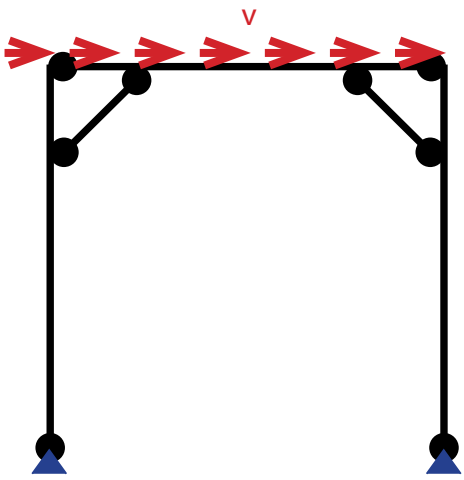

Figure 23. RISA model, lateral loads.

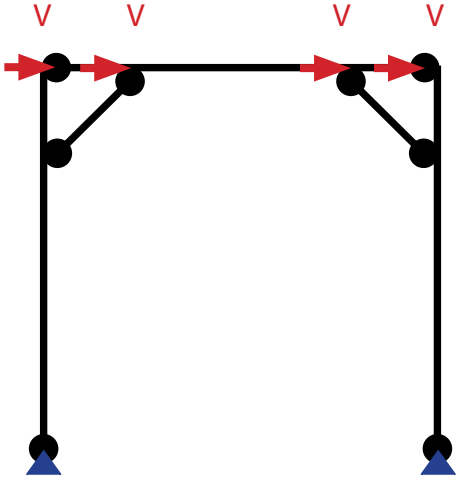

Figure 24. MATLAB model, lateral loads.

contributed to the understanding of force-flow and frame performance in the elastic and inelastic range when solely a lateral load was placed at the top of the frame, see Figures 23 and 24 for the lateral distributed load (v) diagram and the lateral point load (V) diagram. Load demands during an actual seismic event or gust of wind would include dead and live gravity loads distributed along the beam, however, these gravity loads counteract overturning forces, so they were conservatively left out during testing. Excluding gravity loads during testing is also common with wood shear wall testing. To accurately predict the test results gravity loads were excluded from the analysis, further testing may investigate gravity load effects. RISA-2D is a structural analysis software that was used to approximate the linear forces in all frame members. These demands would be checked against PSL material strength for adequacy. ETABS 2015, structural engineering software used for building analysis and design, was used to verify the linear RISA-2D results. MATLAB uses a high-performance language for technical computing. This software was used to code a script that approximated linear (elastic) and nonlinear (inelastic) behavior of the timber frame to be tested. The output in this report does not include gravity loads in order to more accurately predict frame force-versus-deflection test results. Supplementary hand and Microsoft Excel calculations were used to compare capacity-versus-demand stresses. The amount of lateral load applied to the beam for software analysis was based on the ultimate dowel force. For an eight foot by eight foot frame, a 180 pounds per foot (plf) lateral load resulted in a 4,100 pound axial force in the kick braces, see Figure 25, which was then compared to the dowel testing data in Table 4. Commercial structural analysis software allowed for quick approximate analysis. The custom non-linear MATLAB code model was created to accurately approximate the global frame behavior.

3.1.1 RISA linear

After applying a 180 pounds per foot (plf) load, or 1,400 pounds, laterally to the

beam the axial, shear, and moment demands were calculated. To account for friction in the connections, 1,500 pounds was used as the approximate ultimate force resisted by the frame. Paired with an expected lateral deflection an expected ultimate force versus displacement point called "hand calculated" was plotted on the test results graph.

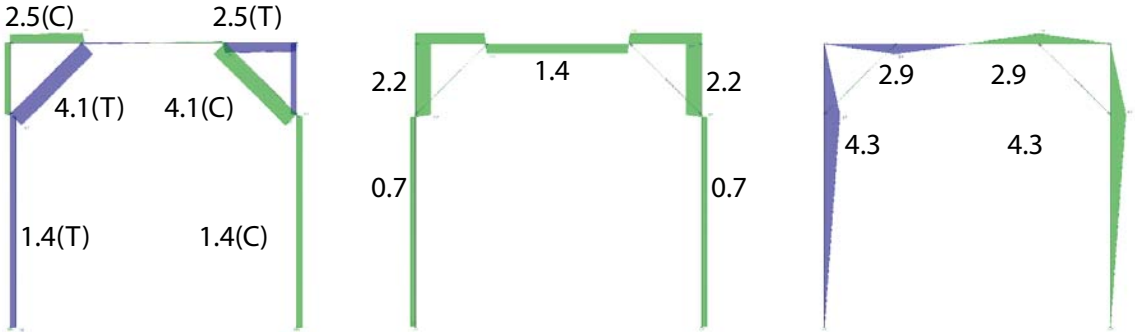

Axial (kips) Shear (kips) Moment (kip-ft)

Figure 25. RISA demand results due to a 180 plf distributed lateral testing load on the beam only.

3.1.2 ETABS Linear

A linear ETABS model was created to verify the RISA results. After the statics matched, a nonlinear pushover model was attempted. Two axial deformation controlled hinges were placed at the ends of each kick brace, representing the two dowels connecting a kick brace to a beam and column. Yield forces and displacements were input into the hinge properties that best represented the dowel testing data, however ETABS uses elastic perfectly plastic hinge force displacement behavior, which does not perfectly represent the dowel test data. Unfortunately ETABS overestimated the stiffness by roughly double, based on the MATLAB analysis and engineering intuition. ETABS was not an accurate tool to use for the pushover analysis of this wood frame with customized dowel stiffness. ETABS accurately calculates axial hinging in

a member with only one plastic hinge, such as a buckling reduced brace frame, and accurately calculates behavior when using steel or concrete, not wood. Because of this the nonlinear pushover curve produced by the MATLAB code, see Appendix F, was used to analyze the global full scale frame behavior.

3.1.3 Hand Calculations

The largest ultimate dowel force in Table 4 was used as the worst case load that would be applied to the connections of the frame. 4,100 pounds was used to design the mortise tenon connection. The base connection used was two three-eighths inch thick plates on either side of the columns and sill beam. The base connection bolts were one inch in diameter, the bolts had at least four and a half inches of wood surrounding it in all directions, with six inches of end grain distance, exceeding minimum bolt spacing and edge distances per the National Design Specifications for Wood Construction (AWC, 2014). The bolts also had one and a half inches of edge distance for the steel plates, exceeding the minimum edge distance given in Table J3.4 of the Steel Construction Manual (AISC, 2011). The failure modes of this conservative base connection design were not calculated. The sill beam and anchor rods were also all so oversized their failures were not a concern. This test was not meant to observe base connection effects. The focus of the project was the dowel behavior. Any base connection design can be engineered to look and perform as required. To ensure no members would be damaged under testing loads the short term load capacities of the frame members were compared to the results from the RISA analysis, in Figure 27, that included loads due to a lateral force only. The design value for compression parallel to grain, F'_{cll}, for the main member compression stress were heavily penalized by the stability factor, C_P, because during testing one column was unbraced along the week axis for the full 8'-0". Reference adjusted stress design values in Appendix B. The worst Case Column and Beam Shear stressed were considered.

V =2,200 lbs

$$F_v = \frac{3*(2{,}200\ \text{lbs})}{2*(35.5\ \text{in}^2)} = \boxed{93\ \text{psi} < 464\ \text{psi okay!}}$$

The worst case column compression stresses were considered. The column was determined to be the governing failure mode in axial compression because the column had the largest unbraced length in both the strong and weak axis. No other members would fail in compression before the column did.

P =1,400 lbs

$$F_{cll} = \frac{1{,}400\ \text{lbs}}{32.5\ \text{in}^2} = \boxed{43\ \text{psi} < 928\ \text{psi okay!}}$$

The worst case column and beam bending stresses were considered. The beam and column moment capacity were analyzed at the mortise pocket, the location of the highest bending demand and smallest moment of inertia (Ix). The smallest section modulus S top (St) was used to calculate the moment capacity.

Table 5. Mortise Pocket Section Properties.

Section Properties		
Area	32.53	in^2
Ix	275.55	in^4
Sb	66.24	in^3
St	51.60	in^3

$$f_b = \frac{M}{S_t} \Longrightarrow Mn = (f'_b)*S_t = (4243^{psi})*(51.6in^3) = 18{,}244\ \text{lb-ft}$$

$$\boxed{M = 4{,}300\ \text{lb-ft} < 18{,}244\ \text{lb-ft okay!}}$$

Two controlling failure modes were considered at the kick brace connection. By

inspection, the kick brace dowel tear out, Z'_T, due to a tension force was the controlling failure mode, see Figure 26. The net area including the countersink depression was used as the tear out plane. For the column or beam splitting failure mode the split would have to fail along the entire length of the member, depicted in Figure 27. It was assumed that this failure mode would not govern, the dowel would tear out of the kick brace controlled. From dowel testing it was known that the axial forced in the kick brace, which is controlled by the dowel stiffness, would reach almost 4,000 lbs.

Z'_T = (464 psi)*(1.25 in.*.5 in. + 2.25 in.*3 in.) = 3,422 lbs < 4,000 lbs. Oh No?

Technically this design check does not pass if the ultimate dowel load is over 3,422 lbs. However, the PSL wood is possibly stronger than the low shear stress limit of 290

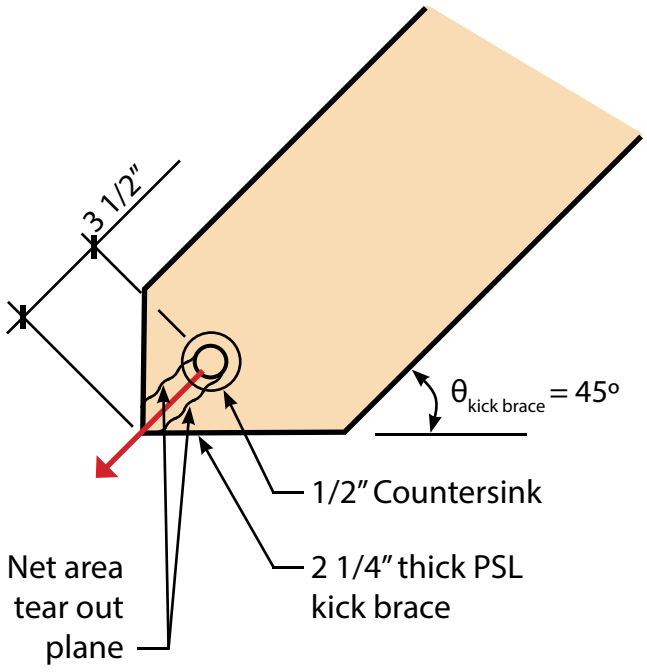

Figure 26. Kick brace dowel tear out.

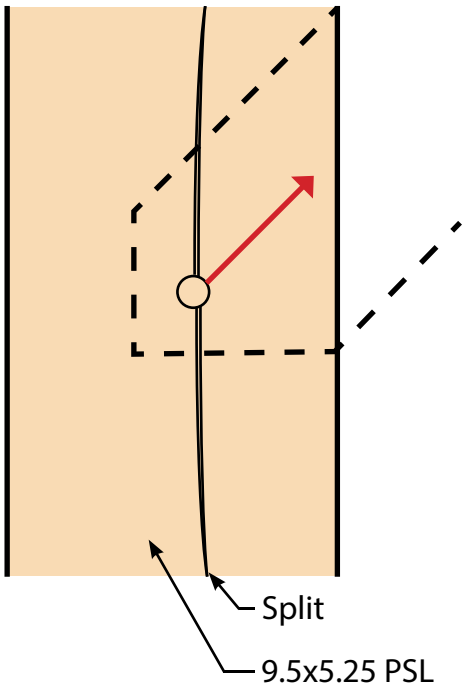

Figure 27. Dowel splitting column or beam.

psi given in the National Design Specifications for wood supplement manual based on PSL test results with a 95% confidence interval (Arwade, S.R., Clouston, P.L., Winans, R., 2010). The equation for tear out also incorporates a factor of safety of one half, and is based on a solid steel bolt, not the special dowel created in this project that is far less stiff than a standard steel bolt.

dowel bearing stress were considered. The 1 inch diameter shall be used as the bearing stress surface length, 1.25 inch shall be used as the bearing stress surface thickness (the thickness within the countersink). Knowing the dowel might reach a force of up to 4,000 lbs:

P =1,400 lbs

$$F_{cll} = \frac{4{,}000 \text{ lbs}}{(1 \text{ in})*(1.25 \text{ in})} =$$ 3,200 psi < 3,770 psi okay!

No further element failure checks were calculated.

Depicted to the right are regions detailed to accommodate all compressive stresses that occur during frame racking. No wood failure analysis needed to be done in these areas, signified by the red highlights, because these regions were protected by detailed gaps or including a layer of rigid foam insulation. These regions were protected for two reasons: to ensure that only the dowels are engaged during testing and to avoid crushing of the main members when the member is in compression. The necessity to include this feature may not be necessary, but for this test engaging the dowels is the most important part so all cautious procedures were taken to isolate the dowel yielding behavior.

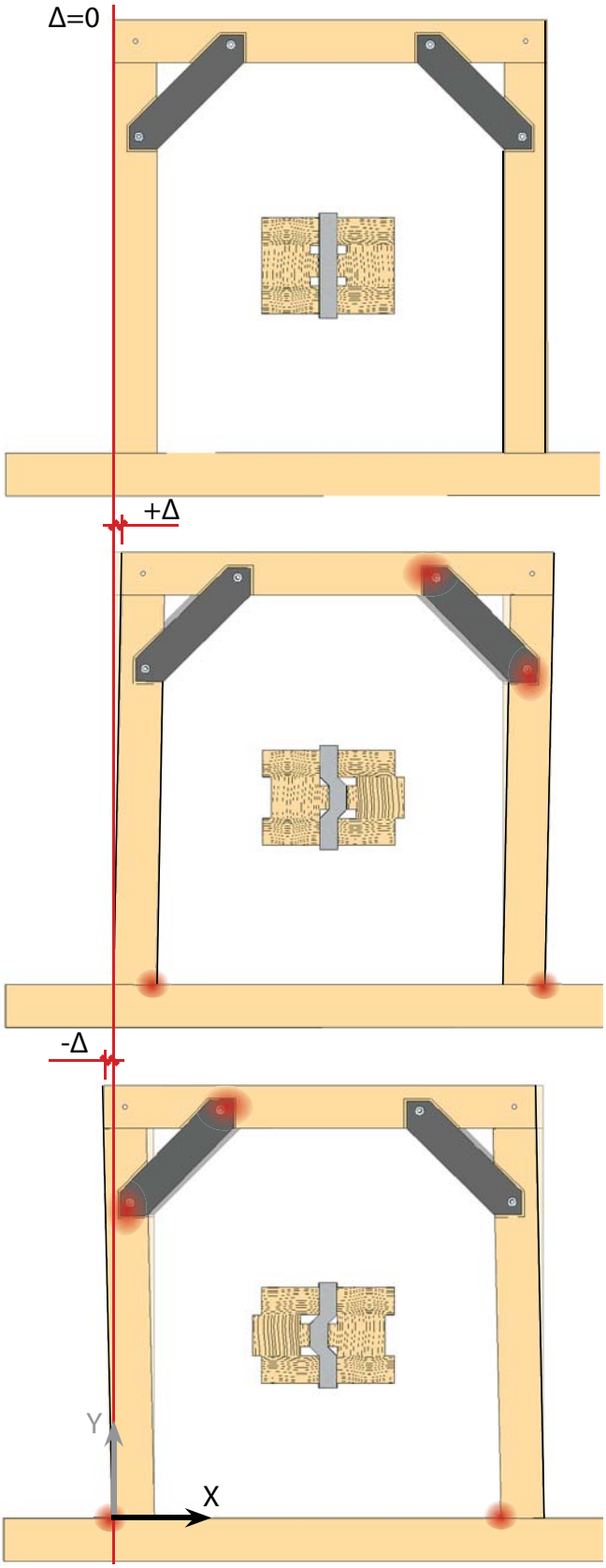

Figure 28. Regions subjected to compressive forces caused by frame racking.

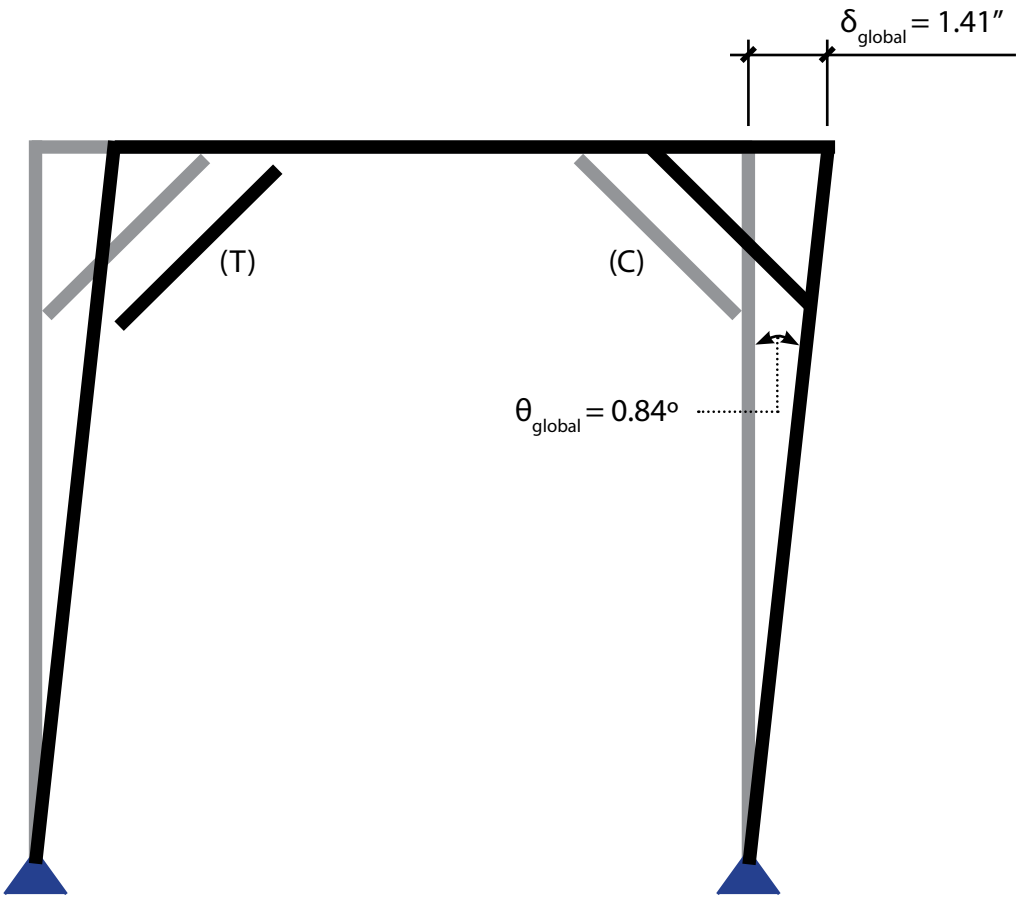

Figure 29. Approximate Lateral frame deflection based on 1/2 inch over-sized mortise pocket, see Appendix A.

Knowing the dowels could handle at least one half of an inch of deflection, and with a 1/2 inch gap for tolerance in the mortise pocket depth, the total amount the frame could deflect based on geometric translation tolerances was estimated as 1.41 inches. This is a deflection calculated using geometry, without contributions due to members deforming (bending, compressing, stretching) which means the frame will likely deflect more than 1.41 inches, but this is a reference point. This deflection is matched with the previously calculated 1,500 pounds lateral load from the 3.21 RISA linear analysis.

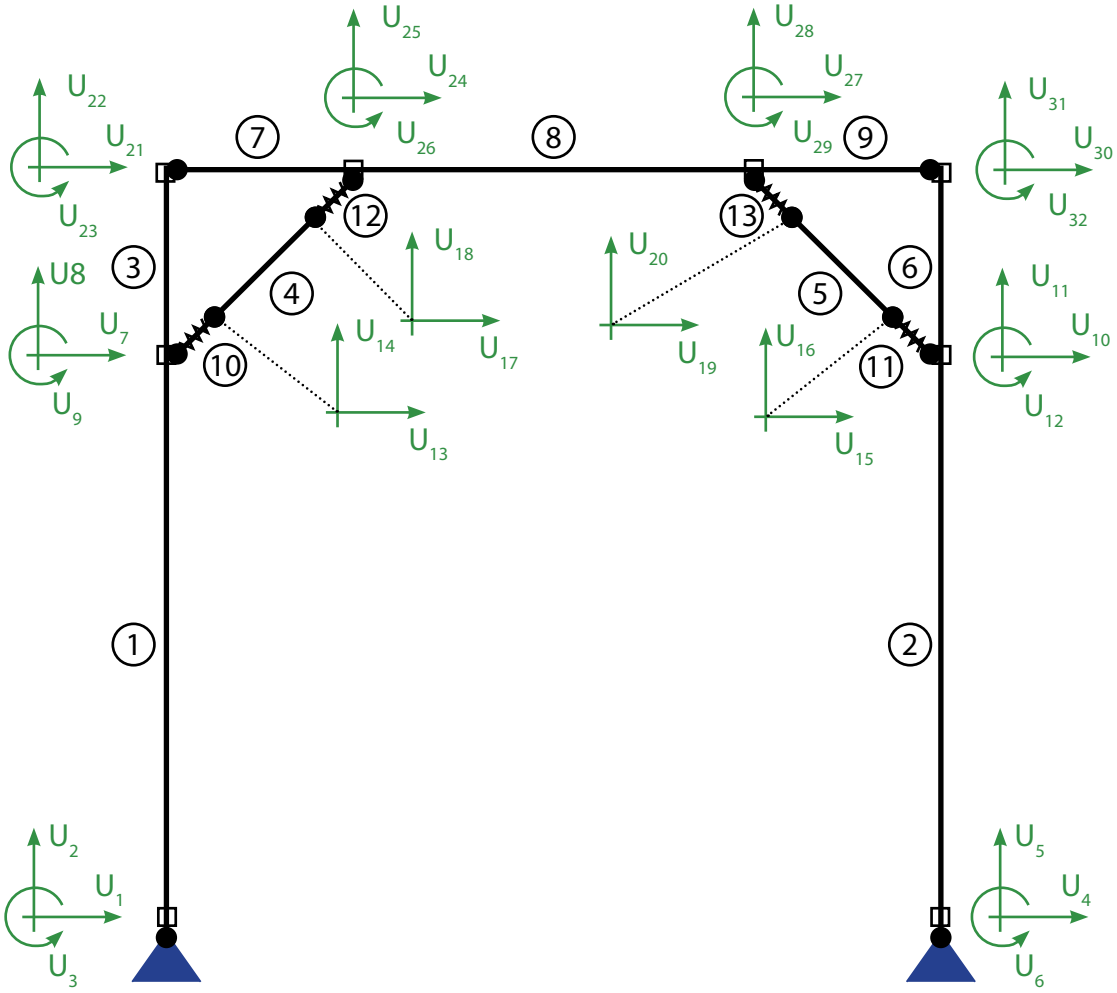

Figure 30. MATLAB Model with degrees of freedom.

3.1.4 MATLAB Linear

A linear MATLAB code was used to check RISA and ETABS. The code executed matrix analysis methods. The results matched the linear RISA and ETABS. MATLAB confirmation reassured that the maximum testing force would be roughly 1,500 pounds.

3.1.5 MATLAB Nonlinear

A nonlinear MATLAB code using Newton Raphson matrix structural analysis was

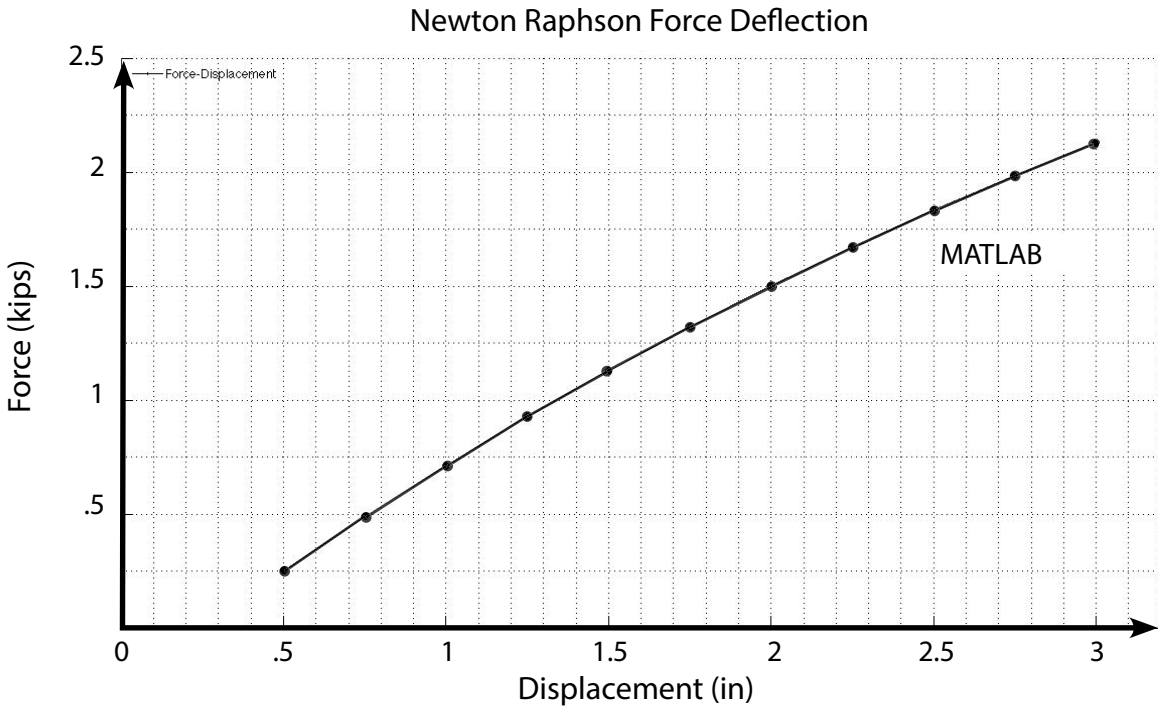

Figure 31. MATLAB output for approximate global lateral frame behavior.

created. Thirty-Two degrees of freedom (DOF) governed the frame model, see Figure 30. Microsoft Excel was used to implement the nonlinear dowel stiffness behavior into the MATLAB code by solving for an equation that best fit the data curve from the steel sleeve with wood peg insert dowel. This equation was used in the stiffness function of the code, changing the frame stiffness as the iterations slowly applied more lateral force to the beam. Thirty-Two degrees of freedom were needed to model this structure in MATLAB. Members one, two, five, six, seven, and nine were modeled as fixed-pinned elements. Member eight was modeled as a fixed-fixed member. Elements four and five were truss elements. Elements ten, eleven, twelve, and thirteen were also truss elements, however, their stiffness was based on the dowel testing data.

Figure 31 is a graph of the non-linear pushover curve output by the MATLAB script. The frame analyzed was the same as the one to be tested: an eight foot by eight foot post-beam frame with kick braces in the top two corners. The best fit curve representing experimental data from the dowel testing was:

$$Fx = -48.95 \cdot x^5 + 86.49 \cdot x^4 - 35.19 \cdot x^3 - 19.54 \cdot x^2 + 19.01 \cdot x - 0.06 \quad \text{(Equation 1)}$$

Equation 1 is an approximate equation for the force versus displacement curve from a dowel compression test in bending. To solve for the stiffness at any point along the curve, the derivative of Fx, ∂Fx, with respect to the varying displacement (x) was taken to get the slope, also known as the stiffness:

$$\partial Fx = -244.77 \cdot x^4 + 345.97 \cdot x^3 - 105.56 \cdot x^2 - 39.07 \cdot x + 19.01 \quad \text{(Equation 2)}$$

Equation 2 is the equation for the stiffness at every point of deflection within the kick brace connections. Equation 6 was implemented into the MATLAB code customizing the overall frame stiffness, see Appendix F.

Figure 32. Dos Osos Timberworks shopyard.

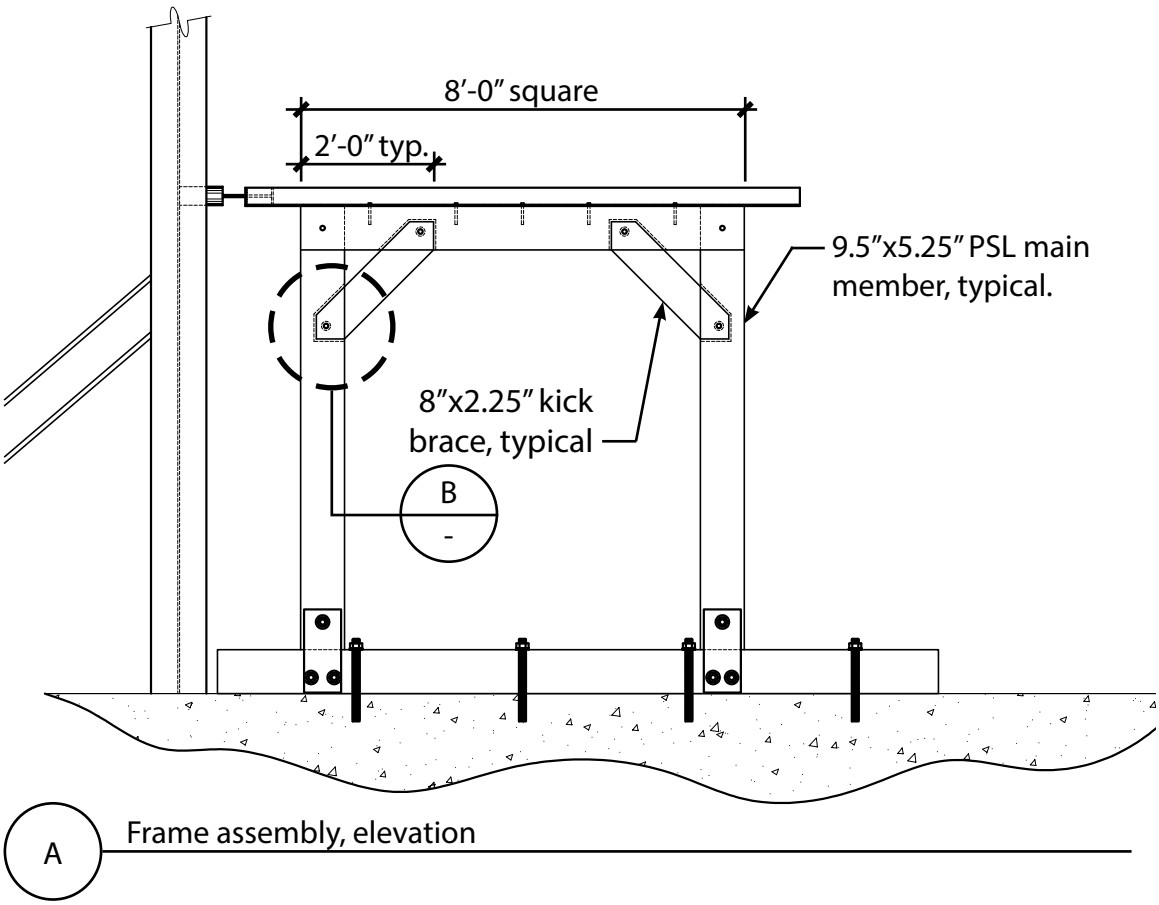

Figure 33. Frame erection and fabrication elevation.

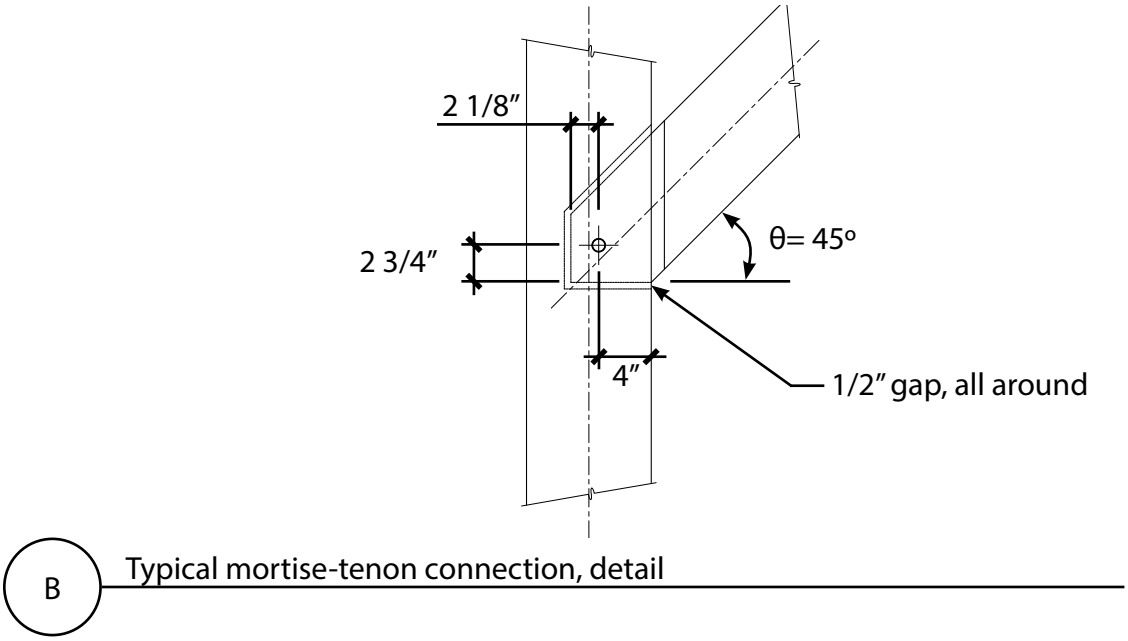

Figure 34. Mortise-tenon kick brace to main member connection

To conduct realistic and cyclic ductile dowel testing a full scale PSL timber frame was constructed. As stated in 3.2 Analysis, three 8'-0" members were used as the columns and beam, and one 13'-0" member was used as a sill beam. All members were 9.5 inches deep by 5.25 inches wide. The kick braces triangulated a right triangle with orthogonal legs measuring 2'-0" and were 8 inches deep and 2.25 inches wide. For the full frame configuration see Figure 33.

Carpentry tools included: an assortment of chisels and gauges, circular saws, a jig saw, a guided power drill, a chisel mortising machine, triangles, and many other common tools. Some pictures of the bigger tools used are depicted in Figures 35, 36, 37, and 38. Wood horses were used to mount the lumber into a working position. Bar-clamps were then used to hold the members in place as they were worked on with powerful tools.

Figure 35. Drill guide aided drilling accuracy.

Figure 36. Circular saw "big foot" was used for large cuts.

Figure 37. Chisel mortising machine carved out the mortise pocket.

Figure 38. Chisel and mallet carved and chipped off wood.

Figure 39. Complete pencil marks on all wood members before cutting.

The first step in wood framing fabrication is drawing every single cut with a pencil on every side of the member, shown in Figure 39. Surfaces were squared using triangles, a ninety degree ruler, and any other measuring or leveling instruments needed to draw the measurements from the drawings. The measurements for the pencil marks were taken such that the saw blade was meant to cut on the drawn line, taking into account the amount of wood the cutting tools will take out of the measurements.

When cutting the PSL wood there were some very hard parts in the wood that even the circular saw had to be forced through. When cutting parallel to grain it was slightly easier to direct the blade. Once the saw blade cut through the wood in either direction a very smooth surface was left. It also left a very nice looking pattern of

Figure 40. Parallel strands of lumber exposed by saw cut.

strands, and made it easier to see how these beams are made up of strands of wood glued together, see Figure 40. The texture of the PSL wood was very different than sawn cut lumber. The way PSLs are made results in the wood chipping off in bits as opposed to long strands of connected wood fibers, see Figure 41. The glue connecting all of the PSL strands causes the strands to come off in layers. This results in splintery chips of PSL.

Figure 41. PSL Wood chips.

When using power tools the wood smoked and even burned when the tool was used slowly. Cleaner cuts were achieved when the machines were used with authority and quickly driven into the material . The chisel mortising machine was clamped to the member and used to carve out the mortise pockets. Steps were created for the forty-five degree sloped portion of the mortise pocket. Once enough of the pocket had been carved out, a chisel and mallet was used to touch up the rest, shown in Figure 42.

After the mortise pockets were complete, the beam to column mortise tenon connections were fabricated. For the mortise end, two intermediate saw lines were cut then the middle chunk of wood was drilled out then cleaned up with a chisel. The tenon insert was more straight forward and could be done just by sawing off a small

Figure 42. Mortise pocket clean up.

rectangle on each side of the middle portion. Both the column mortise and the beam tenon had to be sanded and carved in order to make them fit smoothly, and even then they were very hard to mallet together.

Although the cuts made using large electric saws were fairly accurate, all of the mortise and tenon pieces needed some extra care in order for them to smoothly fit together. To do this, a power sander and a hand chisel were used to smooth and

Figure 43. Hand carving PSL resulted in splinters.

flatten surfaces. When using the chisel, the PSL behaved very differently compared to carving natural wood. Some parts of the wood were extremely hard, but the wood mainly just pealed off in flat plane layers as opposed to carved fiber chunks. This made controlling how much wood was taken off with the chisel very difficult. Figure 43

Figure 44. Frame members partially assembled.

Figure 45. Kick brace installation check

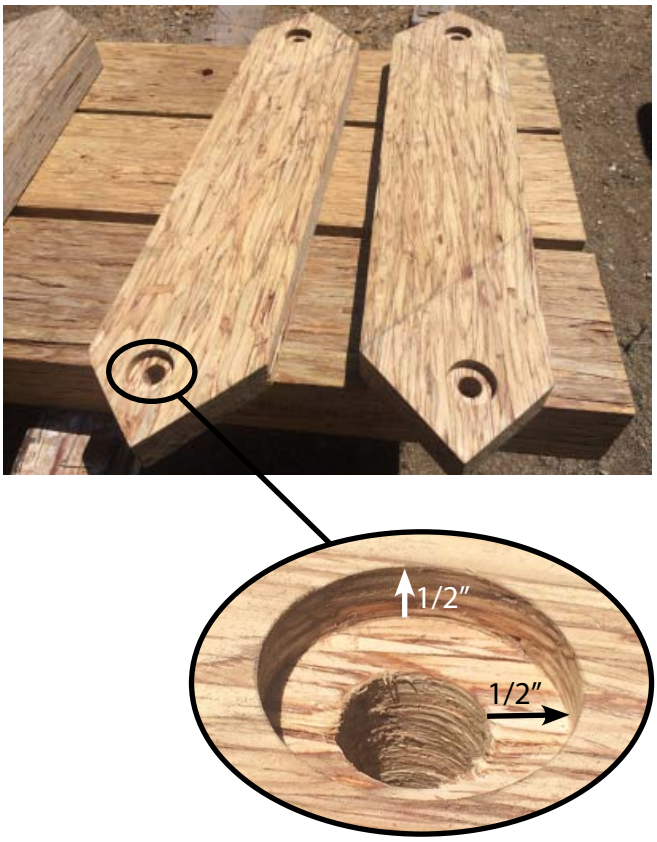

Figure 46. Kick brace countersink

shows some carves that peel off the PSL wood similar to natural sawn-cut wood, but this was a rare occurrence.

Before drilling holes in the kick braces, they were inserted into their respective mortise pocket. Figure 45 shows a triangle being used to make sure the kick braces were in the correct orientation before marking the dowel hole. The entire frame was then assembled, while making sure the main members were orthogonal and the kick braces were in the right locations, with a one-half inch gap surrounding the insert inside of the mortise pocket, see Figure 44. Once everything was aligned, the hole locations on the kick braces were marked. They were then taken out and a one inch diameter hole was drilled almost an eighth of an inch off the mark in the direction that would pull the connection together tightly when the dowel was hammered in. Then, a two inch diameter, one-half inch deep counter sink was drilled on top of the previously


Figure 47. Steel sleeved dowel with notches at kick brace countersink locations.

drilled hole, see Figure 46. This countersink provided the one-half inch gap seen in the test housing configuration during dowel testing. The countersink provides the space required to allow deformation to occur at the desired reduced section locations on the dowel, creating plastic hinges. To fabricate the dowels the steel pipes were cut with a pipe cutter to six inch lengths. The notches were then filed on the wood peg and then the wood insert was sanded down until it slid inside of the metal tube. The pipe cutter indented the ends which forced unwanted sanding down of the wood inserts in order to slide them in easily. The last two inches of the eight inch wood dowel were sanded into a coned taper before encasing it in the steel sleeve, see Figure 47. The pointed tip of the cone was used as a guide when hammering in the dowels, locating the holes of the mortise-tenon connection. There where no notches on the wood inserts for the dowels labeled B to C (Beam to Column). That connection was meant to deform less than the kick brace connection dowels (labeled K.B.).

While hammering the connections together, Bar-clamps were used to hold members in place. To minimize damage from local stressed applied by the Bar-clamps small wood pieces were used to distribute the load and prevent marks from being left on the surface of the main members, shown in Figure 48.

A basic rigid foam insulation was used in the mortise pockets and below the

Figure 48. The frame laying down clamped to wood horses.

column. The rigid insulation was used to protect areas of compression during lateral racking as well as clearly make visible deformations from translational and rotational deformations at the connections. Once all the members were set in place with a rubber mallet, the holes were inspected to make sure everything was aligned. The dowels were then placed into their respective holes and hammered in. Because the holes were purposefully miss aligned, some dowels had to be hit in so hard that it

Figure 49. Rigid foam prevented contributions from and damage to the main members.

actually buckled the tops of the steel sleeve encasements. Fortunately three-eighths of an inch of extra dowel was left on the end. Once all of the dowels were in, the base plates were bolted to each side of the column and the sill beam, creating a true pin connection.

The frame was complete. A crane lifted the frame into a vertical position. To secure the frame to the ground, the testing facility had one and one-half inch diameter holes spaced three feet apart on a square grid embedded into the concrete floor slab. Threaded rods were placed in the holes and the sill beam was bolted down. The crane was left attached to the frame as a safety precaution but the chains were loosened to have some slack.

Figure 50. The frame lifted by an overhead crane from a horizontal assembly position into the vertical testing location.

5 FRAME TEST ONE

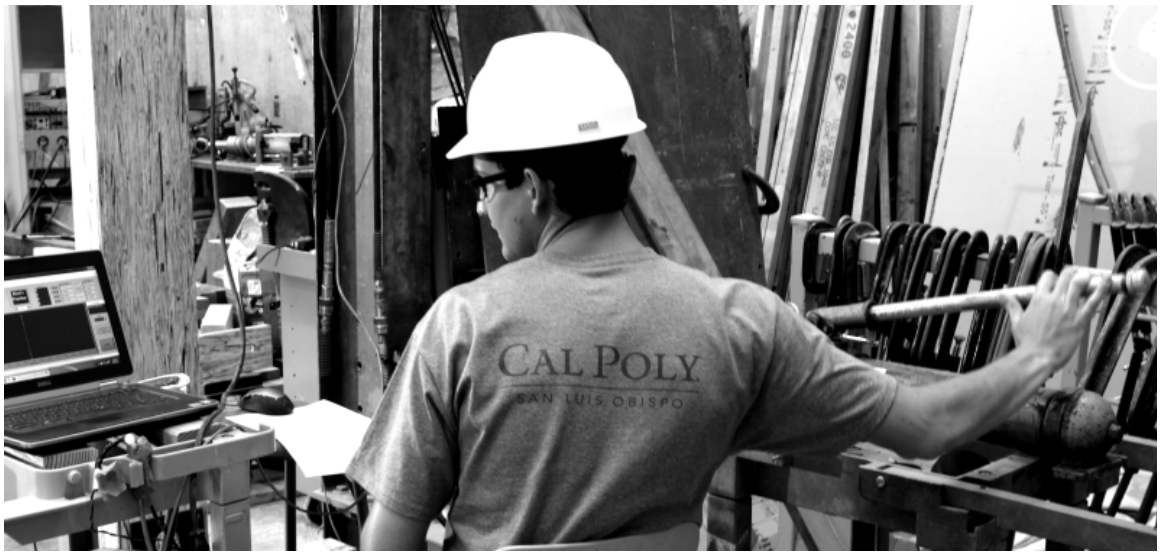

Figure 51. Computer and ram set up in the High Bay Testing Facility, Cal Poly, CA.

The full scale test was used to test the strength, behavior, ductility, and performance of a traditional timber frame with modified dowels. Success would be the frame endured "a minimum of 20 records" or cycles of loading (Ayoub, A., Ibarra L., Krawinkler H., Medina R., Parisi F., 2001). 20 cycles is considered the amount of records needed to "obtain stable statistical estimates" (Ayoub, A., Ibarra L., Krawinkler H., Medina R., Parisi F., 2001). The frame is expected to be elastic and linear up to seven hundred pounds. The toughness of PSLs will also be tested. If the engineered material is stiff enough, the members will be undamaged and reusable once testing has commenced. A load cell (B.L.H.) was attached to the ram to output a force in pounds, and a deflection measuring device called a pull string potentiometer produced by Houston Scientific International Inc was attached from the wide flange to an attachment on the channel and would output deflection in inches. The measuring devices were hard-wired to the computer. The forks on a fork lift were used to prevent out of plane movement would occur, see Figure 53. The column closest to the support frame was left unbraced, but that side of the frame was firmly attached

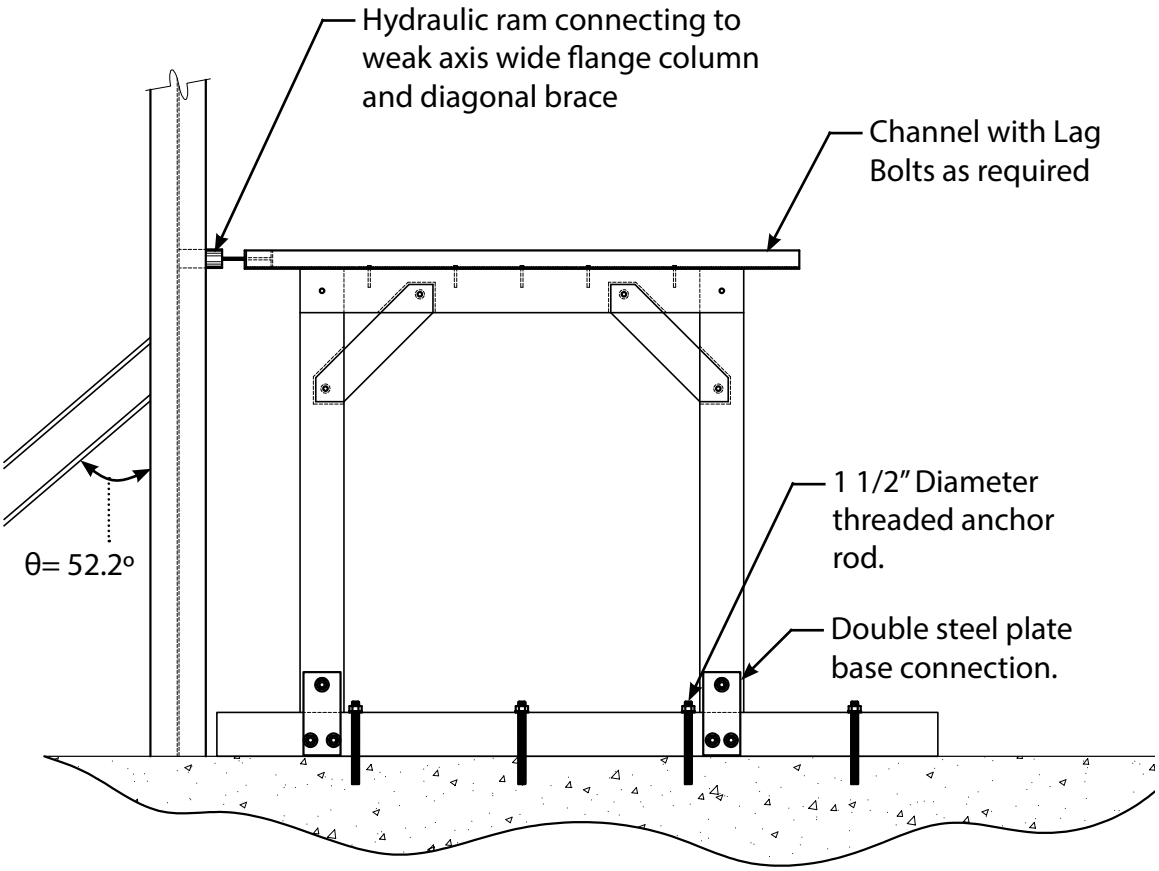

Figure 52. Frame testing configuration.

to the support frame. A channel was lag bolted into the top of the beam to simulate a diaphragm being nailed into the beam, distributing the lateral shear load. A make shift connection attached the channel to the ram. For the complete test configuration see Figures 52 and 53. Figures 54 and 55 show strain gauges that were placed on two of the main steel wide flange supports. This was a precaution taken to make sure the supporting steel structure was not taking away energy from the global frame test system by deflecting the opposite direction as the frame, which was pushing back on the support frame as the ram loaded the system. Ideally the support would be perfectly rigid. A four-ton hydraulic ram was attached to the existing steel support frame in the High Bay Lab made up of large wide flange members. This ram was then

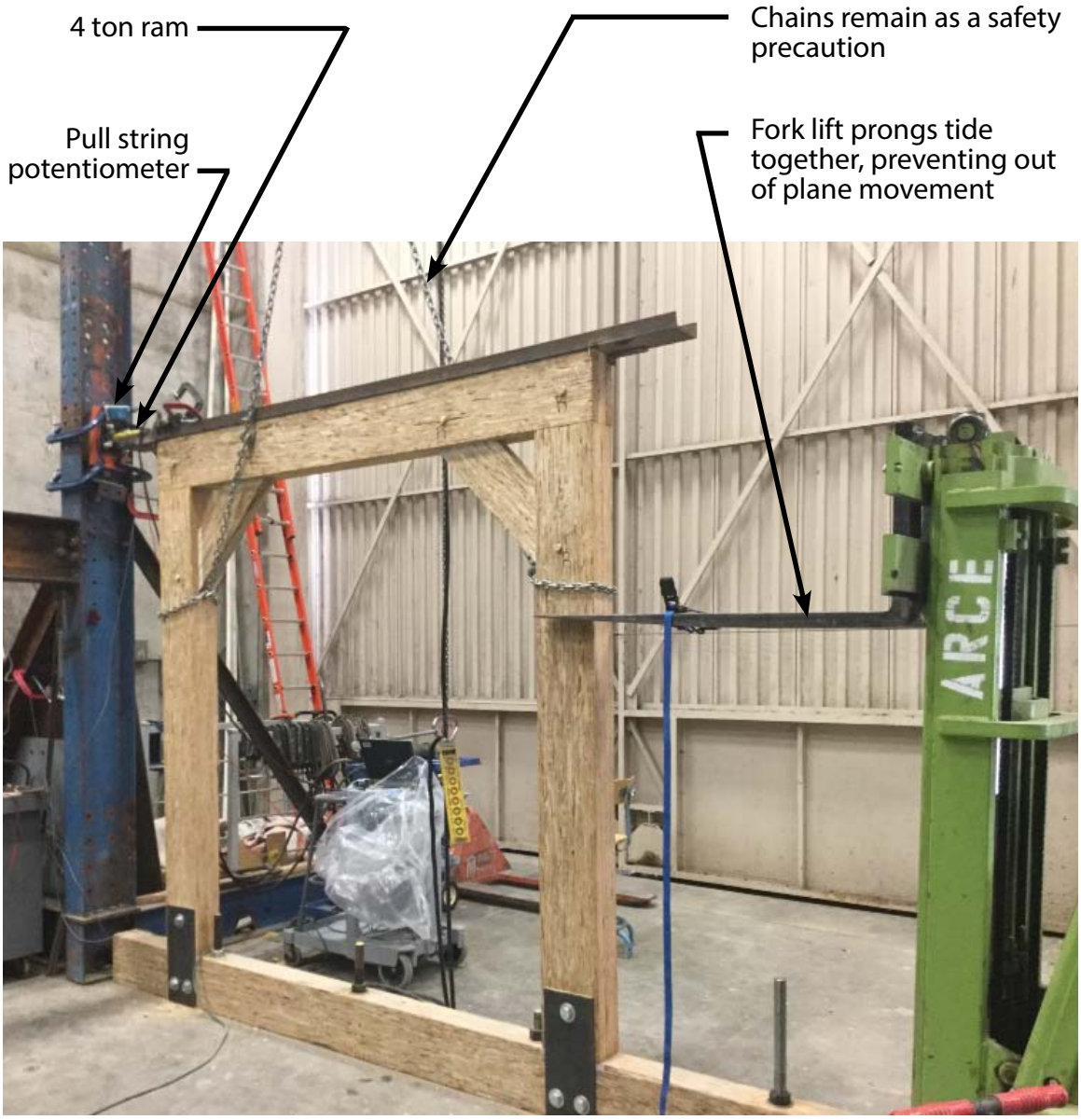

Figure 53. Frame testing arrangement set up in the High-Bay lab at Cal Poly.

attached to a channel that was lag bolted into the top of the beam. The hydraulic ram was manually pumped.

Figure 54. Strain gauge 2 located on the axially loaded wide flange.

Strain gauge 2 was used to measure strains in the diagonal brace that is in plane with the frame in order to estimate deflections during testing. The resistance from the frame could result in tensile and compressive axial strains in the angled member. The horizontal component of the calculated deflection shall be subtracted from the measured frame displacement, see Appendix D.

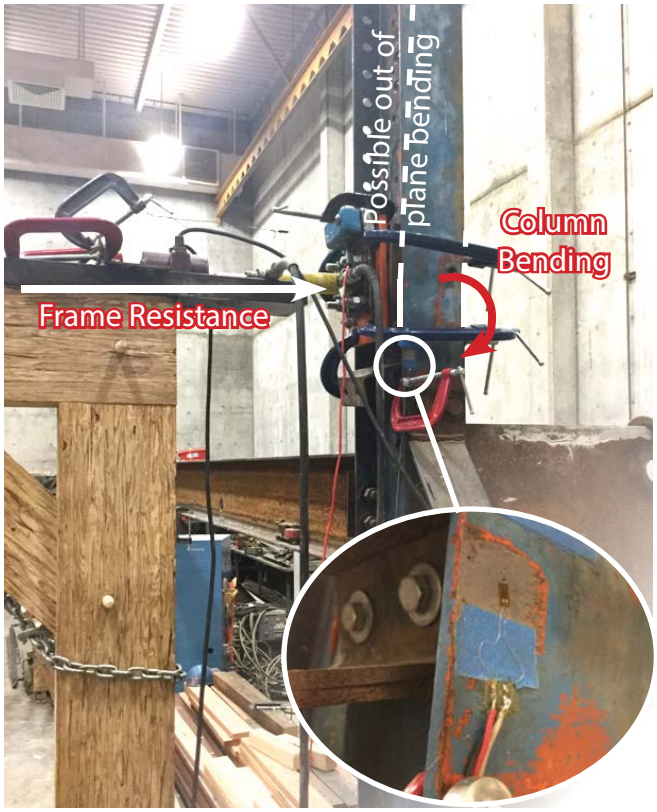

Figure 55. Strain gauge 1 located on the support column in out of plane bending.

Strain gauge 1 was used to measure any bending strains in the wide flange that was being forced to bend about its weak axis by the attached ram. These strains shall be calculated into deflections. Horizontal deflections in this member were subtracted from the measured frame displacement, see Appendix D.

CUREE testing protocol for woodframe structures (Ayoub, A., Ibarra L., Krawinkler H., Medina R., Parisi F., 2001) suggest test loading patterns based on load or deformation that simulate earthquake cycles, see Appendix C. This testing will not push on the frame dynamically as rapidly an actual earthquake would, but the suggested CUREE test pattern will produce a quality hysteresis that tests the cyclic and relatively dynamic capabilities of the frame to resist lateral forces. Δ, also shown as Δ_a,

Table 6. ASCE 7-10 allowable inelastic drift.

	Frame Height h_x	8.0 feet
	Δ_a=.02*h_x	1.92 inches
	Story Drift	0.02
Δ_a - allowable story drift based on story height per ASCE 7-10		
	Δ_a	1.92

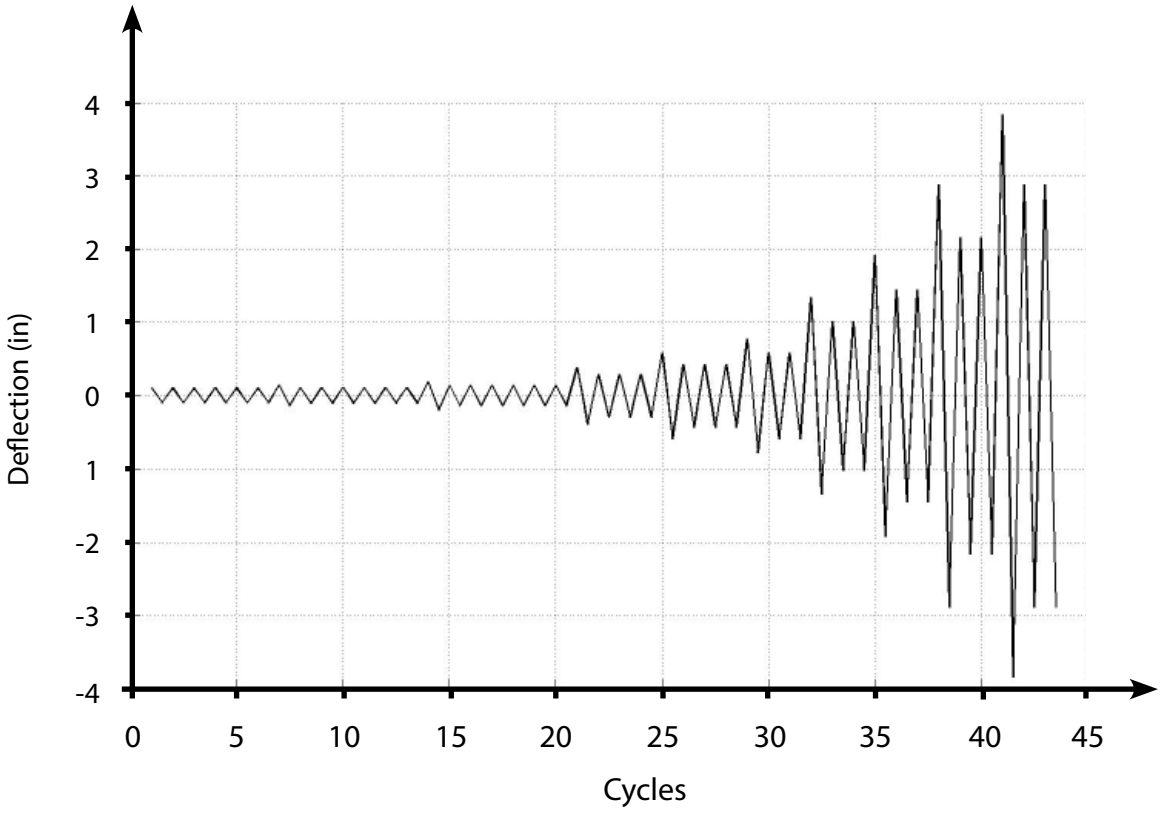

Figure 56. The deformation pattern that will be used for testing.

is the expected maximum drift per ASCE 7-10. This is the ultimate allowable inelastic deflection, meaning the lateral system's force-versus-deflection output should be nonlinear at this deflection, calculated to be just under two inches for an eight foot tall frame per Table 12.12-1 in ASCE 7-10.

5.1 Testing Procedure

The hydraulic press was pumped by hand until the computer read the first data point per the CUREE testing protocol, see Figure 56. Once cycle is a full deflection from right to left then back to zero. Testing may commence once the largest deflection the ram can extend to (three inches in either direction) is reached, or if the frame fails. The force and displacement data points were recorded every three seconds to extract a hysteresis.

5.2 Testing Observations

The frame rebounded elastically until roughly 600 lbs. As the deflections got larger, some rotations occurred at the beam to column connection, and the kick braces either pulled out or were pushed in, made noticeable by the chalk lines drawn on the wood, see Figure 58, Figure 61, and Figure 63. Rotations at the bottom of the columns was also observed, see Figure 60. No crushing at these connections occurred in the main wood members. Movement and rotations were also made very visible by the crushing of the rigid foam insulation. Primarily the foam at the kick brace connections appeared crushed and flattened as the brace translated and rotated due to the dowels deforming. Dowel deformation was the most important sign of proper frame behavior. It could be seen from the outside, shown in Figure 62, that the dowels had been bent and crushed inside of the mortise-tenon connection. The dowels endured sixty cycles - one cycle being a translation of the beam both left and right - of

increasing load without seriously damaging the main timber members.

When the frame racked there were medium-loud cracking noises. It was discovered that these noises came from both the wood dowel inserts breaking, and friction between the surfaces of the mortise-tenon connections as they rubbed against each other during rotations caused by lateral deflections. The connections were so tight tightly fit that it took roughly fifty pounds incrementally to overcome the static friction. When the static friction was eventually overcome, a -medium loud snap or crack sound echoed.

The base connection was fully intact and showed no signs of weakening. The bottom surface of the column rested parallel to the surface of the sill and rigid foam.

Figure 57. Hydraulic ram connected the channel attached to the beam.

Figure 58. Chalk drawn on the kick braces made connection translations and rotations visible.

5.3 Test Results

The maximum load put into the frame was 2,000 pounds with a total lateral deflection of just 2.9 inches. The frame endured over sixty cycles of lateral loading. No members showed signs of damage, they could be reused for another test. The following images show details of the frame while it was pushed out to 1.92 inches of lateral deflection, Δ_a.

5.4 Hysteresis Discussion

Figure 59. Two examples of rigid foam inserts crushing making deformations visible at 1.92 in. of lateral deflection.

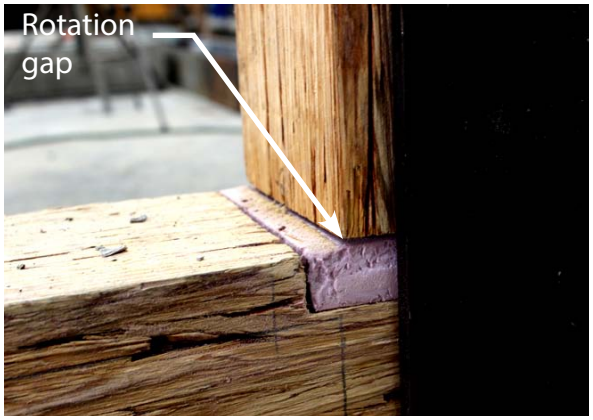

Figure 60. Column base, frame at 1.92" of lateral deflection.

Figure 61. Beam to column connection rotation, frame at 1.92 inches of lateral deflection.

Figure 62. Dowel visibly deforming when the frame was at Δ_a, 1.92 inches of lateral deflection.

Figure 63. Tenon pull out when the frame was at Δ_a, 1.92 inches of lateral deflection.

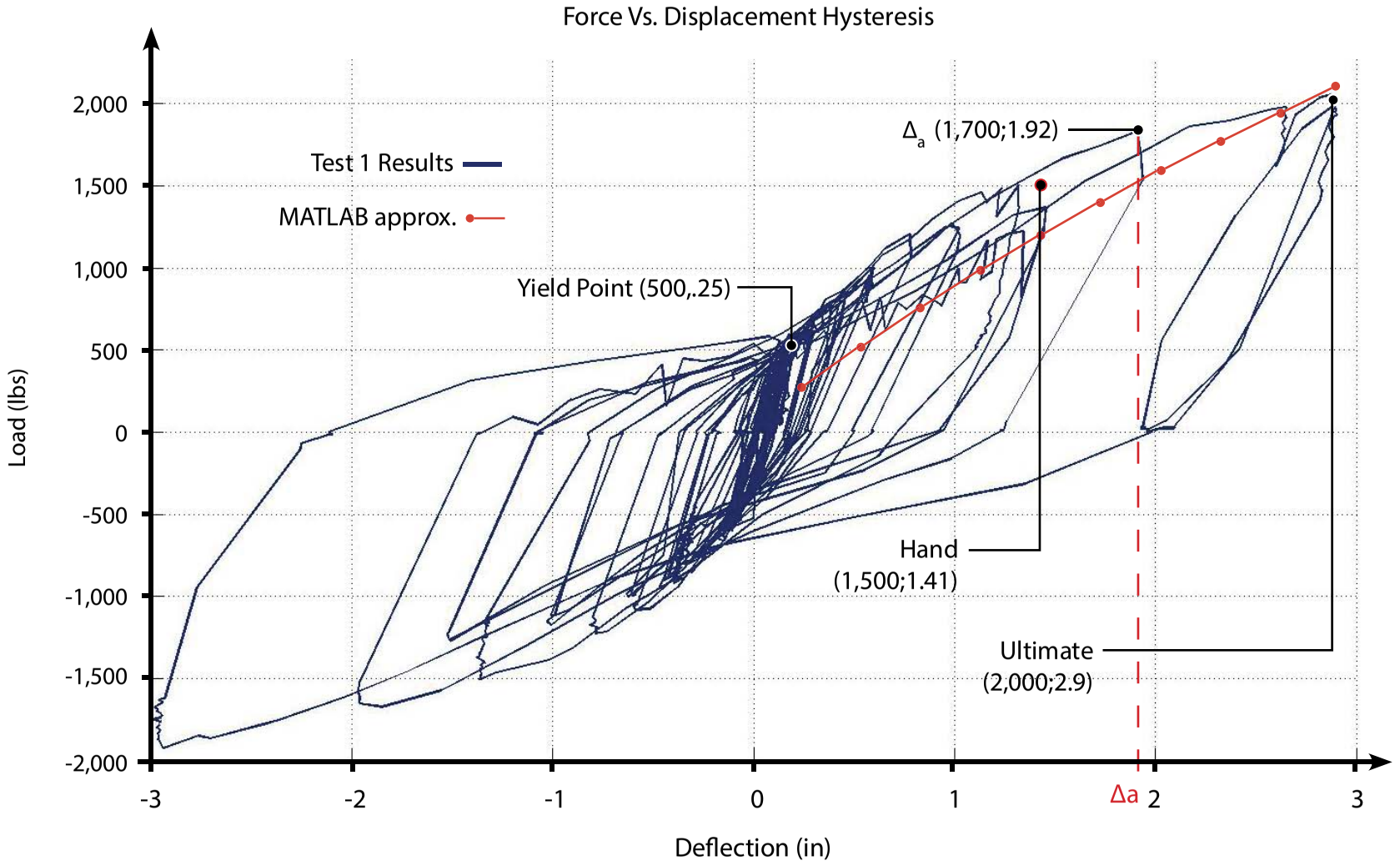

Figure 64. Test 1 results, Δ_a is the allowable story drift point from ASCE 7-10.

(Reference Figure 64) The frame remained elastic until 500 pounds (62.5 plf) with a lateral deflection of 1/2 inch. The inelastic range went up to 2,000 pounds (250 plf) with 3 inches of deflection. The beginning of the hysteresis has a reasonable shape for a frame which has deformation controlled by steel: a straight elastic portion followed by a yield point then a yield plateau of decreasing stiffness shown by a slightly arched shallow angled line. As the load in the frame is reversed, the hysteresis curve is headed to the zero force line at an angle very similar to the initial elastic stiffness slope. However, unlike most steel controlled systems, the force vs. displacement line loses stiffness, shown by a decrease in slope, as the frame force approaches zero. The change in slope and creates a pinch in the overall shape of the graph, similar to the shape of a concrete moment frame hysteresis. The reason concrete moment frame hysteresis graphs have this pinching is because concrete cracks as it bends, changing the moment of inertia of the section. A similar thing is happening to the dowel in the wood frame. As the dowels are pushed in, the hinge locations of the dowel deform the cross-sectional shape, changing the cross-sectional geometry of the region of the dowel that controls lateral movement of the entire frame. With a reduced beam section in steel moment frame the cross-sectional geometry of is able to stay fairly constant when it plastically deforms because the web and flanges are designed to be compact, creating a graph that looks like the outline of an American football, at a forty-five degree angle. In this research the plastic hinge region of the dowel deforms into a smaller cross-sectional shape, meaning the hysteresis pinches decreasing energy absorption. Figure 65, Figure 66, and Figure 67 are depicting the dowel deforming within the mortise tenon connection during four phases of increasing deformation. This diagram helps explain why there is pinching in the hysteresis. As the dowel deforms the controlling hinge section gets pinched,

weakening cross-sectional properties. Because of this, the dowel loses its stiffness much sooner than, say, a steel wide flange that can maintain a more constant cross section throughout the nonlinear range.

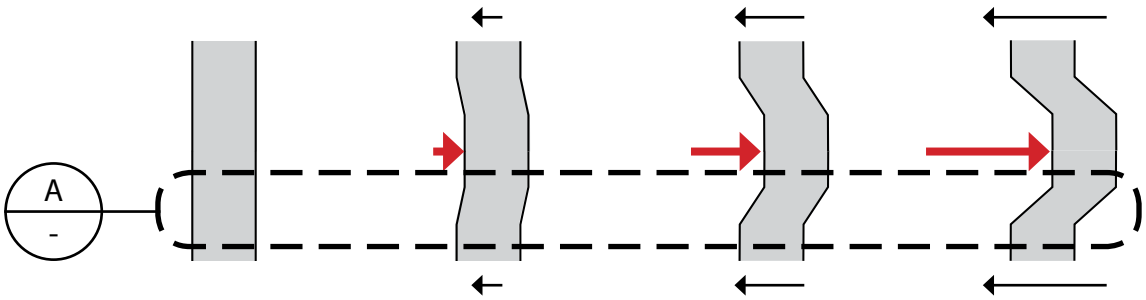

Figure 65. Progressive dowel pinching

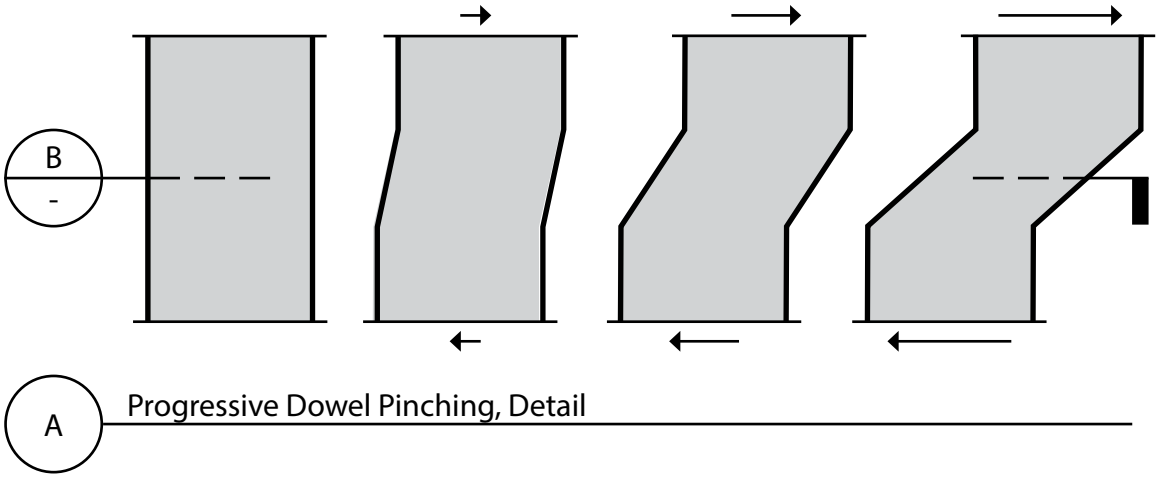

Figure 66. Progressive dowel pinching, detail.

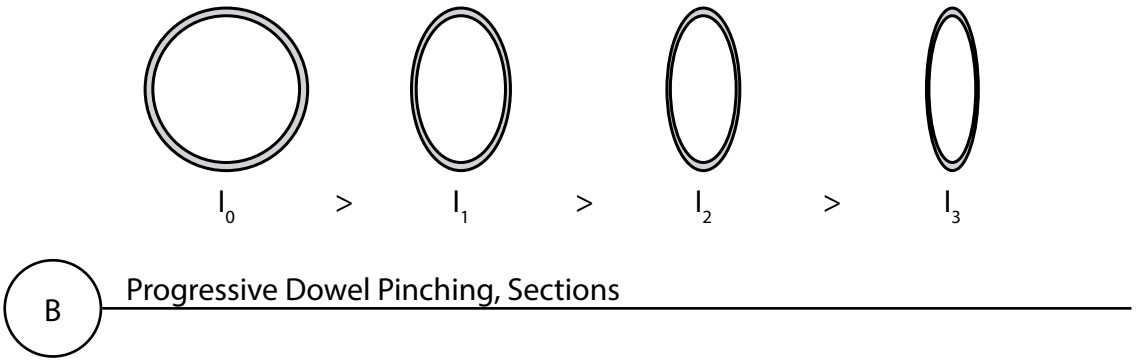

Figure 67. Progressive dowel pinching, section.

The benefits of using stainless steel sleeved dowels is demonstrated by the continuous force-versus-displacement cycle of a traditional timber frame with the dowels tested in this research, see Figure 66. The number of cycles the frame was able to endure was 62, far more than the number of cycles that a timber frame with wholly wood dowels could be expected to endure. A structural engineer seeking to implement a traditional timber frame into a building would not want to be responsible for the liabilities that come with relying on a wholly wood dowel to stabilize a lateral system enduring multiple cycles. Technically, a wood frame with all wood dowels would not have zero capacity after a dowel breaks. As the load reverses there would realistically be some capacity that remains, however the amount of stiffness would be small and unpredictable. The design capacity of a wood dowel that has ruptured should not be relied on and should be taken as zero. The material properties of every wood dowel in a frame differ from each other because wood is a natural material that humans cannot control. Because of this and because of how little strength wood retains after the fibers have been strained passed their yield or rupture point, only half of an inelastic cycle can reliably dissipate energy. Essentially, when wholly wood dowels are used in a traditional timber frame, the dowels cannot be relied on to endure multiple cycles of lateral loading, so the usable portion of the hysteresis is half of a cycle. When the stainless steel sleeve is introduced into the connection, the benefits of steel's ability to endure multiple cycles are seen in the hysteresis in Figure 64. The frame can sway—also known as rack—back and forth, dissipating energy from not just one but numerous complete cycles imposed by seismic events. Building types that require ductile lateral systems are non-essential facilities, which make up a large amount of buildings. Non-essential facilities are all building other than those that are intended to remain operational in the event of extreme environmental loading from flood, wind, snow, or earthquakes (ASCE, 2010). Non-essential structures

are engineered for permanent damage or inelastic performance design in order to dissipate energy and dampen lateral building movement. The timber frame tested in this project would not be used for essential facilities—buildings that are designed to remain elastic during maximum considered earthquakes. For buildings that do not need to be immediately occupied—non-essential facilities—after a seismic event, multiple cycles of nonlinear frame behavior is desired because energy dissipation is the performance goal.

5.5 Test One Summary

The ultimate total force imposed on to the frame was 2,000 pounds. The maximum lateral deflection was three inches. The frame did satisfy the code requirements of being in the non-linear range at a drift two percent, Δ_a. The support frame deflected 0.036 inches, see Appendix D. Based on the support frame deflection measurements all measured test frame deflection values should technically be reduced by 98.8% of the recorded frame deflection, however, this reduction was considered negligible.

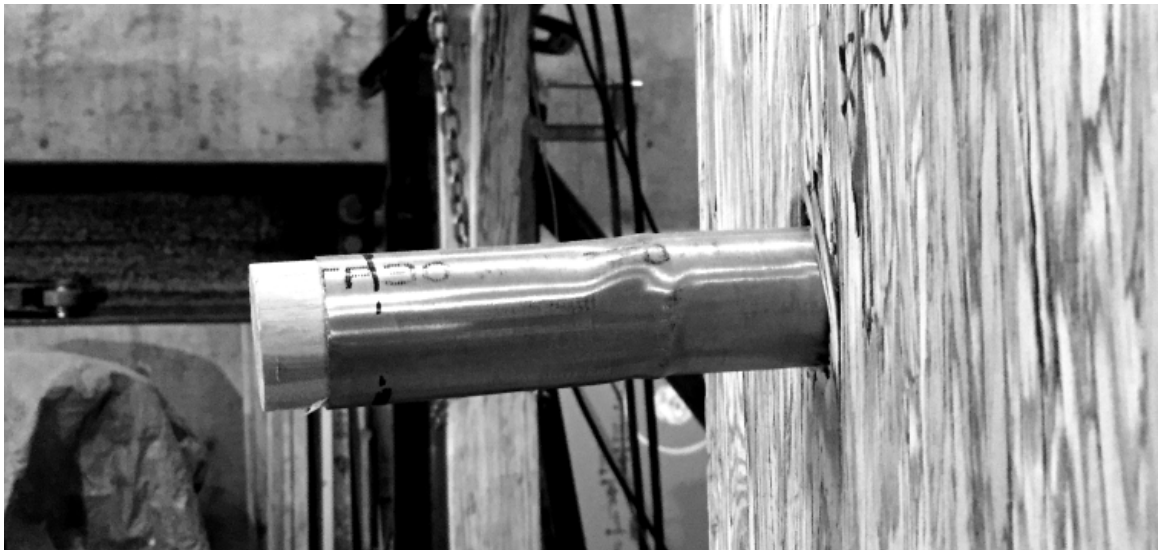

Figure 68. Dowel extraction.

After a successful first test reusability was investigated. This project promotes sustainable building by using wood and that is further reflected within concept of reusability. PSLs were used because of their inherent strengths, but also because of how hard and stiff the material is. The surfaces of many natural woods can be dented with a fingernail, not PSLs. In earlier dowel tests it was seen that the PSL dowel test housing was undamaged around the dowel holes. Just like the dowel test housing, after the first full frame testing had commenced the old damaged dowels were replaced them with new ones, all frame members were reused. The main members were examined and looked adequate to still be used to support a building under gravity loads and even during the another earthquake. To confirm this, a second test was conducted. To replace the dowels the frame was brought back to its zero displacement point. In reality, bringing an entire building back to its zero point may have to be done to replace the dowels, but this is feasible and something that is already done today when repairing damaged structures after an event.

To extract the dowels the first thing done was to hit on them with a hammer from the tapered side that was sticking out the furthest. This pushed the dowel and

Figure 69. Wood peg insert coring during extraction using a power drill.

the sleeve out about an inch or more. The column to beam connection dowels were the most difficult to remove, they were also the most challenging to install. A drill was needed to core out the inner wood peg at the beam to column connections, see Figure 69. A three-quarter inch diameter drill bit was used to leave a small amount of tolerance inside of the steel sleeve. This turned out to be interesting as it gave a unique perspective to observe what happened to the dowel during testing, see Figure 70. Even though the steel tubes were slightly damaged by the drilling process, it was possible to see if hinging occurred on the steel sleeve at the kick brace countersink locations; hinging was visible in all dowels. The face of the main members were hit lightly by the drill bit. Once the drill was put down and all that was left was a steel pipe it was difficult to grab the pipe and pull it out. One end of the pipe was hammered down, then used as a cap, shown in Figure 71. A skinnier long pipe slid through the other side, up to the cap and a hammer pounded the sleeve out. Once the holes were completely empty, the condition of the PSL wood was investigated, see Figure 72 and

Figure 70. Stainless steel sleeve condition post wood peg insert removal.

Figure 73. Besides some fraying on the outside surface, the innards of the hole were not significantly damaged.

It was not difficult to remove the damaged dowels, the extraction process only took about two hours. Pushing the frame back to its zero deflection point made dowel extraction easier than if the frame remained in a deflected shape. If this frame were applied to a real structural framing system, the building may need to be pushed back to its zero point in order to simplify the process of extracting the dowels. Bringing the frame back to zero deflection is also a safety issue. The dowels are stabilizing

Figure 71. A hammered down end of a stainless steel sleeve during extraction

Figure 72. Hole inspection post dowel removal.

the frame in its deformed shape, preventing collapse. If they are removed while the frame is in a racked position the entire system could collapse. The frame tested in this project would be able to be re-centered and used again since only the dowels were damaged. Theoretically they could be reused multiple times to resist the handful of seismic events or extreme gusts of wind a building has potential to experience in its life time. Figure 73 shows the conditions of the dowels post testing. Figure 73a is the best example of the dowel deforming exactly as intended. The pipe looked untouched except for the permanently deformed regions that developed at the two

Figure 73a. Top Left KB Dowel

Figure 73b. Top Right KB Dowel

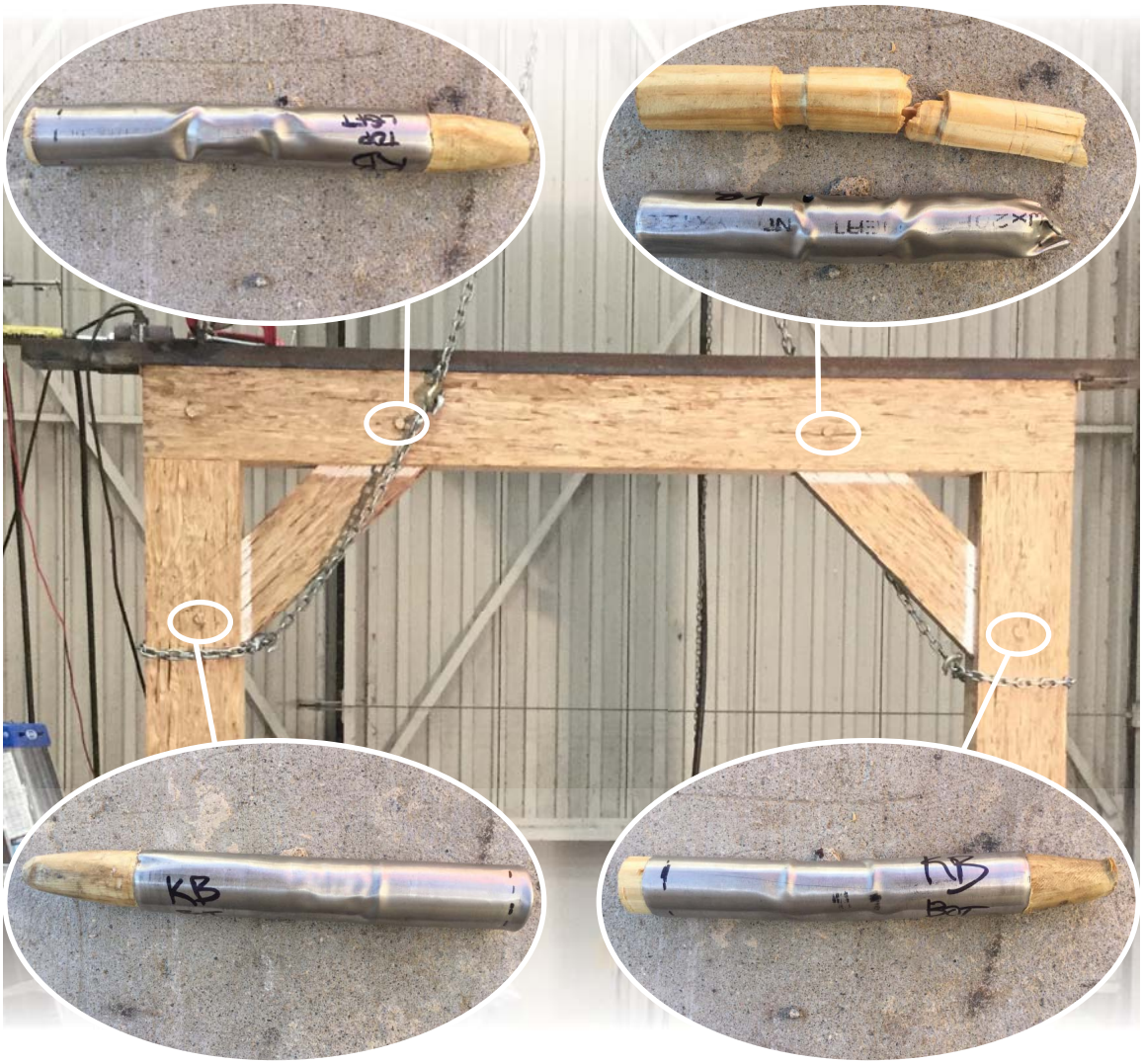

Figure 73c.Bottom Left KB Dowel

Figure 73d. Bottom Right KB Dowel

Figure 73. State of dowels post extraction after the first test.

hinge locations designed to take the damage. This dowel was the most damaged. Figure 73b shows a dowel that was difficult to remove. Figure 73c depicts a dowel that remained intact and was easy to push out during extraction. It shows some minor crushing and damage in the hinge locations, but this dowel was not fully engaged. Figure 73d is another good example of how a dowel was intended to deform.

Figure 74 demonstrates the minimal amount of damage that occurred to the dowel holes. There is some fraying on the outside surfaces, and this damage happened during the dowel removal process, and a little also when drilling the holes

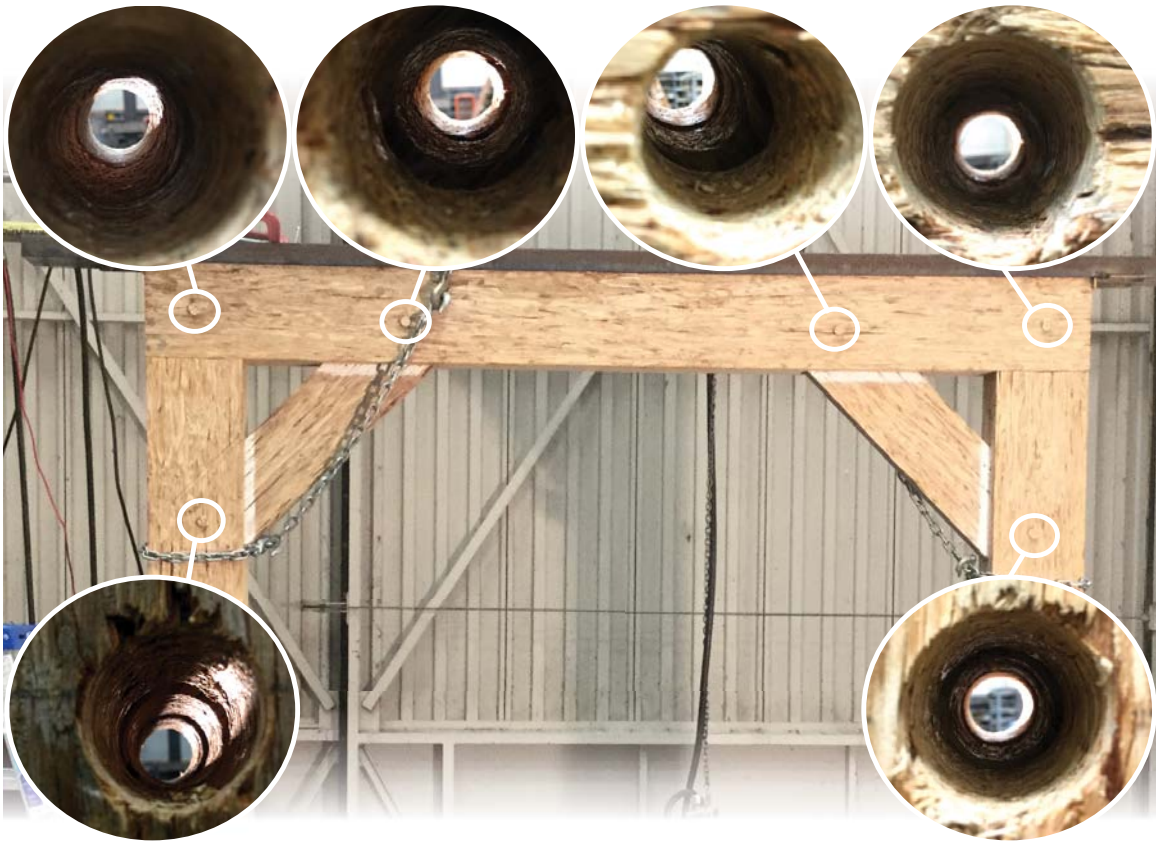

Figure 74. Hole Inspections post dowel removal after first test.

initially. Aside from that the insides do not show major signs of being overstressed. There are some shiny parts on the wood hole walls, and this means some wood fibers were permanently deformed, but not enough to prevent effective strength for reusability.

Replacement dowels were inserted with more ease than the first time. They still had to be tapped in with a mallet, but the ease in inserting hinted at more flexibility

in the second test. The reinstallation took two hours. Once the frame was repaired a second test began.

The second test was almost identical to the first. The frame racked, some snapping noises from movement were heard, as well as cracking of the wood peg dowel inserts. The main members were not damaged.

The test 2 data is very similar to the test 1 data set, however it is ten percent weaker. The frame was able to retain ninety percent of its strength reaching a

Figure 75. Dowel Removal after second test.

maximum load of 1,800 pounds after the process of replacing the dowels. This reduction in strength came from loosening of the mortise-tenon joints from the first test, and some very slight deformation of the dowel holes from the first test. No further testing was conducted.

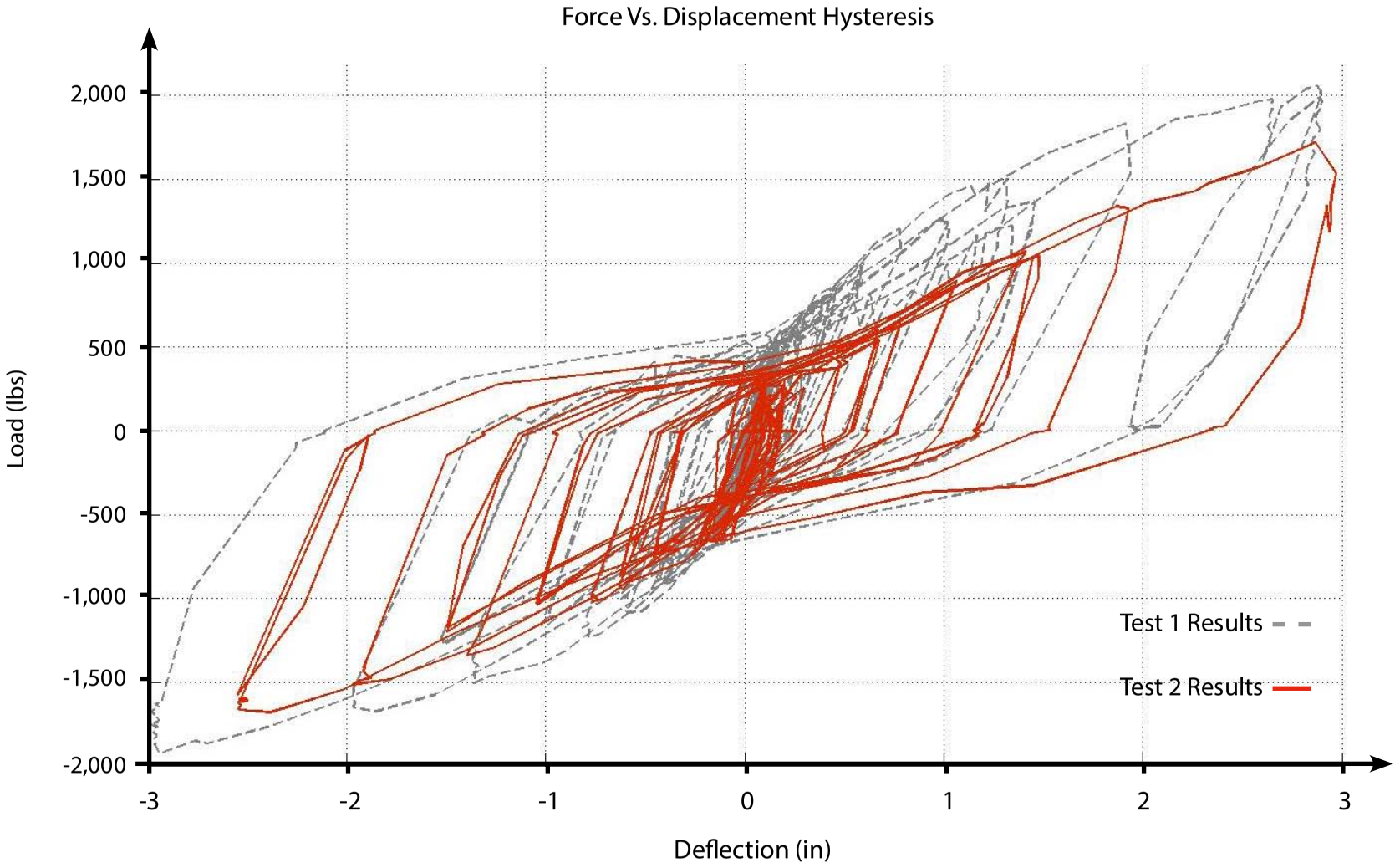

Figure 76. Test 2 results imposed on top of Test 1 results.

7 CONCLUSION

The lateral strength of the frame tested was 2,000 pounds, or 250 pounds per linear foot (plf) for an eight foot frame with an aspect ratio of one to one. 250 plf is enough resisted force to prove that timber frames can be used as a lateral force resisting system, however, the frame is not yet highly competitive from purely a strength standpoint compared to other current lateral systems. If the frame were implemented into building codes a factor of safety would likely be required, reducing the maximum expected capacity of the frame, however, 2,000 pounds of resisted lateral load is enough to demonstrate that timber frames with mortise-tenon-dowel connections are very capable of being reliable lateral systems for residential and small commercial buildings in seismic categories A through C. The frame also retained ninety percent of its strength during the second test exemplifying the frame's ability to retain stiffness after almost 200 cycles, making reusability of heavy timber framing a possibility.

Ductile frame behavior was evident during testing, and is displayed in the hysteresis graphs, Figure 64 and Figure 76. Ductility in a lateral resisting element is directly related to the amount of energy dissipated. The amount of energy dissipated is calculated by quantifying the area inside of a hysteresis loop, per frame cycle. Between the number of trial and recorded test cycles, the frame was racked back and forth over sixty times during both the first and second full scale tests. No PSL members were considerably damaged after two tests. The only significant failures occurred in the isolated stainless steel sleeved dowels, condoning energy-dissipating frame racking. Two last features that can make the frame tested in this thesis desirable to structural engineers are a hinging sequence and an increase in the R value for timber frames (ASCE 7-10). Not all of the dowels engaged at once during both tests. Not engaging all hinges at the same time gives opportunity to create a hinging sequence, creating redundancy in the lateral element. With six dowels per frame, a

complete structure using the structural system in this research would be loaded with redundancies. With properly designed mortise-tenon connections the hinges could be timed to yield in a particular sequence. In ASCE 7-10, Table 12.2-1 the R value given for a wood frame when used as the lateral system is 1.5. Ductile wood frame behavior shown in this research suggests an increase in the R value for timber frames when ductile dowels are introduced to the connections. Design base shears for a building using the wood frame tested in this research should not be penalized by the low ductility factor of 1.5. Knowing the structural system is very ductile and redundant gives designers more confidence in the reliability of the building's performance during a seismic event. Normally, structures that rely on wood as a source of ductility are considered to be very brittle, so they are penalized by a low R value, which increases the design base shear, increasing lateral demands, which translates to economical and architectural costs. Increasing the R value for timber frames would help the wood industry; designers would consider using a wood structural system more often.

A post-beam timber frame with kick braces attached by a mortise-tenon-dowel connection is capable of complying with current minimum design loads per the American Society for Civil Engineers (ASCE 7-10) . With modern analysis and design theories, timber frames can be improved in order to be used as reliable lateral force resisting structural elements, as well as satisfy architectural demands. The advantages of using the metal tube dowels are that they can act as a "fuse" and not only can be replaced, but also allow all other members to remain elastic and reusable after an event. Not only that, but because of metal material properties, dowel deformation inhibits ductile frame action which is important for owners and occupants of a building. Both the MATLAB code created in this project and the structural analysis of wood frames paper from Stanford (Brungraber, 1985) demonstrates the ability to accurately analyze a wood frame's behavior and ability to resist seismic demands. The

benefits discussed regarding wood being cheaper, more sustainable, and aesthetically warm and pleasing emphasize the need to construct buildings with wood. Wood working and hands on construction/fabrication can be an art form. Some of the oldest and most inspiring structures in the world use timber as a building material. With new energy demands, the building industry is being pushed to shift back towards wood construction and adapt timber structural designs to modern structural and architectural demands.

7.1 Recommendations

Further testing can explore stiffer dowels, which will push the boundaries of wood to the material's limits. More parameters to test are: thicker walled steel sleeves, different dowel hinge designs (see Appendix G), different frame dimensions and aspect ratios, tighter-fit mortise tenon connections with no rigid insulation, a smaller or no countersink on the kick braces, adding kick braces to the bottom corners, and alternate base connections. Each of these parameters should be tested individually, altered one at a time in order to clearly demonstrate their affects on the overall frame behavior. Further testing shall aim to make a traditional timber frame with steel sleeved dowels highly competitive amongst modern framing systems. In the future, it is also recommended to cut the tube steel encasement with a saw so that the ends do not bend inward, that way there is a tighter fit between the steel tube walls and the surface of the wood peg insert.

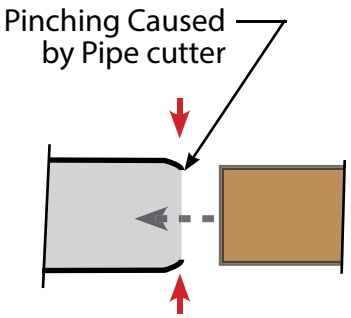

Figure 77. Steel pipe pinching.

REFERENCES

American Institute of Steel Construction (AISC), (2011). Steel Construction Manual 14th Edition. United States of America.

American Wood Council (AWC), (2013). Heavy Timber Construction. American Forest & Paper Association, Washington, DC.

American Wood Council (AWC), (2014, September). National Design Specification (NDS) for Wood Construction 2015 Edition. Leesburg, VA.

American Wood Council (AWC), (2014, September). National Design Specification (NDS) Design Values for Wood Construction 2015 Edition. Leesburg, VA.

Arwade, S.R., Clouston, P.L., Winans, R. (2010, April). Journal of Engineering Mechanics. Variability of the Compressive Strength of Parallel Strand Lumber. PDF. Retrieved March 25, 2017.

ASTM A312 / A312M-00c, (2001). Standard Specification for Seamless and Welded Austenitic Stainless Steel Pipes, ASTM International, West Conshohocken, PA, from www.astm.org. Retrieved December 12, 2016.

ASTM B241 / B241M-16, (2016). Standard Specification for Aluminum and Aluminum-Alloy Seamless Pipe and Seamless Extruded Tube, ASTM International, West Conshohocken, PA, from www.astm.org. Retrieved December 12, 2016.

ASTM B88-16, (2016). Standard Specification for Seamless Copper Water Tube, ASTM International, West Conshohocken, PA, from www.astm.org. Retrieved December 12, 2016.

ASTM E119-16a, (2016). Standard Test Methods for Fire Tests of Building Construction and Materials, ASTM International, West Conshohocken, PA, from www.astm.org. Retrieved December 6, 2016.

Ayoub, A., Ibarra L., Krawinkler H., Medina R., Parisi F. (2001). CUREE Development if a Testing Protocol for Woodframe Structures. Stanford University. Retrieved August 5, 2016, from curee.org

Brungraber, R. L. (1985). Traditional timber joinery: A modern analysis.

Busta, H., & Honesty, L. (2013). How It's Made: Laminated Veneer Lumber and Parallel Strand Lumber. Retrieved April 14, 2016, from architectmagazine.com/

technology/products/how-its-made-laminated-veneer-lumber-and-parallel-strand-lumber_o

Chappell, S. (1998). A timber framer's workshop: Joinery, design & construction of traditional timber frames. Brownfield, Me.: Fox Maple Press.

Croft, W., Henry, P., Woolson, E., Darcey, B., Olson, M. (May, 1984). US Health Care Reform, Seasonal Arsenic Exposure From Burning Chromium-Copper-Arsenate-Treated Wood. Retrieved December 11, 2016 from jamanetwork.com.

Forrest, P.G. (1970). Fatigue of Metals. Head of Queen's Award to Industry Branch, Ministry of Technology: Pergamon Press

Global Structures. (2010). History of timber frame Global Structures. Retrieved April 14, 2016, from globalstructuresltd.com/en/pages/timber-frame/history-of-timber-frame.php

Hugh Lofting Timber Framing (HLTF), (2013). Carriage Shed Project. Retrieved September 24th, 2016, from hughloftingtimberframe.com

Kuzman, M. K., & Kutnar, A. (2014). Contemporary Slovenian timber architecture for sustainability. Cham: Springer.

Lab, R. H. (2007, April). Think Formwork – Reduce Costs. Retrieved April 17, 2016, from http://www.structuremag.org/?p=6141

Lisa, Ana (2013, March). Shigeru Ban's Gorgeous Nine Bridges Golf Club House is Inspired by Traditional Bamboo Cushions. Retrieved December 6, 2016. inhabitat.com/shigeru-bans-gorgeous-golf-club-house-is-inspired-by-traditional-bamboo-cushions/

Myers, Rob. (2016, March). A Timber-Frame House for a Cold Climate. Retrieved December 6, 2016, from http://www.greenbuildingadvisor.com

Ritter, M., Skog, K., Bergman, R. (2011, December). Retrieved December 6, 2016, from United Stated Department of Agriculture, Forest Service. fpl.fs.fed.us/documnts/fplgtr/fpl_gtr206.pdf

Roy, R. L. (2004). Timber framing for the rest of us. Gabriola Island, BC: New Society.

SlideShare, Steel-vs-concrete and timber. (2015, April). Retrieved April 18, 2016, from slideshare.net/sheerazgulabro/aquib-steelvsconcrete

Schmidt, R. J. (2006, May). TTimber Pegs R U C T U R Eimber Pegs® - STRUCTURE magazine. Retrieved April 18, 2016, from structuremag.org/wp-content/uploads/2014/09/SF-Timber-Pegs-March-061.pdf

Strand, R. (2007, August). The Evolution of Structural Composite Lumber. Retrieved April 18, 2016, from structuremag.org/wp-content/uploads/2014/09/D-Prod-Watch-Strand-August071.pdf

Weyerhaeuser (2016, July). Parralam Plus PSL Beams, Headers, and Columns Featuring Trus Joist Parallam PSL with Wolmanized Preservative Protection #TJ-7102 Specifier's Guide. United States: Weyerhaeuser NR Company.

Weyerhaeuser (2016, May). 2.2E Parallam PSL Deep Beam #TJ-7100 Specifier's Guide. United States: Weyerhaeuser NR Company.

White, R. H. (2006, April). Fire Resistance of Structural Composite Lumber Products. Retrieved April 14, 2016, from researchgate.net/publication/238696640_Fire_Resistance_of_Structural_Composite_Lumber_Products

APPENDIX A: APPROXIMATE FRAME DEFLECTION

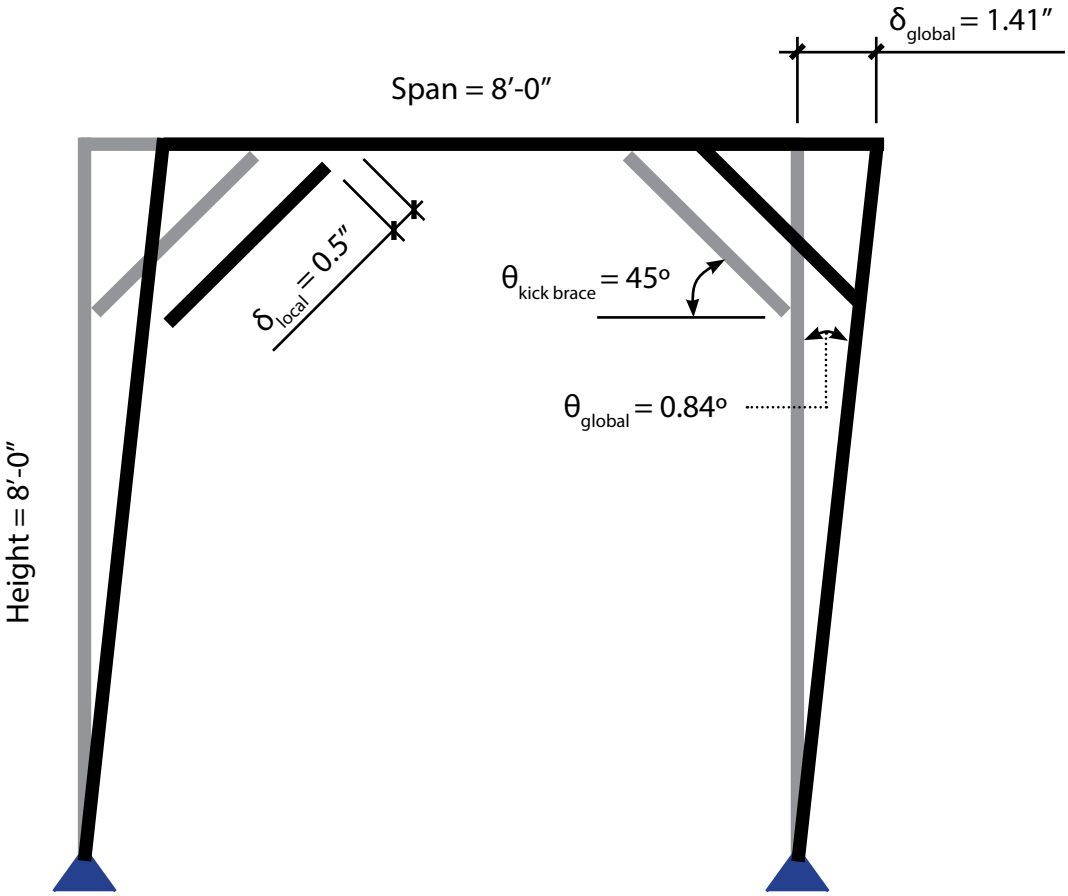

Figure 78. Lateral frame deflection based on 1/2 inch over-sized mortise pocket.

$\delta_{local} = 1/2$ in

$\delta_{kick\ brace} = (2)*(1/2\ in) = 1$ in

$$\delta_{global} = \frac{(1in)}{\cos(45^o)} = \underline{1.41\ in}$$

$\theta_{global} = \tan^{-1}((1.41\ in)/((8\ ft)*(12))) = \underline{0.84^o}$

APPENDIX B: ADJUSTED DESIGN STRESSES

PSL Design Values [p. 53 2015 NDS]

F_b = 2,9000 psi

F_{cll} = 2,900 psi

F_c = 625 psi

E = 2,200,000 psi

E_{min} = 1,118,190 psi

PSL Adjusted Design Values [p. 53 2015 NDS]

F'_b

C_f = .974, C_D = 1.6, C_m = C_t = 1.0, C_L= 1.0, C_v= 0.8775

F'_b = 4,243 psi

F'_{cll} for Column Member Stress

C_D = 1.6, C_p = 0.2

F'_c = 928 psi

F'_{cll} for Dowel Bearing Stress

C_D = 1.6, C_b = 1.3

F'_c = 3,770 psi

F'_v

C_D = 1.6

F'_v = 464 psi

APPENDIX C: CUREE TESTING PROTOCOL

The following is the deformation based point chart from the CUREE testing protocol for woodframe structures (Ayoub, A., Ibarra L., Krawinkler H., Medina R., Parisi F., 2001):

- Six cycles with an amplitude of 0.05Δ (initiation cycles)
- A primary cycle with an amplitude of 0.075Δ
- Six trailing cycles
- A primary cycle with an amplitude of 0.1Δ
- Six trailing cycles
- A primary cycle with an amplitude of 0.2Δ
- Three trailing cycles
- A primary cycle with an amplitude of 0.3Δ
- Three trailing cycles
- A primary cycle with an amplitude of 0.4Δ
- Two trailing cycles
- A primary cycle with an amplitude of 0.7Δ
- Two trailing cycles
- A primary cycle with an amplitude of 1.0Δ
- Two trailing cycles
- Increasing steps of the same pattern with an increase in amplitude of 0.5Δ, i.e., one primary cycle of amplitude equal to that of the previous primary cycle plus 0.5Δ, followed by two trailing cycles.

In concordance with a maximum expected drift, Δ_a, from Table 12.12-1 in ASCE 7-10, Table 7 was calculated to produce the deformation points for every test cycle.

	Frame Height h_x	8.0 feet			
	Δ_a=.02*h_x	1.92 in			
	Story Drift	0.02			
Δ_a - allowable story drift based on story height per ASCE 7-10					
	Δ_a	1.92	in		

Steps	Cycles	Deflection	Calculation	Drift	Θ
1	(6) Initiation Cycles	0.10	.05Δ_a	0.10%	.0597
2	Primary Cycle	0.14	.075Δ_a	0.15%	.0835
3	(6) Trailing Cycles	0.11	.05625Δ_a	0.11%	.0657
4	Primary Cycle	0.19	.1Δ_a	0.20%	.1134
5	(6) Trailing Cycles	0.14	.075Δ_a	0.15%	.0835
6	Primary Cycle	0.38	.2Δ_a	0.40%	.2268
7	(3) Trailing Cycles	0.29	.15Δ_a	0.30%	.1731
8	Primary Cycle	0.58	.3Δ_a	0.60%	.3462
9	(3) Trailing Cycles	0.43	.225Δ_a	0.45%	.2566
10	Primary Cycle	0.77	.4Δa	0.80%	.4596
11	(2) Trailing Cycles	0.58	.3Δ_a	0.60%	.3462
12	Primary Cycle	1.34	.7Δ_a	1.40%	.7997
13	(2) Trailing Cycles	1.01	.525Δ_a	1.05%	.6028
14	Primary Cycle	1.92	1.0Δ_a	2.00%	1.146
15	(2) Trailing Cycles	1.44	.75Δ_a	1.50%	.8593
16	Primary Cycle	2.88	1.5Δ_a	3.00%	1.718
17	(2) Trailing Cycles	2.16	1.125Δ_a	2.25%	1.289
18	Primary Cycle	3.84	2.0Δ_a	4.00%	2.291
19	(2) Trailing Cycles	2.88	1.5Δ_a	3.00%	1.718

Table 7. CUREE testing deformation goals per cycle.

APPENDIX D: SUPPORT FRAME DEFLECTION

The following calculations estimate the supporting steel frame deflection during testing.

Wide Flange Column - Weak Axis Bending

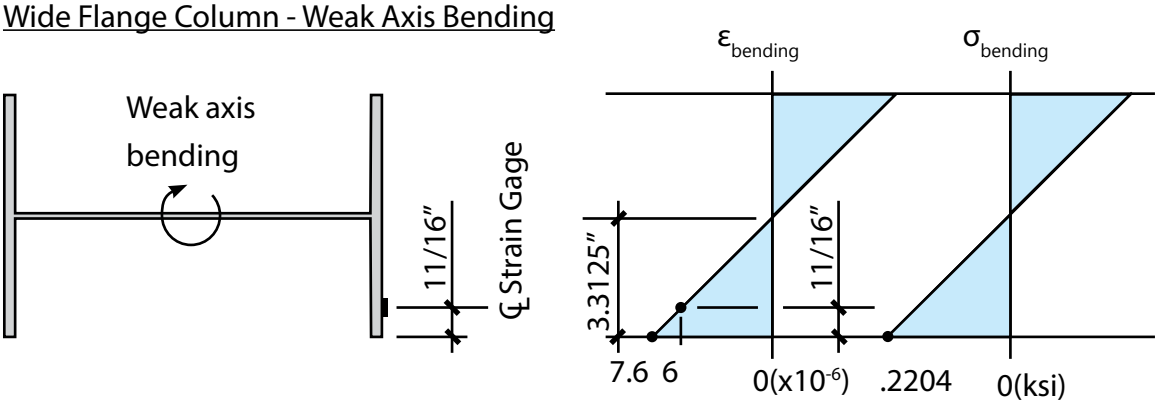

Figure 79. Support Column Stress and Strain.

The bending is caused by the force of the test frame pushing back on the out of plane column, above the column's connection to the diagonal axial brace. The exact wide flange size was not able to be determined, but a W12x30 was the closet section seize and was used to approximate the maximum deformation in the support frame due to bending. The column will be treated as a cantilever above this point, with a 2,000 lb point load 16.5 inches above the connection point. Using slope deflection, the stiffness for a cantilever column is:

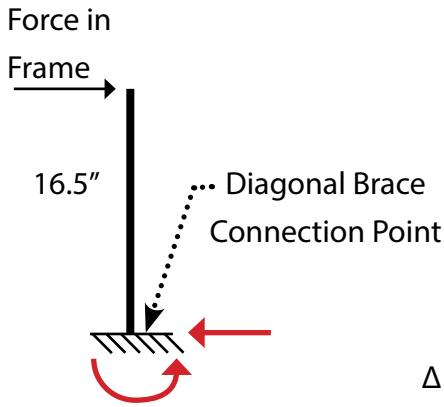

$$K = \frac{3EIL^3}{L^3}$$

and,

$$\Delta = F/K$$

$$\Delta = \frac{(2{,}000\ \text{lb})*(16.5\ \text{in.})^3}{3*(29{,}000{,}000)*(20\ \text{in.}^4)} = \underline{0.005\ \text{in.}}$$

Figure 80. Support Column FBD.

W8x28 Diagonal Brace - Axial Compression and Tension

$A = 8.25\ in^2$

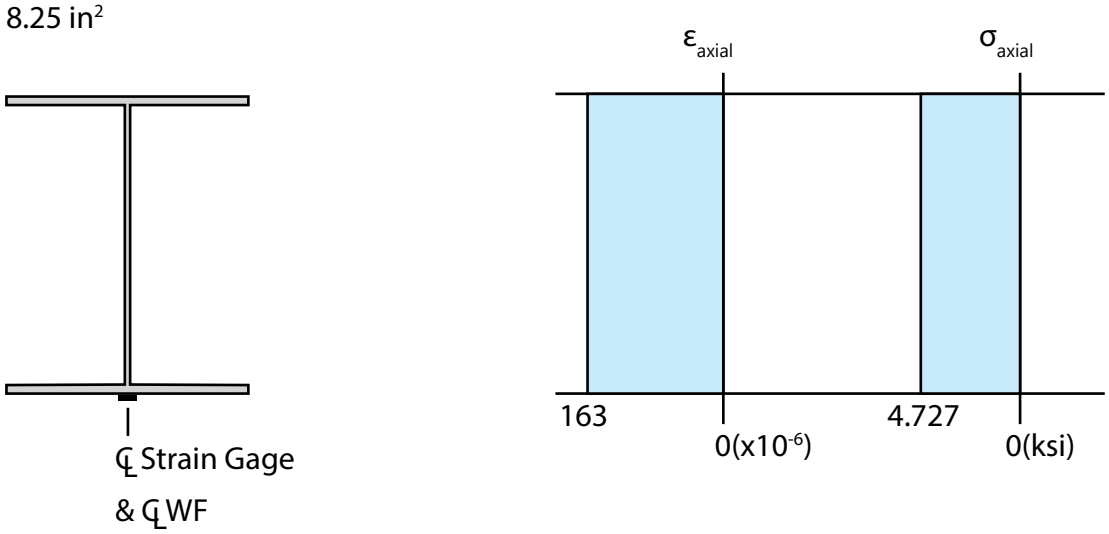

Figure 81. Support brace stress and strain.

Pure axial compression and tension deforms this support member. Using Hook's law, stress and strain are related to derive:

$$\Delta = \frac{PL}{AE}$$

First the stress is found using the simplified Hook's law equation:

$$E = \frac{\sigma}{\varepsilon}$$

$\sigma = (29{,}000\ ksi)*(163x10^{-6}) = 4.727\ ksi$

$P = (4.727\ ksi)*(8.25\ in^2) = \underline{39\ kips}$

$$\Delta_{diagonal} = \frac{(39\ kips)*(116.8\ in.)}{(8.25\ in.^2)*(29{,}000\ ksi)} = \underline{0.019''}$$

Knowing the brace is at an angle of 52.2° (See Figure 52), the diagonal deflection can

be converted into a horizontal deflection by dividing by the cosine of the kick brace angle.

$$\Delta_{horizontal} = \frac{0.019''}{\cos(52.2^{o})} = \underline{0.031''}$$

$$\Delta_{total} = 0.031'' + 0.005'' = \underline{0.036''}$$

0.036 inches is 1.2% of the maximum lateral beam deflection of 3 in.

The supporting steel frame was so stiff it effectively provided a rigid support, resisting the force going into the frame from the ram. Technically, according to the strain gauge calculation, the forces and deflections recorded during the testing should be reduced by 1.2%, but this is such a small amount it was considered negligible.

APPENDIX E: CONCEPTUAL FRAME IMPLEMENTATIONS

Figure 82. Timber frame implemented into residential housing structure, rendered in SketchUp.

Traditional timber framing can be modified to satisfy modern architectural and structural demands in residential construction, which makes up the majority of projects.

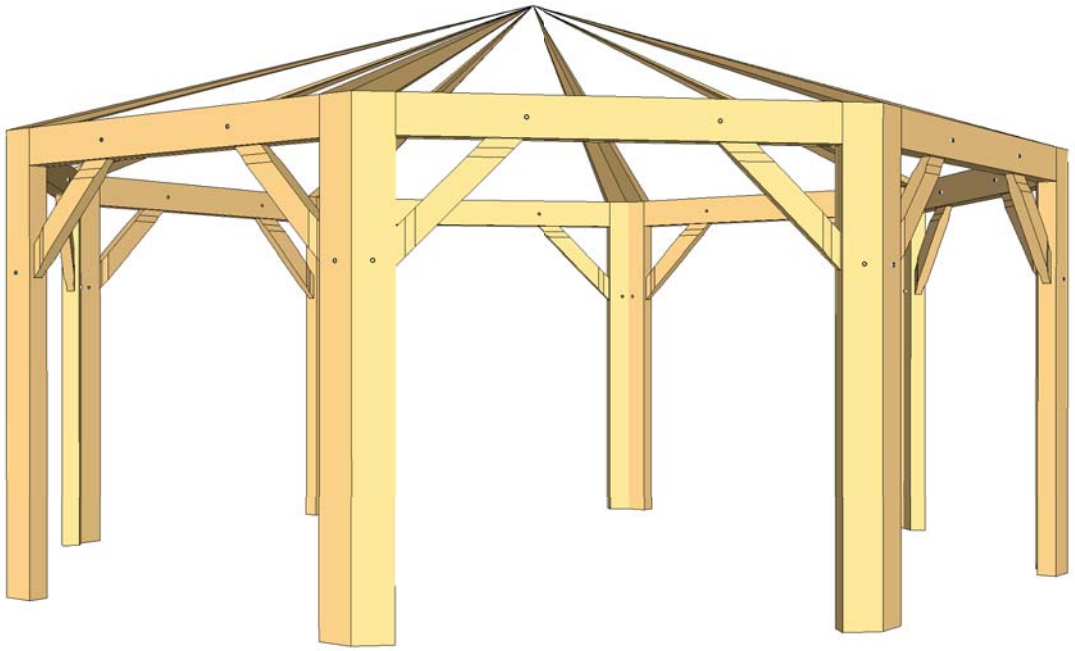

Figure 83. Timber frame implemented into an outdoor gazebo structure, rendered in SketchUp.

The ductile connection to be tested in this project could be reliable support for outdoor trellises and gazebos.

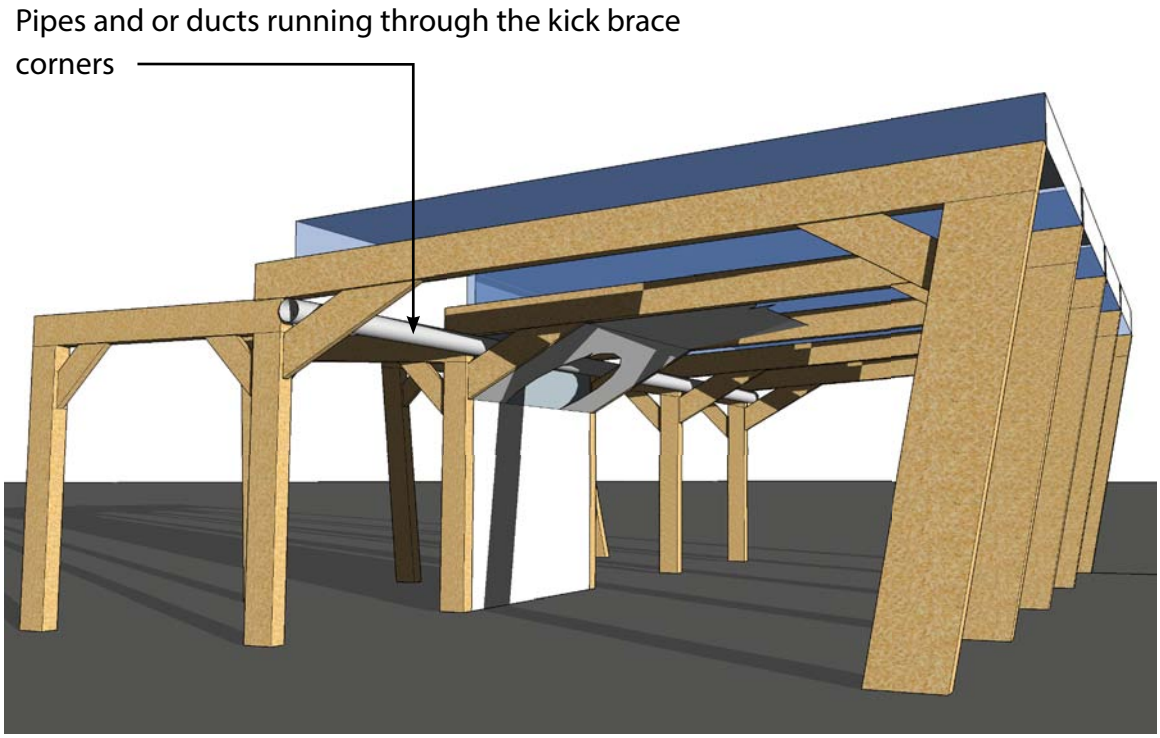

Figure 84. Timber framing integrating mechanical, electrical, and plumbing designs, rendered in Sketchup.

Heating, ventilation, air conditioning, and plumbing ducts can be placed and hidden in the corners of a timber frame with kick braces. Pipes and ducts placed in the corners are very accessible for maintenance and can be hidden by removable interior finishes.

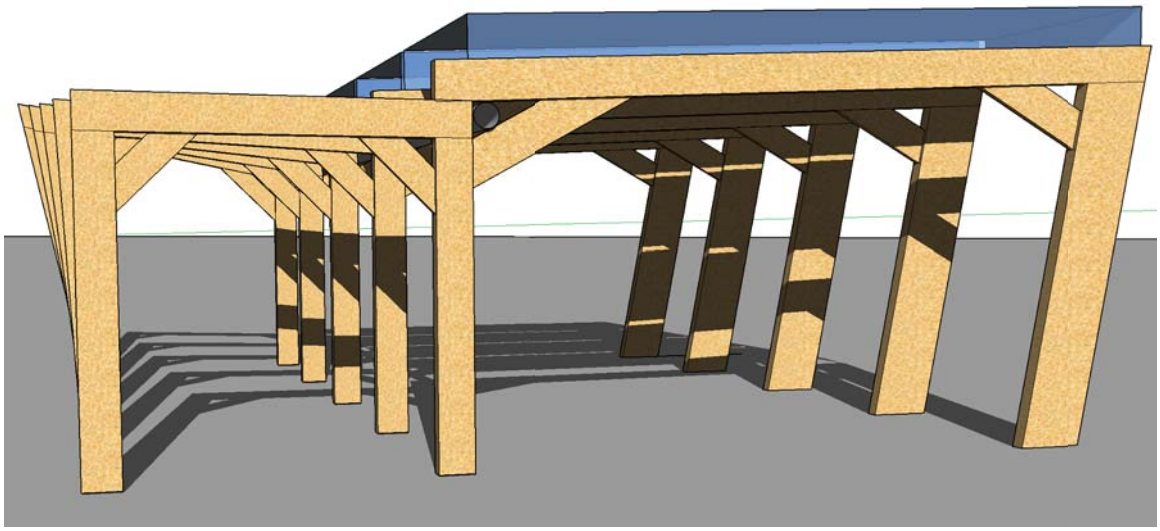

Figure 85. Timber framing satisfying modern structural and architectural demands, rendered in Sketchup.

The same frame in this project can be constructed in non-orthogonal geometries, accommodating both structural and architectural designs.

Figure 86. "A timber frame is beautiful and long lasting." (Myers, 2016)

Figure 87. "...light-filled building...referencing local traditions." (Lisa, 2013)

APPENDIX F: MATLAB CODE

```
% Alexi Kouromenos
% ARCE Masters Thesis
% Non-Linear Pushover of a one bay timber frame
% California Polytechnic State University

clc
clear all
%Concentric one story post beam frame with kick braces
%connected by a mortise tenon dowel connection

   %% Define Variables
% u = global displacement of node
% f = global force at node
% r = local nodal resisting displacement exerted by element on node
% R = local nodal resisting force exerted by element on node
R=trans(b)*S
% v = deformation of member                              v=a*r
% S = action deformation                                s=k*v
% Q = ubalance force (error)                            Q=F-Ri

%%   Member characteristics
E=2000;          %ksi
Acol=50;        %in^2
Abm=50;          %in^2
Akb=20;          %in^2

% PSL Values obtained from Weyerhauser TDJI 9000 Manual, phi already
% applied

% PSL Columns 11 7/8" x 5 1/4"
Icol=(5.25*(9.5^3))/12;
LcolS=2;                    %ft
LcolL=6;                    %ft
colSYtens=2*Acol;                %kips
colLYtens=colSYtens;              %kips
colSYcomp=2.9*Acol;               %kips
colLYcomp=colSYcomp;              %kips
colSyrot=6*E*Icol/LcolS*12;       %k-in
colLyrot=6*E*Icol/LcolL*12;       %k-in
vycolS=colSYtens*LcolS*12/(Acol*E);    %in
```

```
vycolL=colLYtens*LcolL*12/(Acol*E);    %in
vbcolS=-colSYcomp*LcolS*12/(Acol*E);   %in
vbcolL=-colLYcomp*LcolL*12/(Acol*E);   %in
phicolS=colSyrot*(1/(E*Icol));         %rad
phicolL=colLyrot*(1/(E*Icol));         %rad

% PSL Beam 9.5 " x 5 1/4"
Ibm=5.25*(9.25^3)/12;
LbmS=2;                        %ft
LbmL=4;                        %ft
bmSYtens=2*Abm;                %kips
bmLYtens=bmSYtens;             %kips
bmSYcomp=2.9*Abm;              %kips
bmLYcomp=bmSYcomp;             %kips
bmSyrot=6*E*Ibm/LbmS*12;       %k-in
bmLyrot=6*E*Ibm/LbmL*12;       %k-in
vybmS=bmSYtens*LbmS*12/(Abm*E);        %in
vybmL=bmLYtens*LbmL*12/(Abm*E);        %in
vbbmS=-bmSYcomp*LbmS*12/(Abm*E);       %in
vbbmL=-bmLYcomp*LbmL*12/(Abm*E);       %in
phibmS=bmSyrot*(1/(E*Ibm));            %rad
phibmL=bmLyrot*(1/(E*Ibm));            %rad

% PSL Kick Brace 3.5 " x 5.5"
Lkb=sqrt(2^2+2^2);             %ft
kbYtens=2*Akb;                 %kips
kbYcomp=2.9*Akb;               %kips
vykb=kbYtens*Lkb*12/(Akb*E);           %in
vbkb=-kbYcomp*Lkb*12/(Akb*E);          %in

% Dowel Springs

vyD=.18;                       %in
vbD=-vyD;                      %in
kD0=29.7;                      %k/in
% F=-16748*(x^2)+16383*x+90.452;
% K=diff(F,x);
%
% F=subs(F,x,v)
% K=subs(K,x,v)

% LD=1;                        %ft
% DYtens=30;                   %kips, phi=.9
```

```
% DYcomp=10;                    %kips, phi=.9
% vyD=DYtens*LD*12/(AD*E);          %in
% vbD=-DYcomp*LD*12/(AD*E);          %in



%%  Define degrees of freedom DOF
DOF=32;
dof=[1:1:32]';

%%  Define the id vectors to assemble the global stiffness and force matrix

id1=[1 2 3 7 8 9];
id2=[4 5 6 10 11 12];
id3=[7 8 9 21 22 23];
id4=[13 14 17 18];
id5=[19 20 15 16];
id6=[10 11 12 30 31 32];
id7=[21 22 23 24 25 26];
id8=[24 25 26 27 28 29];
id9=[27 28 29 30 31 32];
id10=[7 8 13 14];
id11=[15 16 10 11];
id12=[17 18 24 25];
id13=[27 28 19 20];


theta1=90;
theta2=90;
theta3=90;
theta4=45;
theta5=-45;
theta6=90;
theta7=0;
theta8=0;
theta9=180;
theta10=45;
theta11=-45;
theta12=45;
theta13=-45;

B1=betaframe(theta1);
B2=betaframe(theta2);
```

```
B3=betaframe(theta3);
B4=betatruss(theta4);
B5=betatruss(theta5);
B6=betaframe(theta6);
B7=betaframe(theta7);
B8=betaframe(theta8);
B9=betaframe(theta9);
B10=betatruss(theta10);
B11=betatruss(theta11);
B12=betatruss(theta12);
B13=betatruss(theta13);

r=zeros(DOF,1);
r1=zeros(6,1);
r2=zeros(6,1);
r3=zeros(6,1);
r4=zeros(4,1);
r5=zeros(4,1);
r6=zeros(6,1);
r7=zeros(6,1);
r8=zeros(6,1);
r9=zeros(6,1);
r10=zeros(4,1);
r11=zeros(4,1);
r12=zeros(4,1);
r13=zeros(4,1);



%%  Step 1) Initialize r, u, v, s equal to zero

vcen=0;
mode=0;

%State = [Vb ; Vy ; EA/L ; v curr ; s axial curr ; s rot1 curr, s rot2 curr k curr ; PD]

statem1=[vbcolL; vycolL; phicolL; E*Acol/(LcolL*12); 3*E*Icol/(LcolL*12)^3; 0; 0;
0; 0; 0; 0; E*Acol/(LcolL*12); 3*E*Icol/(LcolL*12)^3; vcen;mode];
statem2=[vbcolL; vycolL; phicolL; E*Acol/(LcolL*12); 3*E*Icol/(LcolL*12)^3; 0; 0;
0; 0; 0; 0; E*Acol/(LcolL*12); 3*E*Icol/(LcolL*12)^3; vcen;mode];
statem3=[vbcolS; vycolS; phicolS; E*Acol/(LcolS*12); 6*E*Icol/(LcolS*12)^3; 0; 0;
0; 0; 0; 0; E*Acol/(LcolS*12); 6*E*Icol/(LcolS*12)^3; vcen;mode];
statem4=[vbkb; vykb; E*Akb/(Lkb*12); 0; 0; E*Akb/(Lkb*12);vcen;mode];
```

```
statem5=[vbkb; vykb; E*Akb/(Lkb*12); 0; 0; E*Akb/(Lkb*12);vcen;mode];
statem6=[vbcolS; vycolS; phicolS; E*Acol/(LcolS*12); 6*E*Icol/(LcolS*12)^3; 0; 0;
0; 0; 0; 0; E*Acol/(LcolS*12); 6*E*Icol/(LcolS*12)^3; vcen;mode];
statem7=[vbbmS; vybmS; phibmS; E*Abm/(LbmS*12); 6*E*Ibm/(LbmS*12)^3; 0;
0; 0; 0; 0; 0; E*Abm/(LbmS*12); 6*E*Ibm/(LbmS*12)^3; vcen;mode];
statem8=[vbbmL; vybmL; phibmL; E*Abm/(LbmL*12); 3*E*Ibm/(LbmL*12)^3; 0;
0; 0; 0; 0; 0; E*Abm/(LbmL*12); 3*E*Ibm/(LbmL*12)^3; vcen;mode];
statem9=[vbbmS; vybmS; phibmS; E*Abm/(LbmS*12); 6*E*Ibm/(LbmS*12)^3; 0;
0; 0; 0; 0; 0; E*Abm/(LbmS*12); 6*E*Ibm/(LbmS*12)^3; vcen;mode];
statem10=[vbD; vyD; kD0; 0; 0; kD0;vcen;mode];
statem11=[vbD; vyD; kD0; 0; 0; kD0;vcen;mode];
statem12=[vbD; vyD; kD0; 0; 0; kD0;vcen;mode];
statem13=[vbD; vyD; kD0; 0; 0; kD0;vcen;mode];

ke1=kePinFix(Acol,Icol,E,LcolL*12);
ke2=kePinFix(Acol,Icol,E,LcolL*12);
ke3=TWODkeframe(E,Acol,LcolS*12,Icol);
ke4=getKTANL(statem4,r4,Lkb*12);
ke5=getKTANL(statem5,r5,Lkb*12);
ke6=TWODkeframe(E,Acol,LcolS*12,Icol);
ke7=kePinFix(Abm,Ibm,E,LbmS*12);
ke8=TWODkeframe(E,Abm,LbmL*12,Ibm);
ke9=kePinFix(Abm,Ibm,E,LbmS*12);
ke10=getKTANLD(statem10,r10);
ke11=getKTANLD(statem11,r11);
ke12=getKTANLD(statem12,r12);
ke13=getKTANLD(statem13,r13);

format long g
K=zeros(DOF,DOF);
K=Assemble(K,ke1,id1,B1);
K=Assemble(K,ke2,id2,B2);
K=Assemble(K,ke3,id3,B3);
K=Assemble(K,ke4,id4,B4);
K=Assemble(K,ke5,id5,B5);
K=Assemble(K,ke6,id6,B6);
K=Assemble(K,ke7,id7,B7);
K=Assemble(K,ke8,id8,B8);
K=Assemble(K,ke9,id9,B9);
K=Assemble(K,ke10,id10,B10);
K=Assemble(K,ke11,id11,B11);
K=Assemble(K,ke12,id12,B12);
K=Assemble(K,ke13,id13,B13);
```

```
m=max(K);
BFS=10^6*max(m);

%%  Step 2) Form Force matrix

% GUESS A BASE SHEAR
V0=1;

DETECTIVEJOHNSON = 0;

for Dtarget = [.5:.25:3];

P=-1;
   DETECTIVEJOHNSON = DETECTIVEJOHNSON +1;
   j=10;

while j>1

u1=zeros(DOF,1);
du=zeros(DOF,1);

r=zeros(DOF,1);
r1=zeros(6,1);
r2=zeros(6,1);
r3=zeros(6,1);
r4=zeros(4,1);
r5=zeros(4,1);
r6=zeros(6,1);
r7=zeros(6,1);
r8=zeros(6,1);
r9=zeros(6,1);
r10=zeros(4,1);
r11=zeros(4,1);
r12=zeros(4,1);
r13=zeros(4,1);


Q=zeros(DOF,1);
Q(21)=100;
F=zeros(DOF,1);
F(21)=(.25)*V0;
F(22)=P;
```

```
F(24)=(.25)*V0;
F(25)=P;
F(27)=(.25)*V0;
F(28)=P;
F(30)=(.25)*V0;
F(31)=P;

runs=0;

%%  Step 3) Increment displacement vector u = u + delta(u)
% Dtarget = Dtarget+Dutarget;

while abs(Q(21))>.001

   if runs>5000
      disp('HA, NICE TRY')
       disp(' ')
        disp('SHOULD NOT BE TAKING THIS LONG')
         disp(' ')
      break
   end
   u1=u1+du;
ue1=[u1(1:3);u1(7:9)];
ue2=[u1(4:6);u1(10:12)];
ue3=[u1(7:9);u1(21:23)];
ue4=[u1(13:14);u1(17:18)];
ue5=[u1(19:20);u1(15:16)];
ue6=[u1(10:12);u1(30:32)];
ue7=[u1(21:23);u1(24:26)];
ue8=[u1(24:26);u1(27:29)];
ue9=[u1(27:29);u1(30:32)];
ue10=[u1(7:8);u1(13:14)];
ue11=[u1(15:16);u1(10:11)];
ue12=[u1(17:18);u1(24:25)];
ue13=[u1(27:28);u1(19:20)];

%%  Step 4) Form r--nodal resisting displacement--for each element (global to
local transformation)

%Global to Local Deformation

r1=B1*ue1;
r2=B2*ue2;
```

```
r3=B3*ue3;
r4=B4*ue4;
r5=B5*ue5;
r6=B6*ue6;
r7=B7*ue7;
r8=B8*ue8;
r9=B9*ue9;
r10=B10*ue10;
r11=B11*ue11;
r12=B12*ue12;
r13=B13*ue13;

%%  Step 5) Update state of each element (re-->ve-->Se)

% statem1=updatestateTANLsrBM(statem1,r1,LcolS*12,E,Icol)
statem1=updatestateTANLsrFixPin(statem1,r1,LcolL*12,E,Icol);
% statem4=updatestateTANLsrBM(statem4,r4,LcolS*12,E,Icol);
statem2=updatestateTANLsrFixPin(statem2,r2,LcolL*12,E,Icol);
statem3=updatestateTANLsrBM(statem3,r3,LcolS*12,E,Icol);
statem4=updatestateTANLsr(statem4,r4);
statem5=updatestateTANLsr(statem5,r5);
statem6=updatestateTANLsrBM(statem6,r6,LcolS*12,E,Icol);
statem7=updatestateTANLsrFixPin(statem7,r7,LbmS*12,E,Ibm);
statem8=updatestateTANLsrBM(statem8,r8,LbmL*12,E,Ibm);
statem9=updatestateTANLsrFixPin(statem9,r9,LbmS*12,E,Ibm);
statem10=updatestateTANLsrD(statem10,r10)
statem11=updatestateTANLsrD(statem11,r11)
statem12=updatestateTANLsrD(statem12,r12)
statem13=updatestateTANLsrD(statem13,r13)

%%  Step 6) Calculate resisting force R of each element (Se-->Re)

Re1=getResistingForceFixPin(statem1,r1,LcolL*12,Icol);
Re2=getResistingForceFixPin(statem2,r2,LcolL*12,Icol);
Re3=getResistingForceBM(statem3,r3,LcolS*12,Icol);
Re4=getResistingForce(statem4,r4,Lkb*12);
Re5=getResistingForce(statem5,r5,Lkb*12);
Re6=getResistingForceBM(statem6,r6,LcolS*12,Icol);
Re7=getResistingForceFixPin(statem7,r7,LbmS*12,Ibm);
Re8=getResistingForceBM(statem8,r8,LbmL*12,Ibm);
Re9=getResistingForceFixPin(statem9,r9,LbmS*12,Ibm);
Re10=getResistingForceD(statem10,r10);
Re11=getResistingForceD(statem11,r11);
```

```
Re12=getResistingForceD(statem12,r12);
Re13=getResistingForceD(statem13,r13);

%Local to Global Force

R1=transpose(B1)*Re1;
R2=transpose(B2)*Re2;
R3=transpose(B3)*Re3;
R4=transpose(B4)*Re4;
R5=transpose(B5)*Re5;
R6=transpose(B6)*Re6;
R7=transpose(B7)*Re7;
R8=transpose(B8)*Re8;
R9=transpose(B9)*Re9;
R10=transpose(B10)*Re10;
R11=transpose(B11)*Re11;
R12=transpose(B12)*Re12;
R13=transpose(B13)*Re13;

%%  Step 7) Assemble element resisting
Ri=zeros(DOF,1);
Ri=ForceAssemble(Ri,R1,id1);
Ri=ForceAssemble(Ri,R2,id2);
Ri=ForceAssemble(Ri,R3,id3);
Ri=ForceAssemble(Ri,R4,id4);
Ri=ForceAssemble(Ri,R5,id5);
Ri=ForceAssemble(Ri,R6,id6);
Ri=ForceAssemble(Ri,R7,id7);
Ri=ForceAssemble(Ri,R8,id8);
Ri=ForceAssemble(Ri,R9,id9);
Ri=ForceAssemble(Ri,R10,id10);
Ri=ForceAssemble(Ri,R11,id11);
Ri=ForceAssemble(Ri,R12,id12);
Ri=ForceAssemble(Ri,R13,id13);

%%  Step 8) Form Reactions at controlled DOFs
%   Create a very stiff spring with stiffness M which is the largest value
%   in the [K] matrix
format long g
RXN=zeros(DOF,1);
RXN(1)=BFS*u1(1);
RXN(2)=BFS*u1(2);
RXN(4)=BFS*u1(4);
```

```
RXN(5)=BFS*u1(5);
RXN(30)=BFS*u1(30);
display('F dof')
[F dof];
display('Ri dof')
[Ri dof];
display('RXN dof')
[RXN dof];
%%  Step 9) Calculate Q - Equilibrium check
Q=F-Ri-RXN;
[Q dof];

%%  Step 10) Form [K] using desired method
[K Q]=penaltyfunc(BFS,K,Q,0,1);
[K Q]=penaltyfunc(BFS,K,Q,0,2);
[K Q]=penaltyfunc(BFS,K,Q,0,4);
[K Q]=penaltyfunc(BFS,K,Q,0,5);
[K Q]=penaltyfunc(BFS,K,Q,Dtarget,30);
for i=1:32
      K(i,i)=K(i,i)+max(m)*10^-8;
end

Kdiagonal=diag(K);
[Kdiagonal dof]

%%  Step 11) Calculate the left over nodal displacement delta(r)=K^-1 * Q

display('Q F Ri RXN u1 dof')
[Q F Ri RXN u1 dof]

du=K\Q;

[du dof];

Dtarget
uint=u1+du;
[du uint dof]
format short g

%%  Step 12) Go to step 3
        %in
runs=runs+1
display('++++++++++++++++++++++++++++++++++ RUNS
```

```
++++++++++++++++++++++++++ RUNS ++++++++++++++++++++++++++++++')

end

Z=(u1(30)-Dtarget)*BFS   %k
V0
V0=(1-Z/(V0))*V0

   if abs(Z)<0.001
   disp('Converged!')
   disp(' ')

      break
   end

end


   hold on
   pushover_plot = plot(0,0);
   iteration_plot = plot(0,0);
   set(pushover_plot,'LineStyle','-','LineWidth',0.025,'Marker','+','MarkerSize',3,'C
olor',[0 0 0])
%    set(iteration_plot,'LineStyle','-','LineWidth',0.025,'Marker','o','MarkerSize',3,'
Color',[1 0 0])
   grid on
   title('Pushover Curve')
   xlabel('Displacement [in]')
   ylabel('Base Shear [kips]')
   legend('Force-Displacement','Location','northwest')
   legend('boxoff')
   set(pushover_plot,'XData',u1(30),'YData',V0);
%    set(iteration_plot,'XData',u1(44),'YData',runs);
   drawnow

   y(DETECTIVEJOHNSON)=V0;
   V0
   x(DETECTIVEJOHNSON)=u1(30);
end

plot(x,y,'k')
title('Newton-Raphson Force Deflection')
xlabel('Drift (in)')
```

```
ylabel('Base Shear (kips)')
grid on
grid minor

%%
% Alexi Kouromenos
% Masters Thesis
% Function - Create Beta matrix for a truss element converting local to global
%            coordinates for Non-Linear Pushover

function [ B ] = beta( theta )

C=cosd(theta);
S=sind(theta);
B=zeros(4,4);
B(1,1)=C;
B(1,2)=S;
B(2,1)=-S;
B(2,2)=C;
B(3,3)=C;
B(3,4)=S;
B(4,3)=-S;
B(4,4)=C;

end

%%
% Alexi Kouromenos
% Masters Thesis
% Function - Create Beta matrix for a frame element converting local
%        to global coordinates for Non-Linear Pushover

function [ B ] = betaframe( theta )

C=cosd(theta);
S=sind(theta);
B=zeros(6,6);
B(1,1)=C;
B(1,2)=S;
B(2,1)=-S;
B(2,2)=C;
B(3,3)=1;
B(4,4)=C;
```

```
B(4,5)=S;
B(5,4)=-S;
B(5,5)=C;
B(6,6)=1;

end

%%
% Alexi Kouromenos
% Masters Thesis
% Function - Create a local stiffness matrix for a pin-fixed element

%%
function [ ke ] = kePinFix(A,I,E,L)

a=(E*A)/L;
b=(3*E*I)/(L^3);
c=(3*E*I)/(L^2);
d=(3*E*I)/(L);

ke=[a,0,0,-a,0,0;0,b,0,0,-b,c;0,0,0,0,0,0;-a,0,0,a,0,0;0,-b,0,0,b,-c;0,c,0,0,-c,d];
end

%%
% Alexi Kouromenos
% Masters Thesis
%%
function [ ke ] = TWODkeframe(E,A,L,I)
%This function generates the stiffness matrix of a element of the structure
%   A 4x4 matrix will be generated representing the 4 degrees of freedom
%   that the element has to move
format short
ks=E*A/L;
ke=zeros(4,4);
ke(1,1)=ks;
ke(1,4)=-ks;
ke(4,1)=-ks;
ke(4,4)=ks;
ksa=12*E*I/(L^3);
ksb=6*E*I/(L^2);
ksc=4*E*I/L;
ksd=2*E*I/L;
ke(2,2)=ksa;
```

```
ke(2,3)=ksb;
ke(2,5)=-ksa;
ke(2,6)=ksb;
ke(3,2)=ksb;
ke(3,3)=ksc;
ke(3,5)=-ksb;
ke(3,6)=ksd;
ke(5,2)=-ksa;
ke(5,3)=-ksb;
ke(5,5)=ksa;
ke(5,6)=-ksb;
ke(6,2)=ksb;
ke(6,3)=ksd;
ke(6,5)=-ksb;
ke(6,6)=ksc;

end

%%
% Alexi Kouromenos
% Masters Thesis
% Function - Create a local stiffness matrix for a pin-pin element

%%
function [ ke ] = getKTANL( state, re, L)

a=[-1 0 1 0];

ke=transpose(a)*state(6)*a;

end

%%
% Alexi Kouromenos
% Masters Thesis
% Function - Create a local stiffness matrix for the dowel element

%%
function [ ke ] = getKTANLD( state, re)
% Return the new stiffness K of an element
%   Detailed explanation goes here

a=[-1 0 1 0];
```

```
b=a;

ke=transpose(b)*state(6)*a;

end

%%
% Alexi Kouromenos
% Masters Thesis

%%
function [ state ] = updatestateTANLsrFixPin(state,r,L,E,I)
%This function updates the current state of a fix-pin element
%   with an old state and new joint coordinates, nodal force vb, vy
%   and element stiffness AE/l and vcurrent and s current and k current
%   will be updated

a=[-1 0 0 1 0 0;
   0 1/L 1 0 -1/L 0;
   0 1/L 0 0 -1/L 1];

ke=[state(4) 0 0;
   0 0 0;
   0 0 (3*E*I)/L];

v=a*r;
S=ke*v;
vN=v(1);
vroty1=v(2);
vroty2=v(3);
vy=state(2);
vb=state(1);
phiy=state(3);
k=state(12);
krot=state(13);
vcen=state(14);
mode=state(15);

state(6)=vN;
state(7)=S(1);
state(8)=vroty1;
state(9)=S(2);
state(10)=vroty2;
```

```
state(11)=S(3);
state(12)=k;
state(13)=krot;
end

%%
% Alexi Kouromenos
% Masters Thesis

%%
function [ state ] = updatestateTANLsrBM(state,r,L,E,I)
%This function updates the current state of a frame element
%   with an old state and new joint coordinates, nodal force vb, vy
%   and element stiffness AE/l and vcurrent and s current and k current
%   will be updated

a=[-1 0 0 1 0 0;
   0 1/L 1 0 -1/L 0;
   0 1/L 0 0 -1/L 1];

ke=[state(4) 0 0;
   0 (4*E*I)/L (2*E*I)/L;
   0 (2*E*I)/L (4*E*I)/L];

v=a*r;
S=ke*v;
vN=v(1);
vroty1=v(2);
vroty2=v(3);
vy=state(2);
vb=state(1);
phiy=state(3);
k=state(12);
krot=state(13);
vcen=state(14);
mode=state(15);

state(6)=vN;
state(7)=S(1);
state(8)=vroty1;
state(9)=S(2);
state(10)=vroty2;
state(11)=S(3);
```

```
state(12)=k;
state(13)=krot;
end

%%
% Alexi Kouromenos
% Masters Thesis

%%
function [ state ] = updatestateTANLsr( state,r)
%THIS FUNCTION UPDATES THE CURRENT STATE OF A TRUSS ELEMENT
%   with an old state and new joint coordinates, nodal force vb, vy
%   and element stiffness AE/l and vcurrent and s current and k current
%   will be updated

a=[-1 0 1 0];

v=a*r;
vy=state(2);
vb=state(1);
k=state(6);
vcen=state(7);
mode=state(8);

if v > (vy+vcen);
   M=1;
elseif v < (vb+vcen)
   M=-1;
else
   M=0;
end

switch mode
   case 0
      switch M
         case 1
            mode=1;
            vcen=v-vy;
            S=vy*state(3);
            k=0;
         case -1
            mode=-1;
            S=vb*state(3);
```

```
        k=0;
        vcen=v-vb;
      case 0
        mode=0;
        S=(v-vcen)*state(3);
        k=state(3);
        vcen=vcen;
  end
case -1
  switch M
    case 1
      mode=1;
      vcen=v-vy;
      S=vy*state(3);
      k=0;
    case-1
      mode=-1;
      S=vb*state(3);
      k=0;
      vcen=v-vb;
    case 0
      mode=0;
      S=(v-vcen)*state(3);
      k=state(3);
      vcen=vcen;
  end

case 1
  switch M
    case 1
      mode=1;
      vcen=v-vy;
      S=vy*state(3);
      k=0;
    case-1
      mode=-1;
      S=vb*state(3);
      k=0;
      vcen=v-vb;
    case 0
      mode=0;
      S=(v-vcen)*state(3);
```

```
            k=state(3);
            vcen=vcen;
        end
end

state(6)=k;
state(4)=v;
state(5)=S;
state(7)=vcen;
state(8)=mode;
end

%%
% Alexi Kouromenos
% Masters Thesis

%%
function [ state ] = updatestateTANLsrD( state,r)
%This function updates the current state of a dowel element
%   with an old state and new joint coordinates, nodal force vb, vy
%   and element stiffness AE/l and vcurrent and s current and k current
%   will be updated

syms x

a=[-1 0 1 0];

v=a*r;
vy=state(2);
vb=state(1);
vcen=state(7);
mode=state(8);

Fx= -48.95354275*(x^5) + 86.49332771*(x^4) - 35.18746611*(x^3) -
19.53645448*(x^2) + 19.00844372*x - .05654322144;

Kx=diff(Fx,x);

F=subs(Fx,x,abs(v));
K=subs(Kx,x,abs(v));

            mode=0;
```

```
            k=K;
            vpa(k);
            S1=K*v;
            vpa(S1);
            S=F;
            vpa(S);
            vcen=vcen;
if v>=0
state(6)=k;
state(4)=v;
state(5)=S;
state(7)=vcen;
state(8)=mode;
elseif v<0
state(6)=k;
state(4)=-v;
state(5)=-S;
state(7)=vcen;
state(8)=mode;
end
end

%%
% Alexi Kouromenos
% Masters Thesis
% Function - Assemble Global Stiffness Matrix for Non-Linear Pushover

%%
function [ K ] = Assemble(K,kei,idi,B)
% This function assembles the global stiffness matrix K composed of
% Element matrices ke
%  The size of K is determined by the number of DOFs squared

format short
S=size(idi);
n=S(1,1);
m=S(1,2);
if S(1,2)==1;
    for i=1:m;
       r=idi(i);
           if r~=0;
              K(r,1)=kei(i,1)+K(r,1);
           end
```

```
    end
end

ken=transpose(B)*kei*B;

if S(1,2)~=1;
     for i=1:m;
        for j=1:m;
        R=idi(i);
        C=idi(j);
           if R~=0;
           if C~=0;
              K(R,C)=ken(i,j)+K(R,C);
           end
        end
     end
  end
 end
end

%%
% Alexi Kouromenos
% Masters Thesis

%%
function [ Re ] = getResistingForce( state, re ,L )
% Retrieves the local nodal resisting force of a pin-pin element

a=[-1 0  1 0];

b=[-1 -(re(4)-re(2))/L 1 (re(4)-re(2))/L];

Re=a'*state(5);

end

%%
% Alexi Kouromenos
% Masters Thesis

%%
function [ Re ] = getResistingForceBM( state, re ,L,I )
% Retrieves the local nodal resisting force of a fix-fix element
```

```
S=[state(7);state(9);state(11)];

E=2000;

a=[-1 0 0 1 0 0;
   0 1/L 1 0 -1/L 0;
   0 1/L 0 0 -1/L 1];

ke=[state(4) 0 0;
   0 (4*E*I)/L (2*E*I)/L;
   0 (2*E*I)/L (4*E*I)/L];

 b=[-1 (re(5)-re(2))/(L^2) (re(5)-re(2))/(L^2);
     (re(5)-re(2))/(L) -1/L -1/L;
    0 1 0;
    1 -(re(5)-re(2))/(L^2) -(re(5)-re(2))/(L^2);
    -(re(5)-re(2))/(L) 1/L 1/L;
    0 0 1];

Re=a'*S;

end

%%
% Alexi Kouromenos
% Masters Thesis

%%
function [ Re ] = getResistingForceFixPin( state, re ,L,I )
% Retrieves the local nodal resisting force of a fix pin element

S=[state(7);state(9);state(11)];

E=2000;

a=[-1 0 0 1 0 0;
   0 1/L 1 0 -1/L 0;
   0 1/L 0 0 -1/L 1];

ke=[state(4) 0 0;
   0 0 0;
   0 0 (3*E*I)/L];
```

```
 b=[-1 (re(5)-re(2))/(L^2) (re(5)-re(2))/(L^2);
     (re(5)-re(2))/(L) -1/L -1/L;
    0 1 0;
    1 -(re(5)-re(2))/(L^2) -(re(5)-re(2))/(L^2);
    -(re(5)-re(2))/(L) 1/L 1/L;
    0 0 1];

Re=a'*S;

end

%%
% Alexi Kouromenos
% Masters Thesis

%%
function [ Re ] = getResistingForceD( state, re)
% Retrieves the local nodal resisting force of a dowel element
%   Detailed explanation goes here

b=[-1 0 1 0];

Re=b'*state(5);

end

%%
% Alexi Kouromenos
% Masters Thesis

%%
function [ F ] = ForceAssemble(F,Re,idi)
% This function assembles the global Force matrix F composed of
% Element force matrices f
%   The number of rows in F is determined by the number of DOFs squared

format short
S=size(idi);
n=S(1,1);
m=S(1,2);
      for i=1:m;
         r=idi(i);
```

```
            if r~=0;
               F(r,1)=Re(i,1)+F(r,1);
            end
        end
end

%%
% Alexi Kouromenos
% Masters Thesis
% This function applies a scalor of x10^6 to the diagonal of the K
% matrix at a specific DOF, and the corresponding DOF in the F vector

%%
function [ K F ] = penaltyfunc( M,K,F,upi,DOF )

K(DOF,DOF)=M;

F(DOF,1)=F(DOF,1)+M*upi;
end
```

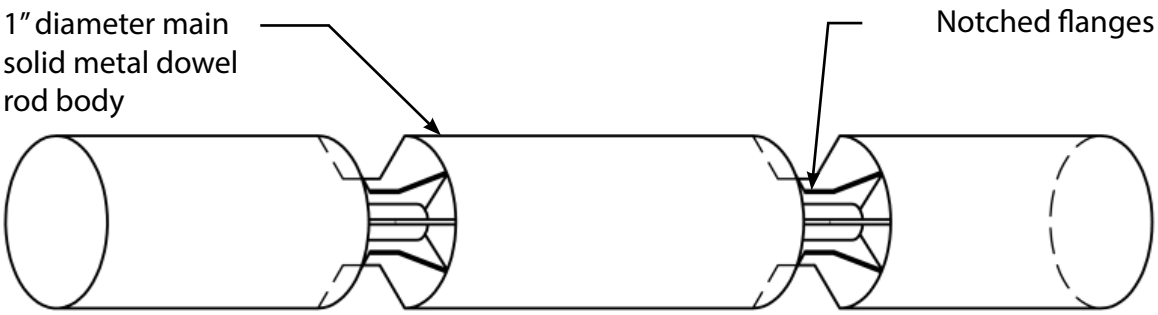

Figure 88. Flange notched dowel.

The optimal number and geometrical shape of the flanges must be tested. The flanges can either buckle or yield in compression depending on the yield strength of the material.

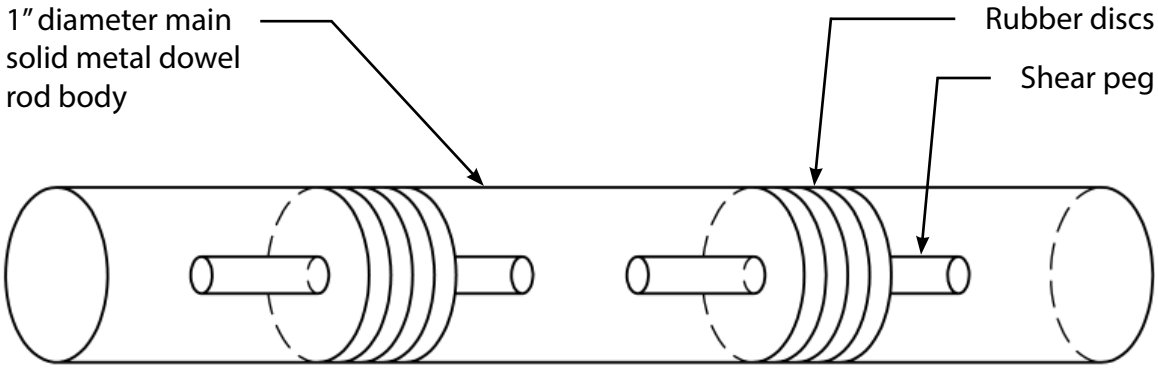

Figure 89. Disk separated dowel.

Combined layers of rubber or plastic and maybe steel can endure large cyclic deformations, similar to the way some base isolators are designed. The optimal layering of materials must be tested.

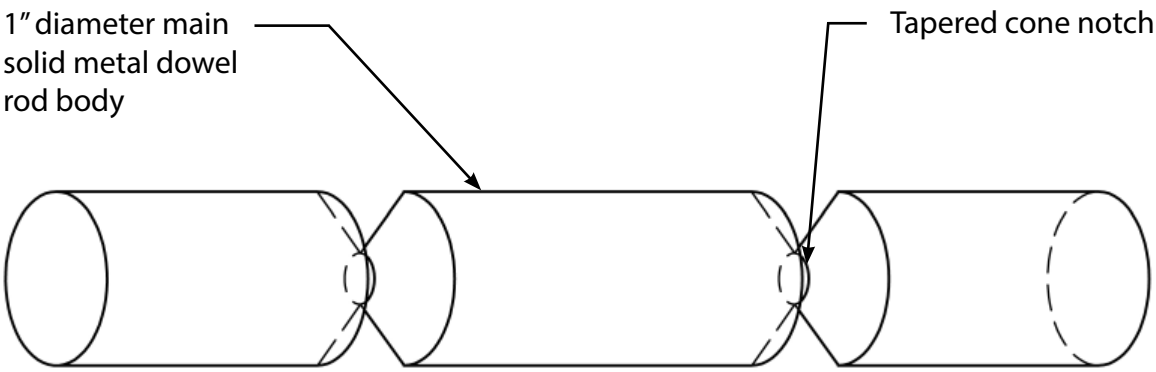

Figure 90. Cone tapered metal dowel.

A solid steel rod is tapered to a smaller diameter cross-section that becomes a plastic hinge. The optimal cone taper to the smaller diameter must be tested.